Medicines for All Institute

Summary of Process Development Work on Synthesis of Ganaplacide

Report Prepared by:

Dr. Ryan Littich
Dr. Justina M. Burns
Dr. Limei Jin
Dr. Chiranjeevi Barreddi
Dr. Pankaj Khairnar
Jason Kelley
Dr. Kevin Robb
Dr. Piyal Singh
Dr. Nakul Telang
Dr. Daniel Cook

Contact: m4all@vcu.edu

Drafted: October 13, 2025

Revised: October 27, 2025

Published to website: November 20, 2025, 1:00 PM EST







Executive Summary

This process development report (PDR) describes the results of synthetic route scouting, process development, scale-up, and documentation efforts of ganaplacide synthesis at Medicines for All Institute (M4ALL). A new, cost-efficient and practical synthetic approach toward the synthesis of 2-(4-fluorophenyl)-8,8-dimethyl-5,6,7,8-tetrahydroimidazo[1,2-a]pyrazine (3.4, an advanced intermediate in the innovator-reported synthesis of ganaplacide) is disclosed. Ganaplacide is a broad acting antimalarial drug that targets both asexual and sexual stages of *Plasmodium* parasites, developed by Novartis Inc. It is in phase 3 clinical trials. Novartis's baseline route for ganaplacide API is an 11-step process commencing from 2-bromo-4'-fluoroacetophenone. The current route is characterized by challenges that impact the overall cost, and manufacturability, at scale. It comprises two Pd-catalyzed steps and features other expensive and hazardous materials (e.g., HATU and Cs₂CO₃), which increase overall raw material costs and create safe-handling concerns. The overall yield of this 11-step route to API is 17% based on 2-bromo-4'-fluoroacetophenone.^{1,2}

Herein, we describe a new approach to make the advanced intermediate **3.4** which is 4 steps removed from ganaplacide. It is a 7-step process from commodity fluorobenzene. The process consists of Friedel-Crafts acylation of fluorobenzene with chloroacetyl chloride (Milestone 1), Bredereck imidazole synthesis (Milestone 2),³ telescoped *N*-alkylation with 2-chloroethylamine followed by Boc protection (Milestone 3), bromination then Boc removal (Milestone 4), and a Pictet-Spengler reaction to give common intermediate **3.4** (Milestone 5). This 7-step process affords **3.4** in 3% overall yield with a purity of 60.3 LCAP (254 nm) and 25.3 wt% (HPLC). Overall yield and **3.4** purity data bely process challenges and opportunities, discussed herein. Technoeconomic (TE) analysis of current process performance shows a 23% reduction in cumulative API raw material cost (RMC), relative to Novartis's first-generation route. Further development and optimization of the Pictet-Spengler annulation has the potential to deliver additional, substantial RMC reduction (Figure 1).



API Raw Material Cost vs. Pictet-Spengler Annulation Yield



Figure 1. Ganaplacide API raw material cost sensitivity as a function of Pictet-Spengler annulation yield, culminating in the advanced intermediate **3.4**. Ganaplacide API RMC calculated in reference to the process disclosed in *J. Med. Chem.* **2012**, *55*, 4244–4273.



$\label{eq:medicines} \textbf{Medicines for All-Contributors to the Research and Report}$

Contributor	Title/Role
Dr. Ryan Littich	Chief Technology Officer
Dr. Limei Jin	Associate Director of Process Development
Dr. Michel Nuckols	Senior Research Scientist (Project Lead)
Jason Kelley	Associate Director of MSAT
Dr. Pankaj Khairnar	Research Scientist
Dr. Nakul Telang	Research Scientist
Dr. Raj Sahani	Research Scientist
Dr. Chiranjeevi Barreddi	Postdoctoral Researcher
Dr. Kevin Robb	Research Scientist
Dr. Piyal Singh	Postdoctoral Researcher
Dr. Daniel Cook	Analytical Chemist
Dr. Justina M. Burns	Assoc Dir of Analytical Chemistry
Dr. Erin Stryker	Project Coordinator
Janie Wierzbicki	Associate Director of Project Management Office



Contents

1	Introduc	ction	6
2	Results	and Discussion	8
2.1	3.0 to 3.	1 (Milestone 1)	10
	2.1.1	Condition screening and optimization	10
	2.1.2	Practical workup and purification for scalability	11
2.2	3.1 to 3.	2 (Milestone 2)	12
	2.2.1	Condition screening and optimization	12
	2.2.2	Practical workup and purification for scalability	14
2.3	3.2 to 3.	.3 and 3.3 to 3.3-Boc (Milestone 3)	15
	2.3.1	Condition screening and optimization	16
	2.3.2	Practical workup and purification for scalability	21
	2.3.3	Safety assessment of the process	25
	2.3.4	Impurities identification, RT markers, mitigation approaches	27
2.4	3.3-Boc	to 3.7-diHBr (Milestone 4)	28
	2.4.1	Condition screening and optimization	29
	2.4.2	Practical workup and purification for scalability	31
	2.4.3	Process safety assessment	36
	2.4.4	Impurities identification, RT markers, mitigation approaches	37
2.5	3.7-diH	Br to 3.4 (Milestone 5)	38
	2.5.1	Condition screening and optimization	38
	2.5.2	Practical workup and purification for scalability	44
	2.5.3	Process safety assessment	47
	2.5.4	Impurities identification, RT markers, mitigation approaches	47
2.6	Conclus	ions	47
3	Append	ix	49
3.1	Experim	nental details	49
3.2	NMR &	HPLC spectra	68
4	Acknow	ledgements	92
5	Doforon	000	02



1 Introduction

Malaria remains one of the most devastating infectious diseases globally, with over 600,000 deaths annually, disproportionately affecting children under five years of age.⁴ Emerging resistance to artemisinin-based combination therapies (ACTs), the current frontline treatment, underscores the urgent need for novel antimalarial agents with distinct mechanisms of action and simplified dosing regimens.

Ganaplacide (development code KAF156), an imidazolopiperazine derivative, is a promising next-generation antimalarial candidate developed by Novartis in collaboration with Medicines for Malaria Venture (MMV). Ganaplacide exhibits potent activity against both *Plasmodium* falciparum and Plasmodium vivax, targeting multiple stages of the parasite lifecycle including liver, asexual blood, and sexual transmission stages. Mechanistically, ganaplacide disrupts protein trafficking and folding within the parasite's endoplasmic reticulum (ER), leading to ER expansion and impaired parasite viability. Although its precise molecular target remains undefined,⁵ resistance has been associated with mutations in PfCARL, PfUGT, and PfACT, suggesting involvement in membrane protein trafficking and fatty acid transport. Preclinical studies demonstrated ganaplacide's efficacy in vitro and in vivo, with favorable pharmacokinetics supporting once-daily dosing.⁶ In combination with lumefantrine, a hemozoin formation inhibitor, ganaplacide has shown synergistic effects and robust activity against artemisinin-resistant strains. This combination, formulated as a solid dispersion (SDF), has progressed through Phase 2 trials and is currently undergoing Phase 3 evaluation across multiple African countries. 8,9 Importantly, ganaplacide-lumefantrine therapy has demonstrated rapid parasite clearance (<48 hours), transmission-blocking potential, and chemopreventive efficacy against liver-stage infection. These attributes position ganaplacide as a strong candidate to replace ACTs in regions burdened by multidrug-resistant malaria.



Novartis's route to ganaplacide API is shown in **Scheme 1.1**.^{1,2} Its challenging imidazolopiperazine core (**3.4**, or *common intermediate*) is constructed by Pall-Knorr-type heterocycle synthesis, lactamization, and redox manipulation sequence.^a

Scheme 1.1 First-generation route to ganaplacide published by Novartis.^{1,2}

Conversion of **3.4** to ganaplacide API proceeds via amidation with *N*-Boc-glycine, electrophilic aromatic bromination, Buchwald-Hartwig amination with 4-fluoroaniline, and protecting group removal. M4ALL technoeconomic analysis of this approach showed that preparation of the imidazolopiperazine 3.4, in particular, introduced significant raw material cost burden. Key starting materials *N*-Cbz-2,2-dimethylglycine and 2-bromo-4'-fluoroacetophenone are expensive (\$188/kg and \$119/kg, respectively) and potentially difficult to source. Other reagents such as BH₃·THF (\$52/kg), Cs₂CO₃ (\$129/kg) and Pd/C (\$6,630/kg) also negatively impact the total raw material cost (RMC) of this route. With support from the Gates Foundation, the development of a new synthesis pathway to imidazolopiperazine **3.4** from more available KSMs was undertaken to reduce the manufacturing cost and maximize patients' access to ganaplacide (via the ganaplacide–lumefantrine regimen) in low- and middle-income countries.

7

^a The necessity of the *gem*-dimethyl moiety to impart pharmacologic activity negated more concise synthetic approaches such as Groebke-Blackburn-Bienaymé (GBB) reaction used to access structurally similar compounds. ¹⁰



2 Results and Discussion

Scheme 2.1 M4All synthesis of ganaplacide intermediate **3.4**. Yields shown are purity-adjusted.

With the aim to lower the RMC for synthesis of ganaplacide API (**Gan-API**), numerous routes were scouted at M4ALL during 2024-2025. Among them, a synthesis of Novartis advanced intermediate **3.4**, from fluorobenzene **3.0**, was identified as the most promising candidate route to move from process research to process development. The key disconnection in this route is the construction of the fused piperazine by a Pictet-Spengler reaction of a decorated imidazole. Attempts to perform the Pictet-Spengler reaction on **3.3**, immediately following *N*-alkylation (**Scheme 2.1**), produced the undesired annulation regioisomer, *iso-3.4*. Bromination was incorporated as a blocking strategy following *N*-alkylation. The physical properties of **3.3** made it difficult to purify and, moreover, bromination in the presence of a free primary amine was low-yielding, so an *N*-Boc protection/deprotection sequence was incorporated to address these issues. The final, optimized route is shown below. Serendipitously, the blocking group is removed *in situ* – the Pictet-Spengler reaction is accompanied by proto-debromination under the reaction

^b For further information regarding the alternative strategies investigated, please contact us via our website: https://medicines4all.vcu.edu/about/contact/

^c Reversing this step order – i.e., bromination of imidazole followed by *N*-alkylation – gave a reduction in yield and isomeric purity of the N-alkylation step.



conditions to afford desired **3.4** as the major species. The conversion of **3.4** to ganaplacide API has been described; ^{1,2} thus **Scheme 2.1** represents a formal synthesis of ganaplacide API.

The optimized route was demonstrated on a decagram scale, with development efforts captured across five project milestones. These are nominated below, accompanied by key observations:

- Milestone 1 (MS1): Friedel-Crafts acylation of fluorobenzene 3.0 to prepare 3.1
 - o Employing heptane as reaction medium improved safety and ease of operation.
- Milestone 2 (MS2): Bredereck-type imidazole synthesis to prepare 3.2
 - 2-Chloro-4'-fluoroacetophenone was demonstrated to be a viable substrate for imidazole construction, replacing the more expensive 2-bromo-4'fluoroacetophenone.
- Milestone 3 (MS3): Telescopic N-alkylation and Boc-protection to prepare **3.3-Boc**
 - Slow, semi-batch addition of the free-based electrophile afforded reproducible conversion and yield. Recrystallization of 3.3-Boc purged the minor alkylation regioisomer and other process impurities.
- Milestone 4 (MS4): Bromination and HBr-mediated Boc-deprotection to prepare 3.7diHBr
 - Direct crystallization of 3.7-Boc from the bromination reaction mixture afforded
 the compound in consistent purity and yield. Following deprotection, 3.7-diHBr
 was isolated by filtration in high yield and purity without the need for additional
 purification.
- Milestone 5 (MS5): Pictet-Spengler reaction to prepare **3.4**
 - Effective management of Pictet-Spengler regiochemistry generated the desired intermediate 3.4. However, further process development is necessary to achieve optimal yield and purity. Further studies must reconcile 3.4's susceptibility to thermal degradation, once formed (i.e., at reaction temperature). Recommendations are presented in Section 2.5.

Here we present a detailed R&D process development of ganaplacide.



2.1 3.0 to 3.1 (Milestone 1)

2.1.1 Condition screening and optimization

Preparation of **3.1** by Friedel-Crafts acylation of fluorobenzene (PhF) with chloroacetyl chloride is a known transformation in the literature and worked well in M4ALL laboratories. Friedel-Crafts reactions are commonly performed in chlorinated solvents, particularly dichloromethane (DCM). Acknowledging recent EPA policy limiting the use of DCM, laternative conditions were investigated for this transformation (**Table 2.1.1**). Using fluorobenzene as solvent and reagent (i.e., neat process) provided **3.1** in high yield and purity, but significant exotherms and reaction mass heterogeneity were observed (entry 2). Heptane proved an effective medium (entries 3-4). It delivered a uniform suspension throughout the reaction and offered enthalpy management benefits via its relatively higher boiling point (98 °C) and higher specific heat capacity (2.26 J/g·K). e

Entin	ELNINI-	Scale	Equiv	Equiv	Solvent (bp)	Yield ^a		Purity		Comments
Entry	ELN No.	3.0	ClCH ₂ COCl	AlCl ₃	[heat capacity]	Y ieid"	quant ¹ H NMR ^b	LCAP ^c	Wt% assay ^d	Comments
1	NT170- X96	5 g	1.1	1.2	DCM 9V 40 °C 0.96 J/g·K	95%	99%	89.3% ^e	nr ^f	
2	NT170- X99	5 g	1.1	1.2	PhF (neat) 85 °C 1.50 J/g·K	86%	95%	nr	nr	larger exotherm, solid rxn mass
3	KR198- X72	5 g	1.1	1.2	heptane 5V 98 °C 2.26 J/g·K	95%	94%	98.6%	100%	no basic aq wash during workup ^g
4	KR198- X73	36 g	1.0	1.0	heptane 3.5V 98 °C 2.26 J/g·K	84%	98%	99.5%	100%	incomplete conversion ^h

-

^d Heterogeneity and heat transfer issues have been addressed in similar systems by using excess arene; in industrial settings, fluorobenzene economics warrant distillative recovery, purification, and reuse.¹⁴

^e The authors note that heptane could be a suitable solvent for a broader range of Friedel-Crafts reactions. It may be a useful alternative to chlorinated solvents (particularly in academic laboratories) or neat reaction conditions when using an excess of arene is not practical.



"Isolated yield, adjusted for purity. bPurity determined by quantitative ¹H NMR using triphenylmethane or mesitylene internal standard. cLCAP; LC-UV area percent at 254 nm, unless noted otherwise. dHPLC Wt% assay. At 260 nm. fnot recorded. When aq NaHCO₃ wash was excluded from workup, product is contaminated with chloroacetic acid (determined by NMR). With exactly 1.0 equiv of reagents, incomplete consumption of 3.0 was observed, which was removed by rotary evaporation during the workup.

Table 2.1.1 Friedel-Crafts acylation of **3.0** to **3.1**.

Further optimization of the Friedel-Crafts reaction was not pursued, per Sponsor-aligned prioritization of Milestones 3, 4, and 5 for process development. The authors note the following variables for further investigation. Further examination of **3.0**-AlCl₃-heptane slurry temperature during the semi-batch addition of chloroacetyl chloride is recommended, to achieve optimal control of reaction enthalpy and product purity. Study of variable (controlled) rates of chloroacetyl chloride addition is recommended, in the same context. Preliminary investigation of stoichiometry – e.g., equimolar amounts of AlCl₃ and chloroacetyl chloride, relative to **3.0** – showed incomplete consumption of starting material but a favorable reaction profile (entry 4; **Table 2.1.1**). Further analysis of reactant stoichiometry (1.0–1.1 equiv AlCl₃; 1.0–1.05 equiv chloroacetyl chloride) is warranted. Thus, the partially optimized reaction conditions are as follows. A detailed procedure for a decagram-scale reaction is in the Supporting Information.

- A Friedel-Crafts acylation was performed using **3.0** (1 equiv), chloroacetyl chloride (1 equiv), and AlCl₃ (1 equiv) in heptane (3.5 V) at 0–15 °C for 1 h. This afforded **3.1** in >90 A% (254 nm).
- Unconsumed 3.0 was observed in <10 A% (254 nm) and was purged during the workup.

2.1.2 Practical workup and purification for scalability

Per the aforementioned prioritization of Milestones 3-5 for process optimization, further workup and purification process development is recommended. A detailed procedure for a decagram-scale reaction is in the Supporting Information.



• The cooled reaction mass (0-5 °C) was cautiously quenched with 0.5 M HCl (8V) and diluted with EtOAc. The organic phase was washed with sat. aq. NaHCO₃. Solvent evaporation afforded **3.1** as a white solid in >98 A% (254 nm).

2.2 3.1 to 3.2 (Milestone 2)

2.2.1 Condition screening and optimization

Preparation of **3.2** from 2-bromo-4'-fluoroacetophenone is a known transformation with a reported 45% isolated yield. M4ALL demonstrated that chloroacetophenone **3.1** was a similarly viable substrate, consistently providing **3.2** in comparable yield and purity under the reported conditions (**Table 2.2.1**). RMC reduction via chloroacetophenone **3.1**'s intermediacy, rather than its bromine analogue 2-bromo-4'-acetophenone, was affirmed. Further optimization of the Bredereck reaction was not pursued, per Sponsor-aligned prioritization of Milestones 3, 4, and 5 for process development. Thus, partially optimized reaction conditions are as follows. A detailed procedure for a decagram-scale reaction is in the Supporting Information.

• Bredereck imidazole synthesis was performed using **3.1** (1 equiv), formamide (12 equiv), and water (2 equiv) at 125–140 °C for at least 4 h. This afforded **3.2** in >85 A% (254 nm).

Entry	ELN No.	Cools 2.1	Toma	Time	IPC LCAP ^a of 3.2	Isolated 3.2				
Entry	ELN NO.	Scale 3.1	Temp	Time	IPC LCAP" 01 3.2	$LCAP^a$	wt% Purity ^b	Yield ^c		
1	BCH199-X44	10 g	140 °C	24 hr	90% (24 hr)	94%	86%	49%		
2	RS171-X75	10 g	125 °C	22 hr	88% (22 hr)	94%	89%	44%		
3	KR198-X74	10 g	125 °C	24 hr	88% (20 hr)	95%	84%	50%		
4	PVK201-X65	50 g	140 °C	6 hr	85% (4 hr)	94%	91%	52%		
5	KR198-X78	50 g	125 °C	6 hr	85% (6 hr)	95%	91%	52%		

^aAt 254 nm; ^bDetermined by quantitative ¹H NMR with respect to internal standard (triphenylmethane or mesitylene); ^cYield shown is corrected for NMR purity.

Table 2.2.1 Bredereck imidazole synthesis of **3.2**.



Conversion of **3.1** to **3.2** is a dynamic process, with characteristics worth noting in the context of scale-up preparation. In-process assays (HPLC-UV) showed a complex medium, comprising numerous intermediates. Bredereck imidazole synthesis involves numerous mechanistic steps, beginning with the hydrolysis of formamide to generate ammonium formate (**Figure 2.2.1**). Substitution of the chlorine atom of **3.1** generated a discrete phenacyl formate ester intermediate, which was present in high concentration as the major species within the first 20 minutes of the reaction (**Figure 2.2.2**). The intermediate ester (retention time 6.3 min; see ADR Section 2.2.2) was consumed within 45-60 minutes, giving way to several downstream intermediates. Intermediates converged to **3.2** as the major species after 1-2 hours of reaction time. **3.2** reached its maximum conversion (85-90 A% at 254 nm) after 4-6 hours of reaction time. Extended reaction duration (12-24 hours) neither increased **3.2** conversion nor proved detrimental to **3.2** (**Table 2.2.1**). Further analysis of reactant stoichiometry (1-3 equiv water; 6-12 equiv formamide) and temperature (80–140 °C) are warranted, in view of the data collected so far and the reports found in the peer-reviewed literature. ^{15,17–20}

Figure 2.2.1 Plausible mechanism for conversion of **3.1** to **3.2** based on analogous reports. ¹⁶ Not all discrete intermediates nor by-products are shown.

13

^f The identity of this compound was confirmed by independent synthesis (see appendix).

^g One of these intermediates is the phenacyl alcohol - the hydrolysis product of the phenacyl formate. Further details are available in the analytical development report (ADR).



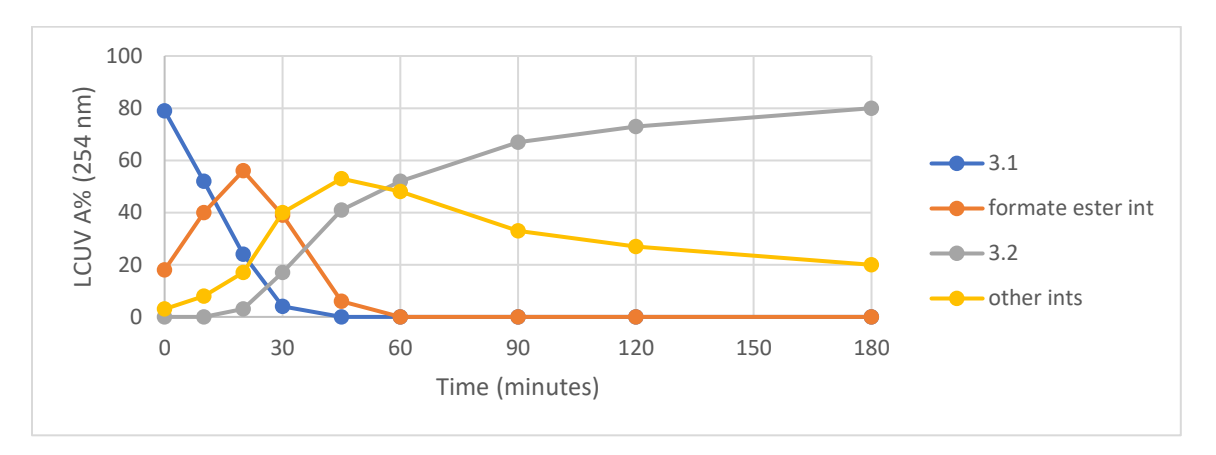


Figure 2.2.2 Typical profile of **3.1** to **3.2** during the first 3 hours of reaction.

2.2.2 Practical workup and purification for scalability

Upon optimal conversion to **3.2**, per LC-UV in process assay, the product mixture was cooled to 20-25 °C, diluted with water (10V), then filtered to remove insoluble impurities.^h The acidic filtrate was adjusted to pH 12 with aqueous NaOH, prompting precipitation of imidazole **3.2** which was collected by vacuum filtration and dried. This procedure afforded **3.2** with consistent yield (44-52%, purity-adjusted) and purity (84-91 wt% by quantitative ¹H NMR).^{i,j}

Per the aforementioned prioritization of Milestones 3-5 for process optimization, further workup and purification process development is recommended. The authors suggest further analysis of the volume of water used (including aqueous NaOH) in order to maximize recovery of 3.2 and minimize losses to the aqueous phase. The partially optimized isolation conditions are as follows. A detailed procedure for a decagram-scale reaction is in the Supporting Information.

• Upon optimal conversion to 3.2, per LC-UV in process assay, the product mixture was cooled to 25 °C then diluted with water (5V). Insoluble impurities were removed by

^h Insoluble impurities consisted of dark orange, tacky, amorphous solids. Analysis by LC and NMR revealed a complex mixture of species which have not been unequivocally identified.

¹ Product losses to the aqueous phase were observed; extraction of the aqueous phase yielded an additional 5-10% of **3.2** albeit with lower purity.

^j Compound **3.2** is also available from a number of commercial suppliers.

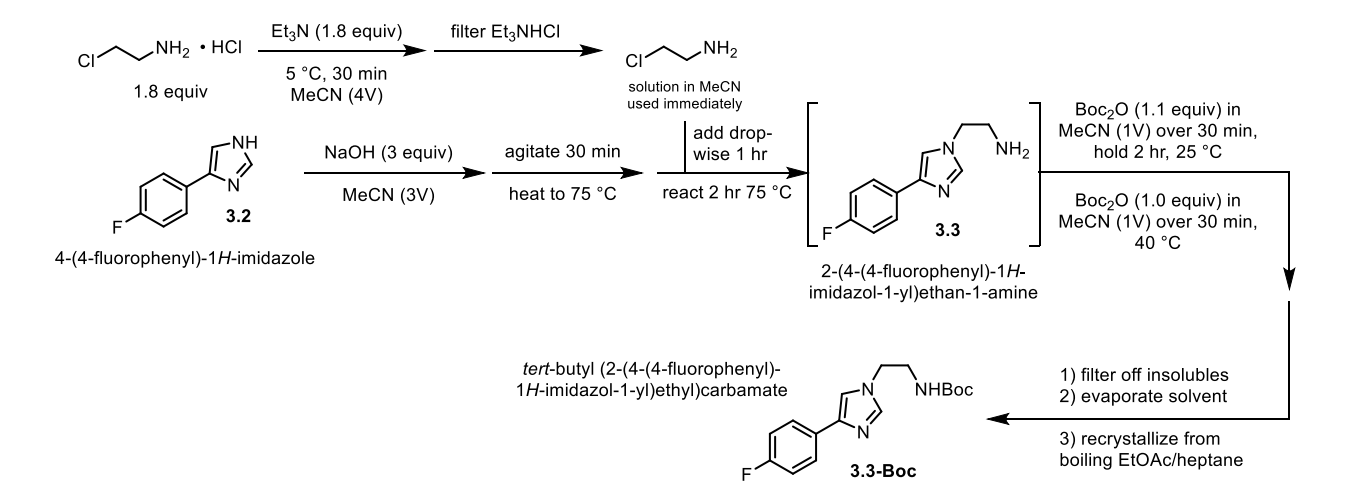


vacuum filtration. The filtrate was adjusted to pH 12 by the addition of 10% (w/w) aqueous NaOH (7.5V). The resulting yellow precipitate (**3.2**) was collected by vacuum filtration and dried at 50 °C.

• Optional recrystallization procedure: **3.2** was dissolved in boiling ethyl acetate (3V), hot filtered, diluted with heptanes (3V) then cooled slowly to induce crystallization. Modest recovery (43%) and excellent purity (100 wt% by quantitative ¹H NMR) were observed.

2.3 3.2 to 3.3 and 3.3 to 3.3-Boc (Milestone 3)

Synthesis of tert-butyl (2-(4-(4-fluorophenyl)-1*H*-imidazol-1-yl)ethyl)carbamate (**3.3-Boc**) is carried out in two steps, starting from 4-(4-fluorophenyl)-1H-imidazole (**3.2**). First, imidazole **3.2** is *N*-alkylated with 2-chloroethylamine to afford 2-(4-(4-fluorophenyl)-1H-imidazol-1-yl)ethan-1-amine (**3.3**). Then, the primary amine **3.3** is Boc protected to yield solid **3.3-Boc**. The crude product is recrystallized from an ethyl acetate—heptane mixed solvent system to purge the minor alkylation regioisomer and other process impurities, affording **3.3-Boc** in high purity (**Scheme 2.3.1**). Development efforts for individual *N*-alkylation and Boc protection reaction steps, **3.3-Boc** workup and purification, and safety assessment of the process are summarized below.



Scheme 2.3.1 M4All telescoped process for **3.3-Boc** synthesis.



Condition screening and optimization

Conditions for the conversion of 3.2 to 3.3 were adapted from a patent describing the alkylation of similar compounds.²¹ In the present application, a mixture of **3.2**, NaOH (4 equiv), 2-chloroethylamine (CEA) hydrochloride (1.1 equiv), and phase-transfer catalyst n-Bu₄N⁺HSO₄⁻ (5 mol%) in acetonitrile (8V), maintained at elevated temperature, afforded 3.3 in an isolated yield of 46% after chromatography (**Table 2.3.1**, entry 1). To improve yield and throughput, several variables – base, solvent, alkylating agent, phase transfer catalyst (PTC; presence or absence), reaction time and temperature – were assessed (**Table 2.3.1**).¹

//	FININI	CEA	D	PTC	G 1	Temp	Time ^a	LC.	AP^b	Isolated
#	ELN No.	equiv	Base	mol%	Solvent	(°C)	(hr)	3.2	3.3	yield ^c
1	KR198-X14	1.1	NaOH (4 eq)	5%	MeCN (8V)	75	42	29^{d}	71^{d}	46%
2	PVK201-X16a	1.1	NaOH (4 eq)	-	MeCN (20V)	75	20	30^{e}	65 ^e	-
3	PVK201-X16b	1.1	NaH (4 eq)	-	DMF (20V)	75	20	100^{e}	0^e	-
4	PVK201-X16c	1.1	K ₂ CO ₃ (4 eq)	-	DMF (20V)	75	20	93 ^e	5^e	-
5	PVK201-X16d	1.3	NaOH (4 eq)	5%	MeCN (20V)	75	20	25^e	70^{e}	-
6	PVK201-X16e	1.3	NaOH (4 eq)	-	MeCN (20V)	75	20	30^{e}	70^{e}	-
7	PVK201-X17	1.5	NaOH (4 eq)	5%	MeCN (10V)	75	68	8^d	92^{d}	78%
8	PVK201-X18	1.8	NaOH (4 eq)	5%	MeCN (10V)	75	24	4^d	96 ^d	89%
9	NT170-X100	1.8	NaOH (4 eq)	5%	MeCN (15V)	75	6	8 ^f	86 ^f	79%
10	PS169-X91	1.2	NaOH (2 eq)	5%	THF (10V)	65	16	72	17	1
11	PS169-X91	1.2	NaOH (2 eq)	5%	Toluene (10V)	110	16	63	25	1
12	PS169-X92	1.2	NaOH (2 eq)	5%	MeCN (10V)	25	3	98	2	1
13	PS169-X92	1.2	NaOH (2 eq)	5%	MeCN (10V)	54	3	87	13	1
14	PS169-X92	1.2	NaOH (2 eq)	5%	MeCN (10V)	75	3	77	23	1
15	PS169-X97	1.8	NaOH (4 eq)	-	Dioxane:H ₂ O 1:2 (16V)	90	22	92	4	1
16	PS169-X98	1.8^{g}	-	-	Dioxane:H ₂ O 1:1 (14V)	90	22	67	22	-
17	PS169-X99a	2^g	-	5%	MeCN:H ₂ O 9:1 (15V)	75	22	70	19	-
18	PS169-X99b	2^g	NaHCO ₃ (4 eq)	5%	MeCN:H ₂ O 9:1 (15V)	75	22	81	10	-
19	PS169-X99c	2^g	NaHCO ₃ (4 eq)	5%	Dioxane:H ₂ O 9:1 (15V)	90	22	85	5	-
20	PS169-X100a	1.8	NaHCO ₃ (2 eq)	5%	MeCN (20V)	80	13	89	5	1
21	PS169-X101	1.8^{h}	NaOH (4 eq)	5%	MeCN (20V)	80	22	7	88	-
22	PS169-X106	1.8	NaOH (4 eq)	5%	MeCN:H ₂ O 2:1 (15V)	80	6	93	5	-
23	PS169-X107	1.8^{i}	NaOH (4 eq)	5%	MeCN:EtOH 3:2 (10V)	75	6	58	39	-

^k Compound **3.3** is a viscous oil and could only be purified by chromatography on screening scales.

¹ In the case of base, alkylating agents, and phase transfer catalyst, stoichiometry was also examined as a variable.



^aOverall maintenance time shown. In most cases, the maximum level of conversion was reached much earlier and did not change appreciably over time. ^bLCAP; LC-UV area percent at 254 nm unless otherwise noted. ^cYields shown are after chromatography. Most experiments were not isolated due to small scale. ^dGCMS TIC A% shown. ^eLC-UV area percent at 210 nm. ^fLC-UV area percent at 260 nm. ^gBEA used in place of CEA. ^hCEA and NaOH added in 3 lots at regular intervals. ⁱCEA added as an ethanolic solution in 3 lots at regular intervals.

Table 2.3.1: *N*-alkylation of **3.2** with CEA hydrochloride: conditions screening. All reactions conducted on small scale (1 gram or less).

Optimal *N*-alkylation results (conversion of **3.2** to **3.3**) were primarily driven by base and solvent selection, and by alkylating agent loading. Sodium hydroxide and acetonitrile proved most effective (entries 7-9, 21; **Table 2.3.1**). Other bases and solvents afforded little conversion (entries 3-4, 10-11, 18-20, 23-24). Exclusion of the phase-transfer catalyst had minimal impact on the reaction (entries 1-2, 5-6). Further to this observation, semi-aqueous reaction media were investigated (entries 15-19, 22-23). Hypothesized improvements via reaction homogeneity, or liquid-liquid rather than liquid-solid phase transfer, were negated by little to no conversion. Increasing the loading of CEA hydrochloride improved the conversion (entries 5-8) although stalling was observed. Decreasing the loading of NaOH from 4 to 2 equiv was detrimental (entries 10-14). Using 2-bromoethylamine (BEA) hydrobromide in place of CEA offered no benefit (entries 16-19). For early material generation campaigns (**Table 2.3.2**), the conditions identified in entry 8 were employed: NaOH (4.0 equiv) and CEA hydrochloride (1.8 equiv) with or without phase-transfer catalyst in acetonitrile, and subsequent heating of the heterogeneous mixture.

M4ALL operators observed reaction stalling at variable levels of conversion (Table 2.3.2) throughout process optimization (inclusive material generation). Extended reaction times did not offer improvement. Additional charges of CEA hydrochloride intermittently improved conversion. Pathways for unproductive CEA consumption have not been confirmed. Unimolecular oligomerization of CEA is suspected, acknowledging improved imidazole alkylation performance via semi-batch addition (entry 21, **Table 2.3.1**). In this instance, wherein CEA concentration is limited (vs. batch addition), the rate of unimolecular *N*-alkylation is likely reduced.



E.	FINA	6 1	PTC	TE: a	LC.	AP^b	G G	V: 11d	q ¹H NMR
Entry	ELN No.	Scale	mol %	Time ^a	3.2	3.3	Conv ^c	Yield ^d	Purity ^e
1	PVK201-X22	9 g	5%	36 hr	21% ^f	77% ^f	79%	66%	nr
2	PVK201-X34 10 g 5% 18 hr		18 hr	1% ^f	96% ^f	99%	77%	66%	
3	3 PVK201-X40 10 g 5%		22 hr	10% ^g	82% ^g	89%	91%	58%	
4	NT170-X101 5 g 5% 4 hr 5% 93%		93%	95%	68%	72%			
5	NT170-X104	27 g	5%	24 hr	22%	70%	76%	75%	80%
6	PVK201-X68	20 g	-	17 hr	17%	67%	80%	76%	56%
7	NT170-X117A	25 g	5%	2 hr	46%	39%	46%	nr	nr
8	NT170-X117B	25 g	5%	1 hr	<1%	86%	99%	89%	62%
9	NT170-X118	25 g	5%	24 hr	19%	72%	79%	88%	80%
10	NT170-X121	50 g	-	17 hr	19%	68%	78%	74%	56%
11	NT170-X131	22 g	-	4 hr	23%	74%	76%	84%	61%
12	PS169-X94	4 g	5%	22 hr	18%	73%	80%	61%	50%
13	PS169-X104	10 g	5%	6 hr	22%	67%	75%	nr	nr
14	PS169-X105	10 g	5%	6 hr	21%	75%	78%	nr	nr

^aOverall maintenance time shown. In most cases, the maximum level of conversion was reached much earlier and did not change appreciably over time. ^bAt 254 nm. ^cConversion = (LCAP **3.3**)/(LCAP **3.2** + **3.3**) ^dCrude yield, adjusted for purity. ^eDetermined by quantitative ¹H NMR, not validated by HPLC wt% assay. ^fGCMS TIC A% rather than LCAP. ^gLCAP at 260 nm.

Table 2.3.2 Reproducibility of alkylation of **3.2**. All reagents are charged to the vessel at once in single lots. The vessel is heated to 75 °C and maintained for several hours.

M4ALL hypothesized that maintaining a low concentration of CEA *in situ* by semi-batch addition over a longer time period would prove beneficial. Entry 21 (**Table 2.3.1**) supported this hypothesis: When 1.8 equiv of CEA hydrochloride were charged in three lots at regular intervals, rather than in one portion, reaction conversion improved to 94%. Reliably controlled dosing of solid CEA hydrochloride was anticipated to be problematic on scale, and the reagent's insolubility in acetonitrile prevented its addition as a solution.^m Literature precedent exists for similar imidazole alkylations using CEA – rather than its hydrochloride salt – added as a solution in

^m CEA hydrochloride is soluble in polar protic solvents like water and ethanol which were found to be unsuitable for this reaction, Table 2.3.1, entries 22-24.



acetonitrile.²² The solution is prepared by treating CEA hydrochloride with an equimolar amount of triethylamine and filtering off the incipient triethylamine hydrochloride. The resulting solution of CEA in acetonitrile must be used promptly after preparation. The concentration of CEA drops by ~2% every hour (**Figure 2.3.2**) as the compound slowly oligomerizes and precipitates out of solution, presumably as polyethyleneimine poly(hydrochloride).

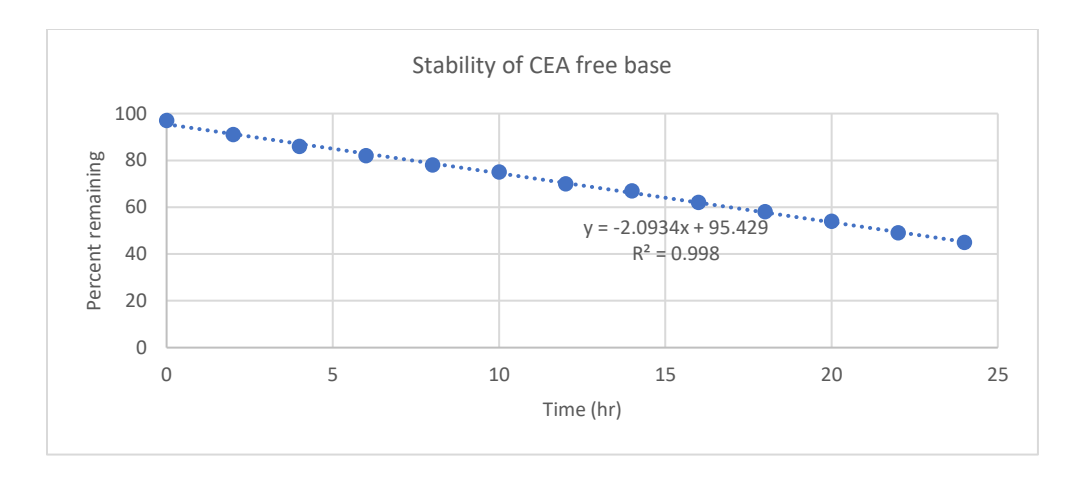


Figure 2.3.2 Stability study of CEA free base (solution in acetonitrile). Reagent concentration was measured every 2 hours by comparing ¹H NMR integral against an internal standard.

In the new baseline experiment, CEA hydrochloride (1.5 eq) was treated with Et₃N (1.5 eq) at 5 °C for 1h to obtain the free base CEA, which was added to a mixture of **3.2** and NaOH (3 eq) at 75 °C over 30 minutes. After completing the addition, the reaction was maintained at 75 °C for several hours. A maximum of 69 LCAP of **3.3** (at 254 nm) was observed after 2h which did not change with longer reaction times. (**Table 2.3.3** entry 1) This procedure was repeated twice more, varying CEA addition time to 60 min (entry 2) and 120 min (entry 3). 60-min addition delivered the best conversion (80 LCAP of **3.3** at 254 nm). Increasing CEA loading from 1.5 to 1.8 equiv (entry 4) further improved conversion (87 LCAP of **3.3** at 254 nm). The alkylation procedure was replicated several times on different scales (entries 4-8) and delivered consistent conversion. Residual **3.2** (~10-15 LCAP at 254 nm) did not impede the subsequent Boc protection and was purged during **3.3-Boc** crystallization. Controlled semi-batch addition of CEA improved



the robustness and reproducibility of this process (**Figure 2.3.3**). Thus, optimized conditions for the alkylation of **3.2**, giving **3.3**, are as follows:

- Triethylamine (1.8 equiv) was added to a suspension of CEA hydrochloride (1.8 equiv) in acetonitrile (4V). Filtration of Et₃N·HCl afforded a solution of CEA in acetonitrile.
- The solution of CEA in acetonitrile was added over 60 minutes to a suspension of **3.2** (1.0 equiv) and NaOH (3.0 equiv) in acetonitrile (3V) at 75 °C.
- The reaction was maintained at 75 °C for 2 hours (>85 LCAP **3.3**, <15 LCAP **3.2**) before proceeding to the Boc protection step.

Enter	ELN No.	3.2 Source	Scale	CEA	CEA addition	LCAP	A% a	Conversion ^b
Entry	ELN NO.	3.2 Source	Scale	equiv	time	3.2	3.3	Conversion
1	KR198-X92	Combi-Blocks ^c 10		1.5	30 min	29%	69%	70%
2	KR198-X94	Combi-Blocks	10 g	1.5	60 min	16%	80%	83%
3	KR198-X95	Combi-Blocks	7 g	1.5	120 min	25%	73%	74%
4	KR198-X96	Combi-Blocks	5 g	1.8	60 min	11%	87%	89%
5	KR198-X102	$M4ALL^d$	7 g	1.8	60 min	10%	90%	90%
6	PS169-X114	Combi-Blocks	10 g	1.8	60 min	17%	82%	83%
7	KR198-X104	M4ALL	13 g	1.8	60 min	14%	85%	86%
8	KR198-X106	Combi-Blocks	40 g	1.8	60 min	10%	88%	90%

^aLCAP (254 nm) measured 2-4 hours after addition was completed. ^bConversion = (LCAP **3.3**)/(LCAP **3.2** + **3.3**). ^c98.7 wt% (by LC-UV assay). ^d99.4 wt% purity (by LC-UV assay), purified by recrystallization.

Table 2.3.3: Reaction of **3.2** with CEA (MeCN solution): optimization & reproducibility.

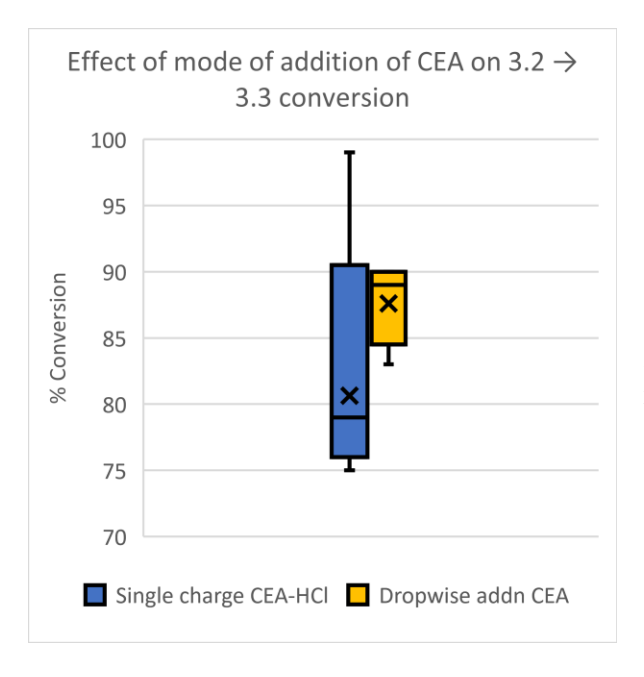


Figure 2.3.3 Blue: distribution of observed reaction conversions when CEA hydrochloride is charged as a single lot. n=14 (from **Table 2.3.2**), median 79%, mean 81%. Yellow: distribution of observed reaction conversions when CEA solution in acetonitrile is added dropwise. n=5 (from **Table 2.3.3**, entries 4-8), median 89%, mean 88%.



With optimized *N*-alkylation conditions, attention turned to Boc protection of **3.3**. In the transition from route scouting to optimization, development of a simple workup and purification strategy was prioritized.ⁿ The authors hypothesized that if Boc protection could proceed in MeCN rather than MeOH, telescoped access to **3.3-Boc** – a solid, suitable for crystallization – could be achieved. In practice, Boc protection proceeded equally well in acetonitrile. Furthermore, filtration between alkylation and Boc protection steps was found to be unnecessary. The presence or absence of NaOH and other insoluble matter had no effect on the outcome of the Boc protection chemistry.^o In the optimized process, once the alkylation step reached its maximum conversion (~90 LCAP of **3.3** at 254 nm, usually within 2 hours), the system was cooled to 25 °C and a concentrated solution of Boc₂O in acetonitrile was added over 30 minutes.

In the telescopic process, 1.1 equiv of Boc₂O was not sufficient for full conversion to **3.3-Boc** and a second charge was generally required (such that a total of 2 equiv were added). Putative byproducts of CEA consumption have amino groups which may competitively consume Boc₂O; the molar quantity of amine functionality was anticipated to be commensurate with the CEA from which it is derived. Boc₂O was added in equimolar amounts to achieve full conversion of **3.3** to **3.3-Boc**. Notably, the telescoped reaction mixture increased in viscosity upon Boc₂O addition and was not satisfactorily stirred by propeller or paddle agitators. Anchor or helical agitators are recommended but have not been investigated in M4ALL laboratories. Once a sufficient quantity of Boc₂O was charged, the reaction completed quickly at 25 °C. The reaction mixture was then filtered and concentrated to afford crude **3.3-Boc**.

2.3.2 Practical workup and purification for scalability

Regioselectivity of *N*-alkylation was consistently ~10:1 across a variety of conditions screened. Compounds **3.3** and *iso-***3.3** co-eluted on normal phase flash chromatography and reverse

ⁿ During route scouting, the *N*-alkylation product mixture was filtered (to remove NaOH and other insoluble components) then concentrated to afford crude **3.3**. **3.3** was purified by chromatographed, dissolved in methanol then treated with Boc₂O to afford **3.3-Boc**.

^o Allowing particulate matter to persist into the Boc protection influenced purification strategy. See Section 2.3.2.

^p Further to this hypothesis, when 3.3 is first purified by chromatography, 1.1 equiv of Boc₂O is sufficient (suspected amine-containing byproducts are removed, negating further stoichiometric excess of Boc₂O).



phase HPLC, but were readily differentiated by ¹H NMR (Figure 2.3.1) and GC retention time. Refer to Section 4.1 for a discussion on how isomerically pure standards of **3.3** and *iso-3.3* were obtained. Compounds **3.3-Boc** and *iso-3.3-Boc* were likewise inseparable by liquid phase chromatography. Developing a purification process for **3.3-Boc** relying on crystallization, which could purge the undesired *iso-3.3-Boc*, was of paramount importance. Two methods for isolating and purifying 3.3-Boc were identified, summarized in Sections 2.3.2.1 and 2.3.2.2.

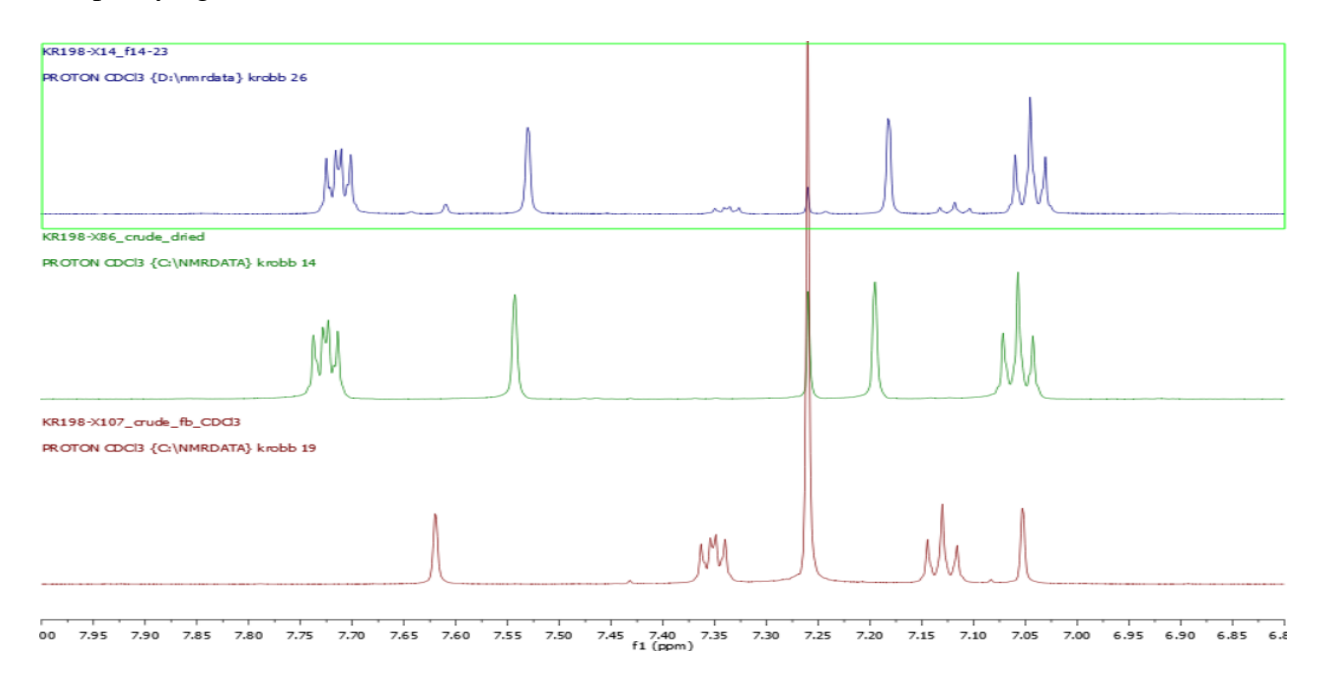


Figure 2.3.1 ¹H NMR spectra (aromatic detail) of **3.3**. Top: appearance after chromatographic purification, showing ~10:1 isomeric ratio; Middle: isomerically pure **3.3**; Bottom: isomerically pure *iso-3.3*. Refer to Section 4 for complete ¹H and ¹³C NMR spectra.

2.3.2.1 Ethyl acetate – heptane crystallization (solvent swap) (Method A)

Upon complete Boc protection of **3.3** (LC-UV), the reaction medium was filtered (glass frit, medium porosity) to remove insoluble matter then concentrated *in vacuo*. Crude **3.3-Boc** was dissolved in a minimal amount of ethyl acetate (EA; 1V) pre-warmed near its boiling point (bp 77 °C). Heptane (2V, bp 98 °C) was then added and the resulting solution allowed to cool (20-30 °C/hr) without stirring. The resultant crystals were isolated by vacuum filtration. The minor *N*-



alkylation regioisomer (*iso-3.3-Boc*) and other process impurities from the telescopic sequence were successfully purged (**Figure 2.3.1**). Recovery improved with increasing scale. Isolated yields greater than 50% (relative to input of **3.3**) were consistently achieved (**Table 2.3.4**, entries 1-3), in consistently high purity.

During process development, acetonitrile was removed by rotary evaporation and crude **3.3-Boc** isolated as a solid before enacting the ethyl acetate-heptane crystallization. A solvent swap procedure will be required in the manufacturing environment. Distillative removal of acetonitrile (bp 82 °C), chasing with ethyl acetate (bp 77 °C) is recommended. Ethyl acetate and acetonitrile form azeotropic mixtures which can facilitate the solvent switch (e.g., an azeotropic bp of 75 °C is reported from a 23 wt% EA – 77 wt% heptane mixture).²³ Alternatively, chasing with heptane (bp 98 °C), which is zeotropic relative to acetonitrile, could be advantageous. Adjusting to 3 volumes 1:2 EA-heptane (by volume) versus **3.3-Boc** and proceeding as previously described is anticipated to deliver comparable outcomes in yield and purity.

2.3.2.2 Direct crystallization and isolation (Method B)

Confirming acetonitrile as a viable replacement for methanol in Boc protection of **3.3** allowed for the direct crystallization and isolation of **3.3-Boc**.^q Once full conversion was achieved, distillation of acetonitrile to ~50% of its original reactor volume (i.e., 5V removed from the initial 10V) then cooling the medium to 0-5 °C caused **3.3-Boc** to crystallize from the reaction mixture, directly. Product purity and yield data were comparable to those observed via ethyl acetate-heptane recrystallization (**Table 2.3.4**, entries 4-6). As with the solvent swap approach in Section 2.3.2.1, a homogenous reaction was required. Insoluble matter (e.g., NaOH) was filtered after the alkylation step and prior to the Boc protection step (although filtration could also be performed after the Boc protection step, as in Method A).^r

^q 3.3-Boc's solubility in acetonitrile is poorer than in methanol. The extent of the differential was not quantified.

As discussed earlier, the presence or absence of NaOH had no bearing on the Boc protection.



Isolation Method A:

- 1) filter off insolubles
- 2) evaporate solvent
- 3) recrystallize from EtOAc/hexane

Isolation Method B:

- 1) concentrate to 50% of initial volume
- 2) cool & collect precipitate

Entry	ELN No.	Input	3.3 ^a	Solvent	Isolation	Output 3.3-Boc			
Entry	ELN NO.	Amount	Purity ^b	Solvelli	Isolation	$LCAP^c$	Purity ^b	Yield	
1	KR198-X50	5.0 g	80%	MeOH	A	nr	100%	2.5 g (42%)	
2	PVK201-X42	8.4 g	58%	MeOH	A	nr	100%	5.2 g (71%)	
3	NT170-X103	7.0 g	72%	MeOH	A	97%	100%	3.9 g (51%)	
4	BCH199-X56	49.0 g	60%	MeCN	В	99.9%	95.2% ^d	24.5 g (58%)	
5	BCH199-X59A	6.5 g	61%	MeCN	В	99.7%	101% ^d	3.4 g (57%)	
6	BCH1990X59B	6.5 g	61%	MeCN	B^e	99.9%	102% ^d	2.5 g (44%)	

3.3-Boc

Table 2.3.4. Isolation of crystalline **3.3-Boc** after conclusion of **3.3** \rightarrow **3.3-Boc** reaction.

Boc₂O (1.1 - 1.6 equiv)

Solvent, 25 °C, 1 hr

then A or B

Results for three trials of the fully telescoped process, leveraging Method A, are summarized in **Table 2.3.5**. Imidazole *N*-alkylation conditions were optimized, with reproducible conversion achieved (refer back to **Table 2.3.3**). The telescoped process afforded **3.3-Boc** in consistently high purity (>98 wt% assay) with variable yields (41-59% over 2 steps from **3.2**). Quantitative analysis of the recrystallization mother liquors revealed residual amounts of **3.3-Boc**, between 10-25% of the theoretical yield. The combined yield of **3.3-Boc** (isolated and residual in ML) is as high as 71-74% of theoretical (**Table 2.3.5** entries 2-3). In view of the available performance gains, further optimization of the Boc protection-crystallization sequence is recommended. Section 4.1 discusses details and proposed strategies.

Entry	ELN	3.2	Scale	Isolate	d, crysta	lline 3.3-Boc	Mother Liquor dissolved 3.3-Boc			
Entry	No.	Source	3.2	$LCAP^b$	Wt%	Yield	$LCAP^b$	Conc assay	Yield	

^a3.3 used here was free of NaOH and other insoluble impurities. ^bPurity determined by quantitative ¹H NMR. ^cAt 254 nm. ^dPurity determined by LC wt% assay. ^eReaction mass was distilled to ~70% of initial volume and diluted with heptane antisolvent.



1	KR198- X102 ^a	M4ALL ^c	7 g	99.0%	98%	5.45 g (41%)	41.6%	12.2 mg/mL 110 mL	1.34 g (10%)
2	KR198- X104	M4ALL ^c	13 g	99.8%	100%	14.40 g (59%)	50.1%	11.9 mg/mL 255 mL	3.05 g (12%)
3	KR198- X106	Combi- Blocks ^d	40 g	99.8%	101%	37.28 g (49%)	62.4%	22.5 mg/mL 820 mL ^e	18.5 g (25%)

^aThis reaction was run with only 1.4 equiv of Boc₂O, and afterwards the mixture was concentrated and the residue partitioned between EtOAc and water (traditional workup). Analysis of the crude **3.3-Boc** revealed some residual **3.3**. ^bAt 254 nm. ^c99.4 wt% (by LC-UV assay), purified by recrystallization. ^d98.7 wt% purity (by LC-UV assay). ^eLoss to the ML was more severe on this scale, which may be due to incomplete acetonitrile removal in the isolation of crude **3.3-Boc**.

Table 2.3.5. Telescoped process for $3.2 \rightarrow 3.3 \rightarrow 3.3$ -Boc.

2.3.3 Safety assessment of the process

Safety assessment of a chemical process is crucial to determine its suitability for scale-up. Reaction calorimetry provides critical insights by measuring the heat evolved or absorbed during a reaction, including parameters such as adiabatic temperature rise (ΔT_{ad}) and maximum temperature of synthesis reaction (MTSR). Among calorimetric techniques, heat flow calorimetry (HFCal) is particularly valuable as it closely mimics the plant-scale operations. In HFCal, a circulation system maintains isothermal conditions by removing heat at the same rate as it evolves during the reaction. To support safe scale-up, we conducted a comprehensive reaction calorimetry study using Mettler-Toledo EasyMax 102 system. This study measured ΔT_{ad} and MTSR for each step of Milestone 3, providing a detailed thermal assessment of the telescoped process.

Four discrete operations were evaluated: 1) neutralization of CEA hydrochloride with triethylamine, 2) addition of NaOH to **3.2**, 3) dosing of CEA solution, and 4) dosing of Boc₂O solution.

1) The addition of triethylamine to CEA hydrochloride was found to be minimally exothermic, even when conducted at a rapid pace (5-minute dosing time) at 20 °C. Total heat of reaction (ΔH_r) of 3.6 kJ/mol was observed, with an MTSR of 24.6 °C ($\Delta T_{ad} = 1.7$ °C) which is below the boiling point of the solvent (MeCN, 81.6 °C). Maximum reaction temperature (MRT), representing the peak temperature reached during the process step, was recorded at 23.4 °C. Maximum heat generation (MHG) during the addition was measured at 2.1 W. Based on standard



reactor cooling capacity thresholds – Low severity: ΔT_{ad} <50 °C and MHG <30 W; Medium: ΔT_{ad} 50-200 °C; High: ΔT_{ad} >200 °C and MHG >30 W) – the step is classified as low severity, indicating minimal thermal hazard.

For the next three operations, reaction calorimetric analysis was conducted using 13 g of 3.2 in a 100 mL vessel. ΔH calculations, based on the moles of 3.2, are summarized in **Table 3.2.6**.

- 2) Batch addition of NaOH to a suspension of **3.2** in acetonitrile at 25 °C was found to be minimally exothermic, with a total heat of the reaction (ΔH_r) of 12.5 kJ/mol. Maximum attainable temperature (MAT) was determined to be 30.8 °C (ΔT_{ad} = 2.8 °C) which is below the boiling point of the reaction solvent acetonitrile (81.6 °C), indicating a low risk of solvent boiling under cooling failure. MRT was recorded at 30.5 °C and the MHG during the addition was measured at 6.4 W. Based on prototypical reactor cooling capacity, the severity is considered low for the addition of NaOH.
- 3) Semi-batch (dropwise) addition of CEA solution (25 °C) to the reaction mass (60 °C), over one hour, was found to be minimally exothermic. Total ΔH_r was found to be 1.48 kJ/mol and MAT was observed to be 63.7 °C ($\Delta T_{ad} = 0.7$ °C) which is lower than the boiling point of the reaction solvent. MRT of 63.1 °C and MHG of -1.0 W were observed during the addition. Based on prototypical reactor cooling capacity, the severity is considered low for the addition of chloroethylamine.

While the transient intermediacy of aziridine (ethylenimine) is suspected, ²⁴ efforts to trap and observe this species during the reaction were unsuccessful.

4) Semi-batch (dropwise) addition of Boc_2O solution over 30 minutes to the reaction mass (25 °C) was found to be modestly exothermic. Total ΔH_r was found to be 7.36 kJ/mol and the maximum temperature of synthesis reaction (MTSR) was determined to be 34.7 °C ($\Delta T_{ad} = 25.8$ °C) which is lower than the boiling point of the reaction solvent. MAT was 53.8 °C; higher, but still lower than the boiling point of the solvent. MRT of 29.8 °C and MHG of 6.9 W were observed

-

^s When this aspect of the process was assessed at 75 °C, reaction enthalpy was not accurately captured. The authors postulate this is likely due to competitive heat of vaporization of solvent. Therefore, the alkylation safety assessment was instead conducted at 60 °C.



during the addition. Based on prototypical reactor cooling capacity, the severity is considered low for the addition of Boc₂O.

Process	ΔH_{r}	ΔH_{r}	ΔH_{r}	ΔT_{ad}	MTSR	MRT	MHG	C _p (J/	(g K)	U (W/	m ² K)
Step	(kJ)	(kJ/g)	(kJ/mol)	(°C)	(°C)	(°C)	(W)	Before	After	Before	After
1^a	0.41	0.031	3.6	1.67	24.6	23.4	2.1	3.39	3.41	136.9	127.1
2^b	1.00	0.077	12.5	2.79	30.8^{e}	30.5	6.4	2.37	5.89	130.6	133.1
3^c	0.12	0.009	1.5	0.68	63.7 ^e	63.1	-1.0	3.04	3.26	105.2	92.7
4^d	7.36	0.566	91.8	25.8	34.7	29.8	6.9	2.96	3.21	71.6	60.3

^aAddition of Et₃N to CEA hydrochloride at 20 °C; ^bAddition of NaOH to suspension of **3.2** at 25 °C; ^cAddition of CEA free base solution to reaction mixture at 60 °C; ^dAddition of Boc₂O solution to reaction mixture at 25 °C. ^eThe maximum attainable temperature (MAT) is shown rather than the MTSR.

Table 2.3.6. Calorimetry data and thermal safety analysis for **3.2** to **3.3** to **3.3-Boc**.

2.3.4 Impurities identification, RT markers, mitigation approaches

N-Alkylation of **3.2**, monitored by LC-UV in-process assays, proceeded cleanly. Primary discernible species were **3.3** (~90 LCAP at 254 nm, present as an inseparable ~10:1 mixture with its undesired regioisomer, *iso-3.3*) and residual **3.2** (~10 LCAP at 254 nm).^t At the conclusion of the Boc protection step, major species consisted of **3.3-Boc** (>80 LCAP at 254 nm, present as an inseparable ~10:1 mixture with its undesired regioisomer, *iso-3.3-Boc*), residual **3.2** (<5 LCAP), and two late-eluting species (RRT 1.15, <5 LCAP; and RRT 1.25, >10 LCAP). The identities of the late-eluting species were not unequivocally ascertained. All process impurities were purged during recrystallization, including the minor alkylation regioisomer.

^t The authors note that putative byproducts of CEA oligomerization (e.g., polyethyleneimine) will not display strong UV absorbance. The composition and quantitation of these byproduct(s) have not yet been determined, as of this writing.



Two impurity mitigation strategies are recommended for further investigation: additional solvent and reaction temperature screening. Higher-boiling polar aprotic solvents (e.g., DMAc, diglyme) – and thereby higher *N*-alkylation temperatures – may further improve **3.3** yield.^u Hastening imidazole alkylation with CEA, via higher temperature, may minimize CEA byproduct formation by better limiting its concentration *in situ*. Examination of higher *N*-alkylation temperatures may grant additional insight into the thermodynamics / kinetics of **3.3** and *iso-3.3* formation, as well. Higher temperatures may further enhance regioselectivity, beyond 10:1.

2.4 3.3-Boc to 3.7-diHBr (Milestone 4)

Preparation of 2-(5-bromo-4-(4-fluorophenyl)-1H-imidazol-1-yl)ethan-1-amine dihydrobromide (**3.7-diHBr**) was accomplished in two steps, starting from intermediate **3.3-Boc**. First, the imidazole nucleus of **3.3-Boc** was brominated at the C(5) position to afford *tert*-butyl (2-(5-bromo-4-(4-fluorophenyl)-1*H*-imidazol-1-yl)ethyl)carbamate **3.7-Boc**. Then, acid-mediated Boc deprotection yielded **3.7**, isolated from the reaction mixture as its dihydrobromide salt **3.7-diHBr** (**Scheme 2.4.1**).

Scheme 2.4.1 NBS-promoted bromination and the subsequent Boc deprotection.

3.7-Boc optimization efforts focused on work up and purification, as product purity was variable (62-86% by qNMR) during route scouting. Extensive reaction condition screening and

-

^u Higher reaction temperatures may be examined while maintaining MeCN as the reaction solvent with the use of a Parr reactor and secondary pressure vessel (the latter, for the introduction of CEA solution against pressure). This would emulate the industrial process for alkoxylations using ethylene oxide (moderate N₂ pressure is used in the nucleophile-containing Parr, to mitigate against catastrophic loss of pressure during ethoxylation / explosion risks).



optimization was not necessary; *N*-bromosuccinimide (NBS) proved regioselective, fast, reproducible, and cost-effective. Boc deprotection focal points included optimization of acid stoichiometry, replacing an ICH class 2 solvent, and improving the product purity profile (50-60% purity was observed by qNMR during process research). As a corollary relevant to the imidazolopiperazine-forming step, several Brønsted acids were screened in Boc removal in order to assess the effect of different counterions on the Pictet-Spengler annulation (3.7 to 3.4; Milestone 5).

2.4.1 Condition screening and optimization

2.4.1.1 Condition screening and optimization of 3.7-Boc formation:

With the above-mentioned parameters affirmed in process research, M4ALL identified the following variables for optimization in **3.7-Boc** preparation: NBS addition rate and NBS addition temperature.

M4ALL assessed the impact of the rate of NBS addition on the quality of **3.7-Boc**. During route scouting, bromination of **3.3-Boc** with NBS was observed to be exothermic. Heat evolution, if inadequately controlled (e.g., if reaction rate outpaced heat transfer), was suspected as a potential contributor to low product purity. Maintaining higher concentrations of NBS relative to **3.3-Boc**, *in situ*, was also hypothesized to contribute to poor quality. Both scenarios would correspond with faster addition. NBS was added as a solution (6V acetonitrile; 25 °C), via syringe pump, to a solution of **3.3-Boc** (4V acetonitrile; 0-5 °C) over periods of 30, 60, and 120 minutes. Rate of NBS addition proved integral to the quality of reaction mass (**Table 2.4.1**). Counter to the hypotheses above, the longest addition time (120 min) delivered poorer performance than either the 30 min or 60 min addition. Adding NBS over two hours delivered only 65 LCAP (at 254 nm) of desired **3.7-Boc**.

-

^v 10-equivalent excesses of acid were observed during process research (route scouting).



ſ	Enter	ELN No.	Addition time	$LCAP^a$		
	Entry	ELN NO.	Addition time	3.3-Boc	3.7-Boc	
	1	NT170-X116-1	30 min	0%	87%	
Ī	2	NT170-X116-2	60 min	0%	89%	
ſ	3	NT170-X116-3	120 min	0%	65%	

^aAt 254 nm. Impurities (remaining mass balance) have not been identified.

Table 2.4.1. Screening of NBS addition rate.

Finally, the effect of NBS addition temperature was assessed. NBS solutions (6V acetonitrile; 25 °C) were added via syringe pump to solutions of 3.3-Boc (4V acetonitrile) maintained at three different temperatures (0-5 °C, 20-25 °C, and 40-45 °C) over 30 minutes. In each trial, upon complete addition of NBS, the reaction medium was adjusted to 20-25 °C and maintained at this temperature for 1 hour. The temperature of addition had no effect on the reaction profile of **3.7-Boc** formation (**Table 2.4.2**).

Enter:	ELN No.	Addition tomm	$LCAP^a$		
Entry	ELN NO.	Addition temp	3.3-Boc	3.7-Boc	
1	BCH199-X53-A	0-5 °C	0%	87%	
2	BCH199-X53-B	20-25 °C	0%	85%	
3	BCH199-X53-C	40-45 °C	0%	86%	

^aAt 254 nm. Impurities (remaining mass balance) have not been identified.

Table 2.4.2. Screening of NBS addition temperature.

Thus, after screening various reaction parameters, optimized reaction conditions were as follows:

• A solution of NBS (1.05 equiv) in acetonitrile (6V) at 20-25 °C was added over 30 minutes to a 0-5 °C solution of **3.3-Boc** (1.00 equiv) in acetonitrile (4V). The

30

w Complete dissolution of NBS was imperative, and sometimes more than 6V of acetonitrile (e.g., 7V or 8V) were required. In such cases, the volume of acetonitrile used to suspend **3.3-Boc** was correspondingly decreased from 4V (e.g., to 3V or 2V) to maintain the total amount of acetonitrile at 10V.



resulting bromination medium was warmed to 20-25 °C for 1 hour, then the optimized workup and purification procedure enacted as described in section 2.4.2.

Acknowledging safety assessment outcomes for the bromination of 3.3-Boc (see Section 2.4.3.1) and the performance observations in Table 2.4.2, the authors recommend deploying the bromination procedure at 20-25 °C.

2.4.1.2 Condition screening and optimization of 3.7-Salt formation

Condition screening and optimization of **3.7-Salt** formation are both discussed in the context of **3.7-Salt**'s practical workup and purification for scalability (Section 2.4.2.2). Screening and optimization aspects of the former related directly to the latter. Specifically, the authors hypothesized that the target ammonium-imidazolium salts of **3.7**, once formed, would precipitate in organic media, allowing isolation by filtration and (if necessary), recrystallization from a suitable organic solvent.

2.4.2 Practical workup and purification for scalability

2.4.2.1 Practical workup and purification for scalability of 3.7-Boc formation

M4ALL pursued two strategies to achieve direct isolation (precipitation) and purification (crystallization) of **3.7-Boc** during process development. First, the reaction medium was treated with varying volumes of aqueous sodium thiosulfate (Na₂S₂O₃). The authors hypothesized that, in addition to serving as anti-solvent, the aqueous reductant would quench any residual NBS, solubilize and purge incipient succinimide during isolation. Addition of 16V of 0.1M aqueous Na₂S₂O₃ (**Table 2.4.3** entry 1) precipitated **3.7-Boc** with improved purity (97 LCAP at 254 nm; 92 wt%) but poor recovery (0.25 g; 30% isolated yield, assay corrected). A second crop of **3.7-Boc** was isolated from the filtrate. It exhibited lower purity (0.35 g; 30% isolated yield, assay corrected) prompting examination of an increased proportion of antisolvent. Doubling the volume of thiosulfate solution (entry 2) improved recovery (0.65 g; 66% isolated yield, assay corrected) but did not meet purity aims. While these experiments did not deliver purity and productivity



targets, they established proof-of-principle for antisolvent-driven, direct isolation of higher purity **3.7-Boc**.

Enters	ELN No.	$Na_2S_2O_3$			Output	t
Entry	ELN NO.	0.1 M aq		Amount	$LCAP^a$	Wt% Assay
1	BCH199-X54	$16V^b$	Crop 1	0.25 g	95.8%	91.8%
1		10 V	Crop 2	0.35 g	74.1%	66.2%
2	BCH199-X54	$32V^b$		0.65 g	83.1%	77.1%

^aAt 254 nm. ^bVolumes shown are relative to grams of 3.3-Boc reaction input.

Table 2.4.3. Direct isolation of 3.7-Boc from reaction mixture by treatment with Na₂S₂O₃ aq.

The following variables for direct **3.7-Boc** crystallization were then examined: volume of added antisolvent (water), product matrix temperature before filtration, and product matrix concentration prior to anti-solvent addition (**Table 2.4.4**). Increasing the water:acetonitrile ratio (entries 1 and 3) and lowering product matrix temperature (entries 1 and 2) benefited recovery. Optimally, distillation of the product mixture to 30% of its initial volume, addition of 6V water, and cooling the medium to 0-10 °C delivered 77% isolated yield of **3.7-Boc** with 95 LCAP purity (254 nm) and 95 wt% purity. Based on an in-process assay of 86 LCAP of **3.7-Boc**, 77% isolated yield represented >90% recovery of the available product in the reaction matrix. Thus, a direct isolation and purification process was demonstrated on screening scale.

		Volume	Volume	Antisolvent:	Maintenance		Ou	tput	
Entry	ELN No.	MeCN	H_2O	Solvent	/ filtration	Raw	$LCAP^a$	Wt%	Active
		removed	charged	Ratio	temp	yield	LCAP"	Assay	$yield^b$
1	BCH199- X57-1	0V	12V	1.2:1	20-25 °C	0.71 g	99.3%	97.9%	55%



2	BCH199- X57-2	0V	12V	1.2:1	0-10 °C	0.79 g	99.3%	97.6%	61%
3	BCH199- X57-3	0V	14V	1.4:1	20-25 °C	0.77 g	99.6%	99.1%	60%
4	BCH199- X57-4	5V (50% removed)	6V	1.2:1	0-10 °C	0.79 g	99.6%	98.8%	62%
5	BCH199- X57-5	5V (50% removed)	6V	1.2:1	20-25 °C	0.73 g	99.7%	99.0%	57%
6	BCH199- X57-6	7V (70% removed)	6V	2:1	0-10 °C	1.02 g	94.6%	95.4%	77%

^aAt 254 nm. ^bIsolated, purity-adjusted yield for the transformation **3.3-Boc** to **3.7-Boc**.

Table 2.4.4. Examining water as an anti-solvent for direct isolation of **3.7-Boc** from reaction mass.

Implementing the anti-solvent strategy, various batches were performed and the results captured below (**Table 2.4.5**). This process afforded **3.7-Boc** in >97 wt% purity and 63-75% yield in most cases (entries 1-4). If the quality of **3.7-Boc** was unacceptable, the purity was improved by redissolving the initially-isolated material in acetonitrile and repeating the purification protocol (entries 5-6). Further investigation to improve the reproducibility of this process is recommended.

Entry	ELN No.	Scale 3.3-Boc	Output 3.7-Boc					
Entry	ELIN INO.	Scale 3.3-Doc	Mass	LCAP ^a	Wt% Assay ^b	Purity-Adjusted Yield		
1	NT170-X127	18.2 g (92.8 wt%)	15.5 g	98.7%	101.4%	73%		
2^c	NT170-X126	11.3 g (95.2 wt%)	9.1 g	99.6%	98.1%	63%		
3	NT170-X128	18.1 g (89.6 wt%)	13.4 g	98.4%	101.2%	66%		
4	NT170-X140	35.1 g (101.2 wt%)	33.9 g	96.8%	97.0%	75%		
5	NT170-X130	25.6 g^d	27.3 g	78.3%	76.0%	64%		
·		re-purification \rightarrow	15.9 g	89.0%	94.5%	49%		
6 NT170-X139		$26.3 g^d$	28.6 g	92.4%	86.6%	74%		
		re-purification →	20.9 g	99.6%	100.4%	63%		

^aLC-UV at 254 nm. ^bDetermined by HPLC assay. ^c12V of water charged after distillation. ^dInput combined from multiple batches.

Table 2.4.5. Results for larger-scale batches of **3.3-Boc** to **3.7-Boc** using optimized process.

2.4.2.2 Practical workup and purification for scalability of **3.7-Salt** formation



M4ALL's efforts to directly isolate and purify **3.7-Salt** focused on solvent selection for the reaction medium and for the acid introduced,^x as well as the acid stoichiometry necessary to achieve complete Boc deprotection.^y The authors hypothesized that the target ammonium-imidazolium salts of **3.7**, once formed, would precipitate in organic media, allowing isolation by filtration and (if necessary) recrystallization from a suitable organic solvent. **3.7** ammonium-imidazolium salts' insolubility were confirmed in a series of experiments, summarized in **Table 2.4.6**.

Entry ^a	ELN No.	Acid (equiv)	Solvent (10V)	IPC 1	LCAP ^b	Isolated yield
			(10 V)	3.7-Boc	3.7-diHX	
1	PVK201-X72-4	2M HCl in EtOAc (4 eq)	EtOAc	9	91	90%
2	PVK201-X72-5	2M HCl in CPME (4 eq)	EtOAc	70	30	-
3	PVK201-X72-6	2M HCl in EtOAc (4 eq)	nBuOH	0	100	90%
4	PVK201-X72-2	33% HBr in AcOH (3 eq)	EtOH	5	95	92%
5	PVK201-X72-1 ^c	conc. H_2SO_4 (2 eq)	EtOH	2	97	nr^d
6	PVK201-X74	conc. H_2SO_4 (2 eq)	nBuOH	0	99	nr
7	PVK201-X64	TFA (5 eq)	CHCl ₃	0	89	91%
8	PVK201-X72-3	conc. H_3PO_4 (2 eq)	EtOH	95	3	-

^aAll reactions were performed on 0.5 g scale; ^bA% measured at 254 nm by LC-UV; ^cReaction time was 1 hour. ^dProduct did not solidify and formed a gel-like adduct with residual EtOH.

Table 2.4.6. Synthesis of various 3.7-diHX salts from 3.7-Boc.

In relatively less polar aprotic organic solvents like ethyl acetate, **3.7-Boc** precipitated as its imidazolium salt prior to Boc deprotection which slowed the conversion to **3.7-diHCl** (entries 1-2). In ethanol and *n*-butanol, conversion to **3.7-diHCl**, **3.7-diHBr**, and **3.7-H₂SO₄** salts (entries 4-6) proceeded without premature precipitation of 3.7-Boc-imidazolium salts. A trifluoroacetate

34

^x During route scouting, use of aqueous acids for Boc deprotection led to low isolated yields, attributable to intrinsic aqueous solubility of **3.7-diHX**. Aqueous acids were discounted as viable options for process development.

^y During route scouting, super-stoichiometric excesses up to 10 equivalents were observed.



salt was also prepared (entry 7).^z Only phosphoric acid failed to convert (entry 8). On complete consumption of **3.7-Boc** (LC-UV in-process assay; 2-5 hr at 50 °C), product mixtures were cooled to 20-25 °C then filtered. The isolated filter cake was rinsed with ethyl acetate (10V) and dried, delivering **3.7-diHX** salts in isolated yields exceeding 90%. *n*-Butanol was selected as the optimal solvent for scale-up, favoring its higher boiling point and relative ease of procurement versus absolute ethanol. ^{aabb}

Optimized conditions for **3.7-Boc** deprotection and direct isolation of **3.7-diHCl** and **3.7-diHBr** salts were demonstrated on decagram scale, as summarized in **Table 2.4.7**. Quality of input (high wt% purity) was crucial for best results (see also section 2.4.4). A minimum of 3 equiv of HX was required; incomplete conversion was observed using 2 equiv or fewer.

		Input	3.7-Boc			Output 3.7-H	ICl salt			
Entry	ELN No.	Mass	Wt% assay	Mass	LCAP ^a	Wt% 3.7 Free Base (expected 80%)	Wt% Cl ^c (expected 20%)	Adjusted yield		
1	NT170-X106 ^d	4.8 g	$72\%^{b}$	4.8 g	79%	54% ^b	17.0%	90%		
2	NT170-X109 ^d	17.0 g	62% ^b	13.2 g	91%	58% ^b	17.8%	87%		
3	PVK201-X66 ^e	9.2 g	87% ^b	7.8 g	92%	60% ^b	18.5%	70%		
4	BCH199-X62	4.0 g	103% ^c	3.7 g	99.9%	77.6% ^c	18.3%	97%		
5	PVK201-X79	8.5 g	98% ^c	7.7 g	99.7%	77.8% ^c	18.7%	96%		
6	BCH199-X60	24.0 g	101% ^c	22.2 g	99.7%	77.6% ^c	19.2%	97%		
		Input	3.7-Boc			Output 3.7-HBr Salt				
Entry	ELN No.	Mass	Wt% assay	Mass	LCAP ^a	Wt% 3.7 Free Base (expected 64%)	Wt% Br ^c (expected 36%)	Adjusted yield		
7	PVK201-X91	14.0 g	94.5% ^c	15.6 g	92.3%	56.0% ^c	34.7%	84%		
8	BCH199-X68	5.0 g	97.0% ^c	6.1 g	98.4%	55.0% ^{c,f}	31.5%	93%		
9	BCH199-X66	17.0 g	100% ^c	19.1 g	99.9%	64.3% ^c	34.3%	97%		

z

^z 3.7-diTFA was prepared in chloroform for the purpose of screening the salt's performance in the Pictet-Spengler. It performed poorly in the annulation. Efforts to solvent swap (to nBuOH) were, therefore, not made.

^{aa} Procurement of high purity ethanol can be complicated in certain jurisdictions (e.g., via controlled substance regulations).

^{bb} M4ALL envisioned that conducting this reaction in *n*-butanol could enable a telescopic 3.7-Boc $\rightarrow 3.7 \rightarrow 3.4$ process since the subsequent Pictet-Spengler reaction is also conducted in *n*-butanol. The viability of this prospect was not investigated in this Scope of Work.



^aLC-UV (254 nm). ^bDetermined by quantitative ¹H NMR assay. ^cDetermined by HPLC assay. ^dSolvent was ethyl acetate. ^eSolvent was chloroform. ^fSample contains 10% water by weight (most samples of **3.7-diHX** are <3% water), resulting in artificially low wt% assays of **3.7** and Br.

Table 2.4.7. Multigram-scale preparations of **3.7-diHCl** and **3.7-diHBr**.

2.4.3 Process safety assessment

2.4.3.1 Bromination of **3.3-Boc** to **3.7-Boc**

Calorimetric analysis of the bromination reaction was conducted using 9 g of **3.3-Boc** in a 100 mL vessel. ΔH calculations, based on the moles of **3.3**, are summarized in **Table 2.4.8** (entry 1). Addition of NBS solution (1.05 equiv in 6V acetonitrile) over 30 minutes to the solution of **3.3-Boc** in 4V acetonitrile at 0 °C proved minimally exothermic, with a total heat of the reaction (ΔH_r) of -94.8 kJ/mol. MAT and MTSR were determined to be 16.5 °C and 4.8 °C, respectively (ΔT_{ad} = 13.5 °C), both below the boiling point of the reaction solvent acetonitrile (81.6 °C), indicating a low risk of solvent boiling under cooling failure conditions. MRT was recorded at 4.0 °C and MHG during the addition was measured at 6.8 W. Based on prototypical reactor cooling capacity, severity is considered low for the addition of NBS.

Process	ΔH_{r}	ΔH_r	ΔH_{r}	ΔT_{ad}	MTSR	MRT	MHG	C _p (J/	g K)	U (W/	m ² K)
Step	(kJ)	(kJ/g)	(kJ/mol)	(°C)	(°C)	(°C)	(W)	Before	After	Before	After
1^a	-2.8	-0.31	-94.8	13.5	4.8	4.0	6.8	3.84	0.85	209.5	93.6
2^b	0.8	0.21	80.2	4.4	30.9	28.5	2.8	2.98	1.32	119.8	96.0
3^c	4.2	0.85	325.5	6.7	44.3	31.8	93 ^d	2.8	14.2	136	104

^aAddition of NBS to **3.3-Boc** at 0 °C; ^bAddition of HCl to **3.7-Boc** at 25 °C; ^c Addition of HBr to **3.7-Boc** at 25 °C. ^dThe MHG is artificially high as a result of maintaining constant T_r (rather than constant T_j) during addition. In this situation, the ΔT_{ad} is a more reliable indicator of the thermal hazard associated with the process, and should be prioritized over the MHG in the severity assessment.

Table 2.4.8. Calorimetric data & thermal safety analysis for Milestone 4.

2.4.3.2 Boc deprotection of 3.7-Boc to 3.7-diHX salt

Calorimetric analysis of the Boc deprotection reaction to form **3.7-diHCl** was conducted using 4 g of **3.7-Boc** in a 100 mL vessel. ΔH calculations, based on the moles of **3.7-Boc**, are summarized in **Table 2.4.8** (entry 2). Addition of HCl (2M in ethyl acetate, 4 equiv) over 10



minutes to the solution of **3.7-Boc** in 10V n-butanol at 25 °C was found to be minimally exothermic, with a total heat of the reaction (ΔH_r) of 80.2 kJ/mol. MAT and MTSR were determined to be 32.4 °C and 30.9 °C, respectively ($\Delta T_{ad} = 4.4$ °C), both below the boiling point of the reaction solvent n-butanol (118.0 °C), indicating a low risk of solvent boiling under cooling failure conditions. MRT was recorded at 28.5 °C and MHG during the addition was measured at 2.8 W. Based on prototypical reactor cooling capacity, severity is considered low for the addition of HCl.

Calorimetric analysis of the Boc deprotection reaction to form **3.7-diHBr** was conducted using 5 g of **3.7-Boc** in a 100 mL vessel. ΔH calculations, based on the moles of **3.7-Boc**, are summarized in **Table 2.4.8** (entry 3). Addition of HBr (33 wt% in acetic acid, 3 equiv) over 5 minutes to the solution of **3.7-Boc** in 7V *n*-butanol at 25 °C was found to be slightly exothermic, with a total heat of the reaction (ΔH_r) of 325.5 kJ/mol. MAT and MTSR were determined to be 34.7 °C and 44.3 °C, respectively ($\Delta T_{ad} = 6.7$ °C), both below the boiling point of the reaction solvent *n*-butanol (118.0 °C), indicating a low risk of solvent boiling under cooling failure conditions. MRT was recorded at 31.8 °C and the MHG during the addition was measured at 93 W. Based on prototypical reactor cooling capacity, severity is considered low for the addition of HBr.

2.4.4 Impurities identification, RT markers, mitigation approaches

Under optimized bromination conditions, once **3.3-Boc** had been fully consumed, in-process assays revealed approximately 85 LCAP (254 nm) of **3.7-Boc**, with the remaining ~15 A% attributed to several individually minor impurities. The authors have not yet succeeded isolating and identifying these impurities. LC-MS analysis of the crude reaction mixture revealed multiple high MW ions, including m/z 608, which might correspond to oxidative dimerization of **3.3-Boc** (m/z 305 + 305 – 2 = 608). Impurity generation was exacerbated by longer NBS addition times (**Table 2.4.1**, entry 3) and curtailed by shorter addition times (entries 1-2). Impurities with the same MW as **3.7-Boc** were not observed by LC-MS; other bromination regioisomers were not generated. All process impurities were consistently purged to low levels by the optimized isolation procedure.



Acid-mediated Boc deprotection and salt formation exhibits a clean reaction profile; **3.7-diHX** is the only species observed by LC-UV once **3.7-Boc** has been fully consumed. Since the product is isolated by filtration with no additional operations, input purity is key for this reaction. Using lower wt% assay **3.7-Boc** results in lower wt% assay **3.7-diHCl** and **3.7-diHBr** (**Table 2.4.7**, entries 1-3, 7).^{cc}

2.5 3.7-diHBr to 3.4 (Milestone 5)

The synthesis of 2-(4-fluorophenyl)-8,8-dimethyl-5,6,7,8-tetrahydroimidazo[1,2-a]pyrazine (3.4) was achieved through a Pictet-Spengler reaction between 3.7-diHBr and acetone (Scheme 2.5.1). During the course of the reaction, the transient blocking group (bromine atom at C(5) position of the imidazole) was cleaved. A detailed discussion of this blocking group approach is provided in the following Section.

Scheme 2.5.1. Conversion of **3.7-diHBr** to **3.4** via Pictet-Spengler reaction.

2.5.1 Condition screening and optimization

Initial efforts to convert compound **3.3** to **3.4** under Pictet-Spengler reaction conditions were unsuccessful. Treatment of **3.3** with acetone in the presence of a variety of acid catalysts at 80-100 °C failed to yield the desired product **3.4** (Scheme **2.5.2**). dd 1H NMR analysis revealed a species

^{cc} Efforts to recrystallize **3.7-diHX** were unsuccessful.

^{dd} The desired product molecular weight (245 amu) was observed by both GC-MS and LC-MS, however, the ¹H NMR showed no evidence of **3.4** generation An authentic reference standard of **3.4** was prepared according to the published route. ¹



consistent with the structure of **3.3-imine**. Suspecting that the temperature was insufficient to drive the cyclization, the temperature was increased to 120 °C using DMF as a solvent. However, this modification resulted exclusively in the formation of a formylated byproduct.^{ee}

Scheme 2.5.2. Attempted conversion of 3.3 to 3.4 via Pictet-Spengler reaction.

To assess the feasibility of Pictet-Spengler cyclization of imidazole **3.3**, control experiments were conducted using more reactive aldehydes (**Scheme 2.5.3**). Imidazole **3.3** reacted readily with either benzaldehyde or tolualdehyde, affording Pictet-Spengler products in >40% isolated yield, however, cyclization occurred exclusively at the C(5) position leading predominantly to the undesired regioisomer.

39

^{ee} Presumably N-(2-(4-(4-fluorophenyl)-1H-imidazol-1-yl)ethyl)formamide (m/z 233 observed by GC-MS) resulting from transamidation of DMF with the primary amino group of **3.3**.

ff There are scant examples of imidazoles partaking in such reactions, 25 compared to more traditional substrates like indoles and methoxyarenes.



Scheme 2.5.3. Control experiments to establish feasibility and regioselectivity preferences.

These findings guided the development of a blocking group strategy. Halogens were identified as suitable candidates due to their facile removal and minimal electronic influence on the imidazole ring. Accordingly, a series of precursors **3.7-diHX** bearing different counterions^{gg} (see synthetic details in Section 2.4) were subjected to Pictet-Spengler reaction conditions. The outcomes of these experiments are summarized in **Table 2.5.1** below.

Entry ^a	ELN No.	3.7-Salt	Time	IPC LCAP b			
			(hr)	3.7-Salt	3.4	3.3	
1	PVK201-X67-12	3.7-diHCl	17	3	58	3	
2	PVK201-X73-2	3.7-diHBr	6	0	66	28	
3	PVK201-X74	3.7-H ₂ SO ₄	17	10	71	11	
4	PVK201-X71-11	3.7-diTFA	6	12	3	0	

^aAll reactions were performed on 250 mg scale using type A sodium zeolite (Sigma-Aldrich product no. 96096). ^bLCAP measured at 254 nm by LC-UV. Major contributors to the remaining LCAP balance include mesityl oxide (from acetone self-aldol condensation) and a reaction intermediate (halogenated 3.4). Further details are located in the analytical development report (ADR).

Table 2.5.1. Effect of counterion on Pictet-Spengler reaction of **3.7-diHX** to **3.4**.

With the C(5) position of the imidazole blocked by a halogen atom, **3.7-diHX** successfully yielded the target compound **3.4** in 58-71 LCAP (254 nm). Reaction of **3.7-diHCl** with acetone and zeolite in *n*-butanol at 150 °C afforded **3.4** in 58 LCAP after 17 hours (**Table 2.5.1**, entry 1). Under identical conditions, **3.7-diHBr** exhibited a faster reaction rate, delivering 66 LCAP of **3.4** and complete consumption of **3.7** within 6 hours. However, a significant amount of **3.3** (28 LCAP) was formed via debromination of **3.7** (entry 2), likely due to the higher acidity of HBr compared to HCl. A similar outcome was observed with **3.7-H₂SO₄** under the same conditions (entry 3), however, its hygroscopicity rendered it less practical than the hydrohalide salts. In contrast, **3.7-**

gg These salts are easier to handle than 3.7, which is a viscous oil like 3.3.

hh Approximately 35 LCAP of halogenated **3.4** (reaction intermediate) was observed under these conditions, with LCMS analysis revealing a mixture of bromo- and chloro-**3.4** derivatives. Refer to the ADR for additional details.



diTFA proved unsuitable for the Pictet-Spengler reaction – TFA reacted with the amine to form the corresponding trifluoroacetamide (53 LCAP at 254 nm) instead (entry 4). Based on these findings, **3.7-diHCl** and **3.7-diHBr** were selected for further screening and optimization.

Zeolite was employed to facilitate the initial condensation of **3.7** with acetone; initial investigations (data not shown) indicated that zeolite outperformed other desiccants such as silica gel and sodium sulfate in promoting this transformation. To evaluate its influence, various types and loadings of zeolite were tested in the Pictet Spengler reaction of **3.7-diHCl**. Using 100 wt% if of type A sodium zeolite (Sigma-Aldrich) yielded **3.4** in 47 LCAP (254 nm), along with 18 LCAP of **3.3** after 17 hours of reaction time (**Table 2.5.2**, entry 1). Omitting zeolite altogether led to a decrease in product formation, with only 29 LCAP of **3.4** detected (entry 2). Lowering the reaction temperature from 150 °C to 130 °C resulted in poor conversion, yielding 9 LCAP of **3.4** after 17 hours (entry 3). Additionally, four other types of zeolites were evaluated at 100 wt% loading (entries 4-7); these produced inferior outcomes (complex reaction profile with new impurities).

Enteria	ELN No.	Zaalita tuma	Zeolite loading	Temp	IPC LCAP ^b		
Entry ^a	ELN NO.	Zeolite type	(w/w %)		3.7	3.4	3.3
1	PVK201-X80-1	Type A sodium	100	150	0	47	18
2^c	PVK201-X80-3	Type A sodium	0	150	0	29	40
3	PVK201-X80-4	Type A sodium	100	130	47	9	39
4^c	PVK201-X80-5	Beta, hydrogen	100	150	4	21	40
5^c	PVK201-X80-6	Mordenite, ammonium	100	150	0	24	51
6 ^c	PVK201-X80-7	ZSM-5, ammonium	100	150	0	27	38
7^c	NT170-X136	Type Y	100	150	22	25	6

[&]quot;All reactions were performed on 0.25 g scale; "LCAP measured at 254 nm by LC-UV. A major contributor to the remaining LCAP balance is a reaction intermediate (halogenated **3.4**). Further details are located in the analytical development report (ADR). "Messy reaction profile with multiple new species (not shown in table).

Table 2.5.2. Effect of zeolite type and loading on the conversion of **3.7** to **3.4**.

41

ⁱⁱ While higher **3.4** LCAP was observed using 200 wt% of zeolite (**Table 2.5.1**), M4ALL sought to limit the zeolite loading to 100 wt% for process development, out of concern for mass transfer/heterogeneity issues.



Given the high temperature requirements of the Pictet-Spengler reaction, higher-boiling acetone analogues, such as 2,2-dimethoxy propane (2,2-DMP) and acetone dibutyl acetal (ADBA), were evaluated as alternative condensation partners. However, these substitutions did not yield significant improvements in reaction yields (**Table 2.5.3**).

^aAll reactions were performed on 0.25 g scale; ^bLCAP measured at 254 nm by LC-UV. Contributors to the remaining LCAP balance include mesityl oxide (from acetone self-aldol condensation) and a reaction intermediate (halogenated **3.4**). Further details are available in the analytical development report (ADR).

Table 2.5.3. Effect of acetone substitutes (acetals) on the conversion of **3.7** to **3.4**.

Throughout these studies, formation of compound **3.3** was observed to varying degrees, potentially contributing to the generation of the undesired regioisomer of **3.4** (*vide supra*). To mitigate this side reaction, the addition of one equivalent of base was found to suppress the formation of **3.3** during the Pictet-Spengler reaction (**Table 2.5.4**).^{jj} As shown in the table, bases such as triethylamine, DBU, or DABCO effectively inhibited premature debromination. Among them, triethylamine provided the highest conversion to **3.4** (entry 1) and was selected for subsequent scale-up studies. Its beneficial effect was also evident in reactions involving the **3.7-diHBr** salt, which had previously shown substantial **3.3** formation (**Table 2.5.1**, entry 2). In the presence of one equivalent of triethylamine, **3.7-diHBr** salt delivered 70 LCAP of **3.4** (at 254 nm) and only 8 LCAP of **3.3** (**Table 2.5.4**, entry 4). A similar result was obtained on a 15-gram scale

^{jj} Given that **3.7-diHX** contains two equivalents of acids, whereas the Pictet-Spengler reaction requires only a substoichiometric amount, we hypothesized that adding one equivalent of base would lower the pH and suppress the formation of **3.3**.



in a Parr reactor (77 LCAP of **3.4** and 11 LCAP of **3.3**), but the isolated yield of **3.4** for this reaction was only 25% (**Table 2.5.4**, entry 5). Initially, the low isolated yield was attributed to potential losses during workup, however, analysis of the aqueous phases confirmed that no significant amount of **3.4** was lost.

Enter	ELN	C = =1 =	3.7-diHX	Base	IPC LCAP ^a			
Entry	ELN	Scale			3.7salt	3.4	3.3	
1	NT170-X134	0.5 g	3.7-diHCl	Et ₃ N	2	74	2	
2	NT170-X135	0.5 g	3.7-diHCl	DBU	34	32	0	
3	BCH199-X61	0.5 g	3.7-diHCl	DABCO	32	36	0	
4	PVK201-X90	2.0 g	3.7-diHBr	Et ₃ N	0	66	7	
5	PVK201-X92	15.0 g	3.7-diHBr	Et ₃ N	0	$76(22\%)^b$	7	

[&]quot;LCAP measured at 254 nm by LC-UV. Contributors to the remaining LCAP balance include mesityl oxide (from acetone self-aldol condensation) and a reaction intermediate (halogenated **3.4**). Further details are available in the analytical development report (ADR). ^bYield determined by HPLC wt% (concentration) assay of **3.4** in the crude isolate.

Table 2.5.4. Effect of basic additives on the Pictet-Spengler reaction.

These findings indicated that intrinsic side reactions might occur during the Pictet-Spengler reaction. Detailed LC analysis revealed that although compound **3.4** accounted for up to 77 LCAP in the reaction mixture (at 254 nm), the LC baseline displayed numerous small, broad signals, suggesting the formation of a complex mixture of high-molecular weight oligomeric impurities. Additionally, the reaction mixtures consistently darkened in color, potentially indicating nonspecific thermal decomposition to elemental carbon. Thermal gravimetric analysis (TGA) of pure **3.4** confirmed its thermal instability (**Figure 2.5.1**), with mass loss initiating around 100 °C. By the time the sample reached 150 °C (the operating temperature of the reaction), approximately 25% of the compound's mass had been lost. These results support the hypothesis of nonspecific decomposition and help explain the discrepancy between LCAP values and both wt% assay and



isolated yield. In light of this, alternative conditions were explored, including lower temperatures (120–140 °C) and shorter incubation times at elevated temperatures (200 °C); however, these adjustments did not yield improvements.

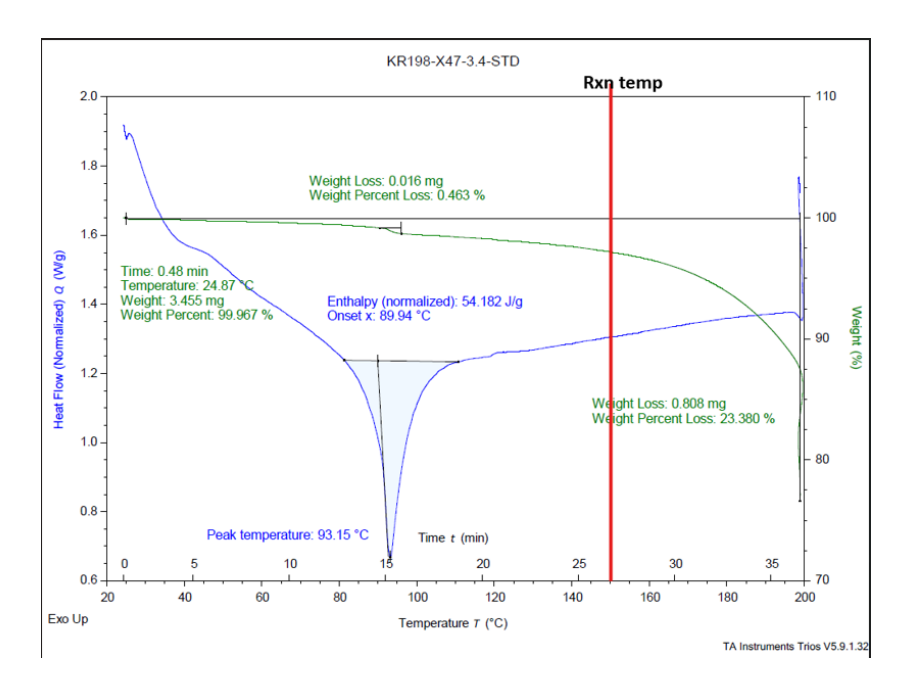


Figure 5.2.1. Thermogravimetric analysis (TGA) of pure 3.4.

Thus, the partially optimized Pictet-Spengler reaction conditions for synthesis of **3.4** from **3.7-diHX** are provided below:

• Reagents: 3.7-diHBr (1 equiv), acetone (4 equiv), Et₃N (1 equiv), zeolite (100 w/w %)

• Solvent: *n*-butanol (10V)

• Temperature: 150 °C

• Reaction time: 10 hours

• Assay yield: 25% (HPLC)

2.5.2 Practical workup and purification for scalability

The current reaction conditions yielded crude **3.4** in 20-30 wt% purity after workup, which involved filtration to remove the zeolite, neutralization with aqueous NaHCO₃, extraction with ethyl acetate, multiple water washes to remove residual *n*-butanol, and concentration of the organic



phase. This process resulted in a black tar-like residue. To establish a practical purification process, several approaches were explored, ultimately leading to the adoption of an acid-base extraction protocol (**Figure 5.2.2**). The tar was dissolved in methyl *tert*-butyl ether (MTBE) and insoluble materials were removed by filtration. The filtrate was acidified with hydrochloric acid to pH = 1, allowing protonated **3.4** to partition into the aqueous phase. The aqueous layer was washed with MTBE to remove organic impurities, then sequentially adjusted to pH = 3 and pH = 5, with each step followed by MTBE washes to further eliminate organic-soluble impurities. Finally, the aqueous phase was basified to pH = 11, and the free base **3.4** was extracted into MTBE. A dramatic improvement in the color of the organic phase was observed, from brown-black prior to acid-base treatment to light orange post-extraction. Subsequent charcoal treatment further improved the color of the MTBE phase to pale yellow. Solvent removal yielded **3.4** as a friable, yellow solid. The purification process was verified on a 1-gram crude, affording **3.4** in 55% recovery with 93 LCAP (254 nm) and 81 wt% purity (**Table 2.5.5**). For detailed experimental procedures, refer to Section **4.1**.

To identify a suitable recrystallization solvent system for **3.4** (81 wt% purity), a solubility screen was conducted (**Table 2.5.6**). The material exhibited high solubility in most organic solvents, typically dissolving completely in just 5 volumes at 25 °C. Notably, **3.4** was insoluble in *n*-heptane at 25 °C (entry 2). These results suggest that heptane, or a mixed solvent system such as MTBE—heptane, may be viable for recrystallization. However, this hypothesis was not fully pursued due to time and material constraints.



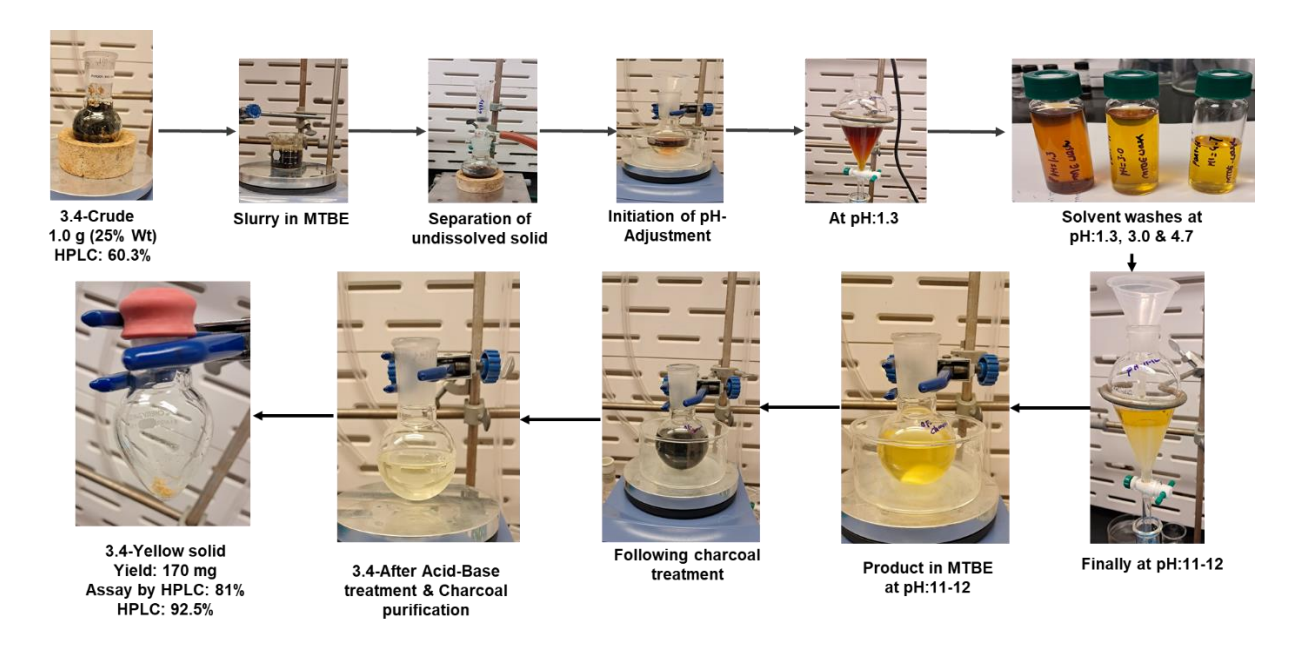


Figure 5.2.2. Process flow diagram for acid-base purification of 3.4.

Input				Output				
Raw mass	LCAP 3.4 ^a	Wt% 3.4	Mass 3.4	Raw mass	LCAP 3.4 ^a	Wt% 3.4	Mass 3.4	Recovery
1.00 g	60.3%	25.3%	253 mg	170 mg	92.5%	81.0%	138 mg	55%

^aMeasured by LC-UV at 254 nm.

Table 2.5.5. Acid-base purification of **3.4**.

Destar d	Solvent	Class@ ICH	Doiling point	Solubility of 3.4			
Entry ^a	Solvent	Class@ ICH	Boiling point	Vol	at 25 °C	at boiling point	
1	MTBE	Class-III	55 °C	9	Soluble	ND	
2	<i>n</i> -Heptane	Class-III	98 °C	10	Insoluble	Soluble	
3	DMSO	Class-III	189 °C	5	Soluble	ND	
4	Ethyl acetate	Class-III	77 °C	5	Soluble	ND	
5	Acetonitrile	Class-II	82 °C	5	Soluble	ND	
6	THF	Class-II	65 °C	5	Soluble	ND	
7	Isopropanol	Class-III	82 °C	5	Soluble	ND	
8	Ethanol	Class-III	78 °C	5	Soluble	ND	
9	2-Methyl THF	Class-III	78 °C	5	Soluble	ND	
10	Acetone	Class-III	56 °C	5	Soluble	ND	
11	Toluene	Class-II	110 °C	5	Soluble	ND	

^aAll studies were performed on 25 mg scale; ND = Not determined.

Table 2.5.6. Solubility study of 3.4.



2.5.3 Process safety assessment

As the Pictet-Spengler operating temperature (150 °C) is greater than the boiling point of n-butanol (118 °C), appropriate safety precautions must be taken. Small-scale reactions (up to 2 grams **3.7-diHX** and 20 mL solvent) were conducted in thick-walled pressure flasks behind a polycarbonate blast shield. Large-scale reactions (up to 15 grams **3.7-diHX** and 150 mL solvent) were conducted in a Parr reactor. The Parr reactor is rated up to 2000 psi and allows for continuous monitoring of internal temperature and pressure, so its use is preferred over glass pressure flasks. Conducting large-scale reactions in a glass pressure flask is not recommended. During the Pictet-Spengler reaction, the maximum pressure exerted by n-butanol vapor was 40 psi, well below the safe operating threshold for this Parr reactor.

2.5.4 Impurities identification, RT markers, mitigation approaches

Refer to the accompanying analytical development report (GFN-001-GAN-ADR) for a detailed discussion.

2.6 Conclusions

A novel and promising 7-step synthetic approach toward the synthesis of the advanced ganaplacide intermediate **3.4** has been developed for the first time. The process begins with the Friedel-Crafts acylation of fluorobenzene, followed by Bredereck imidazole synthesis with telescoped *N*-alkylation and Boc protection. Subsequent bromination, Boc-deprotection and a final Pictet-Spengler cyclization afford intermediate **3.4**. This 7-step process affords **3.4** in 3% overall yield, with a purity of 60.3 LCAP (254 nm) and 25.3 wt% (HPLC) on decagram scales. The sequence has been successfully developed up to the penultimate step, yielding the precursor of **3.4** (**3.7-diHBr** or **3.7-diHCl**) in an overall yield of ~15%. Although the challenges associated with the final Pictet-Spengler reaction have been identified, further optimization was not pursued due to the time constraints. Notably, an efficient acid-base liquid-liquid extraction strategy has been developed for the purification of intermediate **3.4**. This method enables isolation of **3.4** from the crude mixture (25.3 wt% and 60.3 LCAP at 254 nm), enhancing its purity to 81.0 wt% (92.5 LCAP



at 254 nm) with a recovery rate of 55% on gram scale. The recovery rate is expected to improve further upon scale-up.

Although the current Pictet-Spengler reaction yields remain low, technoeconomic (TE) cost analysis suggests that, compared to Novartis's first-generation route, M4ALL's new approach offers ~23% reduction in raw material cost (RMC) for **3.4**. This cost advantage is expected to increase further with optimization of the final step.



3 Appendix

3.1 Experimental details

General Experimental: Reagents and solvents were obtained from commercial suppliers and used as received unless otherwise indicated. Compound 3.1 was purchased from Chem-Impex (catalog no. 30340, 98.95% purity) or prepared as described below. Compound 3.2 was purchased from Combi-Blocks (catalog no. QB-0221, 98% purity) or prepared as described below. Aluminum chloride was purchased from Acros (catalog no. 217465000, anhydrous, 98% purity). CEA (2chloroethylamine hydrochloride) was purchased from aablocks (catalog no. AA00336K, >97% purity). Zeolite was purchased from Sigma-Aldrich (catalog no. 96096). Reactions were conducted under an inert atmosphere (nitrogen) unless otherwise noted. Reactions (in-process controls, IPCs) were monitored by Agilent HPLC – to prepare the samples, an aliquot (~100 μL) was withdrawn from the reaction mixture, diluted with ~1 mL methanol, and filtered to remove any insoluble components. Refer to the analytical development report (GFN-001-ADR) for information on analytical methods. TLC was visualized with UV light or by treatment with phosphomolybdic acid (PMA), ninhydrin, and/or KMnO₄. ¹H NMR and ¹³C NMR spectra were routinely recorded on Bruker Avance III HD Ascend 600 MHz spectrometer. All chemical shifts are reported in parts per million (ppm) relative to residual chloroform (7.26 ppm for ¹H, 77.16 ppm for ¹³C), dimethyl sulfoxide (2.50 ppm for ¹H, 39.52 ppm for ¹³C), or methanol (3.31 ppm for ¹H, 49.00 ppm for ¹³C). ¹⁹F NMR spectra were reference to a benzotrifluoride internal standard ($\delta = -63.0$ in CDCl₃). ¹³C and 19 F NMR spectra are proton-decoupled. Coupling constants J are reported in hertz (Hz). The following abbreviations were used to designate signal multiplicity: s, singlet; d, doublet; t, triplet; q, quartet, p, pentet; dd, doublet of doublets; m, multiplet; br, broad.



Synthesis of 2-chloro-1-(4-fluorophenyl)ethan-1-one 3.1

A 3-necked, 1-L round bottomed Morton flask was equipped with an overhead stirrer, Tefloncoated thermocouple probe, 50-mL addition funnel, and gas outlet tube with aqueous base trap. Caution: A significant amount of HCl vapor is generated during this reaction, so the gas outlet and trap are necessary to relieve pressure and protect equipment from corrosion. The flask was charged with fluorobenzene (36.1 g, 376.0 mmol, 1.0 eq.) and heptane (123.0 mL, 3.5 V) and stirring was initiated (250 rpm). To the resulting clear, colorless solution, AlCl₃ (51.3 g, 385.2 mmol, 1.01 eq.) was added in one portion at 25 °C. The resulting yellow suspension was cooled to 0-5 °C using an ice/salt bath. Then chloroacetyl chloride (30.5 mL, 380.8 mmol, 1.01 eq.) was added dropwise using the addition funnel over a period of 20-30 minutes. Caution: The addition of chloroacetyl chloride generates a significant exotherm and care should be taken to maintain the internal reaction temperature below 15 °C. Once the addition was completed, stirring was continued at 0-5 °C. Reaction conversion was monitored by HPLC. Process notes: With 1.01 equiv of AlCl₃ and chloroacetyl chloride, incomplete conversion was observed. Increasing the loading to 1.05 or 1.10 equiv is recommended. With these loadings, the reaction completes in less than one hour. After completion, the reaction mixture was cautiously quenched with 300 mL of 0.5 N HCl (aqueous) at 0-5 °C. Caution: This quench is initially highly exothermic. The quench solution should be added dropwise or in small portions. If large exotherms are observed, the operator should wait for the mixture to cool before adding more quench reagent. Addition of the first 10 mL of quench solution caused the internal temperature to rise by as much as 30 °C, and the second 10 mL caused a 20 °C temperature rise. After this, exotherms were smaller and ceased entirely once 50-60 mL of quench solution had been added. The remainder was added without incident. An inverse quench protocol may mitigate these issues, but this hypothesis was not investigated. To the resulting beige-white suspension, ethyl acetate (250 mL) was added in one portion. The cold bath was removed and stirring was continued at 25 °C for 15 minutes. All of the solids dissolved and a liquid-liquid biphase was observed. The organic and aqueous layers were



separated, and the organic layer was washed with aq. sat NaHCO₃ (200 mL) and brine (200 mL), dried over MgSO₄, filtered, and concentrated under reduced pressure to afford **3.1** as a white solid, which was pulverized and dried under high vacuum. (55.3 g, corrected assay yield: 84%, purity: 100% by HPLC wt% assay) Caution: Compound **3.1** is a mild lachrymator and vesicant.

¹H NMR (600 MHz, CDCl₃): δ 8.02–7.97 (m, 2H), 7.20–7.14 (m, 2H), 4.66 (s, 2H). These data are in agreement with published literature.²⁶

¹³C NMR (151 MHz, CDCl₃): δ 189.78, 166.32 (d, J = 256.6 Hz), 131.48 (d, J = 9.5 Hz), 130.76 (d, J = 3.0 Hz), 116.28 (d, J = 22.1 Hz), 45.75. These data are in agreement with published literature.²⁶

¹⁹F NMR (564 MHz, CDCl₃): δ -103.37. These data are in agreement with published literature. 26

Synthesis of 5-(4-fluorophenyl)-1*H*-imidazole **3.2**

A 2 neck-500 mL round bottle flask equipped with an overhead stirrer is charged with 2-chloro-1-(4-fluorophenyl)ethan-1-one **3.1** (50.12 g, 290.4 mmol, 1.0 eq.), formamide (139 mL, 3.485 mol, 12.0 eq.) and water (10.5 mL, 580.8 mmol) at room temperature. The resultant heterogeneous solution is heated to 140 °C for 6 h. After completion, the reaction mixture was cooled to 25 °C and poured into a large beaker containing 250 mL (5V) water. The mixture was stirred at 25 °C for 15 minutes. The orange precipitates (undesired byproducts) were removed by vacuum filtration. The pale, yellow filtrate (pH 4-5) was basified by the dropwise addition of 10% (w/w) aqueous NaOH (approx. 375 mL) with stirring to a pH of 12. The light brown-yellow precipitated **3.2** was collected by vacuum filtration and rinsed with cold water (2 x 75 mL). After air drying, the solid was crushed and dried in a vacuum oven (40 Torr, 65 °C) for at least two hours to remove water. (26.79 g, corrected assay yield: 52%, purity: 91% by quantitative ¹H NMR). **Process notes:** If desired, the purity of **3.2** may be increased by recrystallization. Dissolution in 3V of warm ethyl



acetate, hot filtration, addition of 3V hexanes antisolvent, and slow cooling afforded crystalline **3.2** in modest recovery (43%) and excellent purity (100% by quantitative ¹H NMR and HPLC wt% assay).

¹H NMR (600 MHz, CDCl₃): δ 7.76–7.66 (m, 3H), 7.28 (d, J = 1.0 Hz, 1H), 7.11–7.04 (m, 2H). These data are in agreement with published literature. ¹⁷ The N–H signal is not visible.

¹³C NMR (151 MHz, CDCl₃): δ 162.14 (d, J = 245.8 Hz), 138.83 (broad), 135.70, 129.57, 126.73 (d, J = 8.0 Hz), 115.77 (d, J = 21.6 Hz), 114.25 (broad). These data are in agreement with published literature.¹⁷

¹⁹F NMR (564 MHz, CDCl₃): δ -115.68.

¹H NMR (600 MHz, MeOD): δ 7.72–7.67 (m, 3H), 7.37 (d, J = 0.8 Hz, 1H), 7.11–7.05 (m, 2H). The N–H signal is not visible.

¹³C NMR (151 MHz, MeOD): δ 163.29 (d, J = 244.2 Hz), 139.27 (broad), 137.10, 131.02, 127.67 (d, J = 7.9 Hz), 116.36 (d, J = 21.8 Hz), 115.79 (broad).

¹⁹F NMR (**564 MHz, MeOD**): δ -116.79.



Synthesis of tert-butyl (2-(4-(4-fluorophenyl)-1*H*-imidazol-1-yl)ethyl)carbamate **3.3-Boc**

A 500-mL jacketed glass reactor equipped with an overhead stirrer, baffle, thermocouple probe, 250-mL addition funnel, and nitrogen inlet adapter was charged with 5-(4-fluorophenyl)-1*H*-imidazole **3.2** (40.00 g, 246.7 mmol, 1.0 equiv) and anhydrous acetonitrile (120 mL, 3V) under dry, inert atmosphere. Stirring was initiated at 250 rpm. To the resulting pale, yellow suspension, freshly ground NaOH (29.60 g, 740.0 mmol, 3.0 equiv) was added in a single lot. **Process notes:** The use of flake NaOH has not been investigated but should be explored as an alternative to powdered NaOH during future process development. The resulting orange-beige suspension was maintained for 30 minutes at 25 °C and then warmed to 75 °C. **Process notes:** At this temperature, some etching of the glass reactor by NaOH was observed. We have not investigated whether or not etching occurs at lower temperatures. We do know that the alkylation proceeds with equal efficiency at 60 °C as at 75 °C (see section 2.3.3). Potentially the temperature could be reduced even further to help mitigate etching. **Caution:** Hydrolysis of acetonitrile by NaOH at elevated temperatures has been reported, which may present a risk of runaway reaction.²⁷

Meanwhile, a separate 500-mL three-necked round-bottomed flask equipped with an overhead stirrer, 125-mL addition funnel, and nitrogen inlet adapter was charged with 2-chloroethylamine hydrochloride (51.53 g, 444.3 mmol, 1.80 equiv) and anhydrous acetonitrile



(160 mL, 4V) under dry, inert atmosphere. Stirring was initiated at 250 rpm and the white suspension was cooled to 0-5 °C using an ice-water bath. Triethylamine (62 mL, 44.93 g, 444.0 mmol, 1.80 equiv) was added dropwise via the addition funnel over 15 minutes. The suspension thickened over the course of the addition. Once addition was completed, the suspension was maintained at 0-5 °C for an additional 15 minutes and then vacuum filtered thru a fritted glass funnel to remove Et₃NHCl. An additional portion of anhydrous acetonitrile (40 mL, 1V) was used to complete the transfer and rinse the cake. The pale, yellow filtrate (~200 mL) containing CEA free base dissolved in acetonitrile was used immediately.

The CEA solution thus prepared was added dropwise over one hour to the suspension of **3.2** and NaOH in acetonitrile at 75 °C using the 250-mL addition funnel. The reaction mixture lightened to a cream-colored suspension as the addition occurred. Once the addition was complete, the reaction was maintained at 75 °C for 2 hours. Conversion was monitored by HPLC (~90 A% of **3.3** at 254 nm and ~10 A% of **3.2** after 1-2 hours is a typical result). The reaction mixture was cooled to 25 °C and the 250-mL addition funnel was exchanged with a 125-mL addition funnel in anticipation of the Boc protection step.

Process notes: The Boc protection step has not been fully optimized. The main issue we encounter is that the reaction mixture becomes very thick as the Boc anhydride is added and is not adequately stirred by our paddle- or propeller-shaped impellers. Solids near the top of the reaction mass tend to clump together into a foamy, torus-shaped mass. This necessitated multiple *ad hoc* measures noted below in red text. This issue could perhaps be mitigated by using a helical- or anchor-shaped impeller, although this was not investigated in our laboratories.

Additionally, the procedure below calls for two charges of Boc anhydride solution (~1.0 equiv each). We have determined that a total of ~2.0 equiv of Boc anhydride is required to achieve full conversion to **3.3-Boc**. Provided the aforementioned stirring issues are addressed, we anticipate that the total amount of reagent can be added in one charge (~2.0 equiv over 1 hour) and give the same result as adding half the reagents in two separate charges.



In an Erlenmeyer flask, di-*tert*-butyl dicarbonate (62 mL, 59.2 g, 271 mmol, 1.1 equiv) was dissolved in anhydrous acetonitrile (40 mL, 1V). The resulting clear, colorless solution was added dropwise to the reaction mixture at 25 °C over 30 min using the 125-mL addition funnel, resulting in a thick, non-uniform, beige-cream suspension. An additional portion of anhydrous acetonitrile (80 mL, 2V) was added to the reactor. The temperature was increased to 40 °C. The mass of solids near the top of the reactor was mechanically separated. The stir rate was increased to 500 rpm. These interventions led to a marginal improvement in the reaction mass uniformity. In an Erlenmeyer flask, a second portion of di-*tert*-butyl dicarbonate (55 mL, 52.2 g, 239 mmol, 1.0 equiv) was dissolved in anhydrous acetonitrile (35 mL, 1V). The resulting clear, colorless solution was added dropwise to the reaction mixture at 40 °C over 30 min using the 125-mL addition funnel, resulting in a thick, uniform, cream-colored suspension. Once the addition was complete, the reaction was maintained at 25 °C for 1 hour. Conversion was monitored by HPLC (~80 A% of **3.3-Boc** at 254 nm and 0 A% of **3.3** after 1 hour is a typical result).

Upon completion, the reaction mass was drained from the reactor and vacuum filtered through a fritted glass funnel to remove insoluble components. Anhydrous acetonitrile (250 mL, 6V) was used to complete the transfer and rinse the filter cake. **Process notes:** The filtration proceeds slowly. The process took more than 1 hour on this scale. Mechanical agitation of the filter cake during filtration and rinsing seemed to improve the filtration rate. The solids removed during the filtration had a sticky, amorphous quality. Physical entrapment of desired **3.3-Boc** within this matrix is a possibility and may have a detrimental impact on yield. Maintenance of the filtration assembly (including slurry and cake) at an elevated temperature (40-45 °C) may improve the rate of filtration and increase the amount of **3.3-Boc** extracted from the filter cake into the rinse acetonitrile. The filtrate was concentrated by rotary evaporation in a 1-L flask to afford 109.68 g of crude **3.3-Boc** as a clumpy, wet-looking, pale, yellow solid.

Ethyl acetate (100 mL) was added to the crude material and the mixture was stirred (200 rpm) at 85 °C until all solids were dissolved. To the resulting orange solution, heptane (200 mL) was added at 85 °C. Stirring was stopped and the solution was slowly cooled to 25 °C over 2 hours, resulting in crystallization of **3.3-Boc**. The mixture was further maintained at 0-5 °C for several



hours to complete the crystallization. The crystals were collected by vacuum filtration and rinsed with two portions of cold solvent (each portion = 100 mL ethyl acetate and 200 mL heptane, for a total rinse volume of 600 mL). The off-white crystals were air-dried and then dried under high vacuum for 2 hours to afford 37.28 g of **3.3-Boc** (101 wt% assay, 100 LCAP, 49% yield for the telescoped process). **Process notes:** A significant amount of **3.3-Boc** is observed in the mother liquor (see section 2.3.2). Further optimization of the recrystallization conditions (including reducing the volume of solvents used) may increase the recovery of **3.3-Boc**.

¹H NMR (600 MHz, CDCl₃): δ 7.73–7.67 (m, 2H), 7.46 (d, *J* = 1.1 Hz, 1H), 7.13 (d, *J* =0.9 Hz, 1H), 7.08–7.03 m, 2H), 4.79 (bs, 1H), 4.09 (t, *J* = 5.3 Hz, 2H), 3.45 (q, *J* = 5.9 Hz, 2H), 1.44 (s, 9H).

¹³C NMR (151 MHz, CDCl₃): δ 162.12 (J = 245.3 Hz), 155.92, 142.04, 137.75, 130.40 (d, J = 3.2 Hz), 126.45 (J = 8.0 Hz), 115.61 (J = 21.6 Hz), 114.30, 80.26, 46.90, 41.69, 28.46.

¹⁹F NMR (564 MHz, CDCl₃): δ -116.06.

Synthesis of 2-(4-(4-fluorophenyl)-1H-imidazol-1-yl)ethan-1-amine (3.3)

To obtain a pure standard of **3.3** as a single regioisomer, the following procedure was applied. A scintillation vial equipped with a magnetic stir bar was charged with purified, crystalline **3.3-Boc** (500.8 mg, 1.64 mmol, 1 equiv) and *n*-butanol (5 mL, 10V). Stirring was initiated (250 rpm) at 25 °C and a homogeneous, pale, yellow solution resulted within 5 minutes. Then, a solution of 2M HCl in ethyl acetate (3.28 mL, 6.57 mmol, 4 equiv) was added dropwise over 1 minute. The vial was capped, heated to 50 °C, and maintained for 2.5 hours. Within 10 minutes, white



precipitates were observed. The white suspension was cooled to 25 °C and the precipitated **3.3-diHCl** was collected by vacuum filtration and washed with ethyl acetate (4 x 5 mL). The white solid was dried in a vacuum oven (40 Torr, 50 °C, 2 hours) to afford 413.9 mg (91%) of **3.3-diHCl**. ¹H NMR of the **3.3-diHCl** salt was acquired in MeOD. To acquire spectra of the free base form **3.3**, a small portion of the salt was partitioned between 3M aqueous NaOH and CDCl₃ (about 1 mL each) in a dram vial. The CDCl₃ phase was dried over MgSO₄, filtered, and analyzed by ¹H and ¹³C NMR.

3.3-diHCl

¹**H NMR (600 MHz, MeOD)**: δ 9.19 (d, J = 1.5 Hz, 1H), 8.10 (d, J = 1.5 Hz, 1H), 7.84–7.74 (m, 2H), 7.36–7.26 (m, 2H), 4.68 (t, J = 6.2 Hz, 2H), 3.61 (t, J = 6.2 Hz).

3.3

¹**H NMR (600 MHz, CDCl₃)**: δ 7.74–7.68 (m, 2H), 7.52 (s, 1H), 7.17 (s, 1H), 7.07–7.01 (m, 2H), 3.98 (t, *J* = 5.8 Hz, 2H), 3.07 (t, *J* = 5.8 Hz, 2H).

¹³C NMR (151 MHz, CDCl₃): δ 162.03 (d, J = 245.2 Hz), 141.80, 137.69, 130.47 (d, J = 3.1 Hz), 126.41 (d, J = 7.9 Hz), 115.53 (d, J = 21.5 Hz), 114.43, 50.53, 42.74.

¹⁹F NMR (**564 MHz, CDCl**₃): δ -116.22.



Synthesis of *t*-butyl (2-(5-bromo-4-(4-fluorophenyl)-1*H*-imidazol-1-yl)ethyl)carbamate **3.7-Boc**

A 250-mL three-necked round-bottomed flask equipped with an overhead stirrer, nitrogen inlet adapter, and addition funnel was charged with tert-butyl (2-(4-(4-fluorophenyl)-1H-imidazol-1-yl)ethyl)carbamate **3.3-Boc** (18.2 g, 93 wt%, 55.34 mmol, 1 equiv) and anhydrous acetonitrile (36 mL, 2V). Stirring was initiated (200 rpm) and the heterogeneous mixture was cooled to 0–5 °C. A solution of NBS (10.34 g, 58.11 mmol, 1.05 equiv) in anhydrous acetonitrile (146 mL, 8V) was added dropwise to the reaction mixture at 0–5 °C over a period of 30 minutes using the addition funnel. After the addition, the reaction mixture was warmed to 20–25 °C and maintained at this temperature for 1 hour. As the reaction proceeded, a homogeneous solution was observed. After full conversion was observed by HPLC, the reaction mixture was filtered to remove any insoluble matter. The filtrate (~192 mL) was distilled to a volume of ~65 mL and transferred to a 250-mL round-bottomed flask. The solution was heated to 50–55 °C, and water (115 mL, 6V) was added dropwise to the stirred solution over a period of 30 minutes using an addition funnel. The homogeneous mixture was maintained at 50-55 °C for 10 minutes and then cooled slowly to 20-25 °C and finally to 0–10 °C. The mixture was maintained at this temperature for 1 hour, over which time an off-white suspension was observed. The precipitates were collected by vacuum filtration, slurry washed with water (65mL), and dried in a vacuum oven (40 Torr, 50 °C, 2 hr) to afford 3.7-Boc as pale, yellow solid. (15.45 g, 73% yield, 101.4 wt% assay, 98.7 LCAP at 254 nm).

¹H NMR (600 MHz, CDCl₃): δ 7.92–7.86 (m, 2H), 7.57 (s, 1H), 7.12–7.06 (m, 2H), 4.99* (bs, 1H), 4.14* (t, J = 5.4 Hz, 2H), 3.43 (dd, J = 11.7, 6.0 Hz, 2H), 1.44 (s, 9H). Rotameric signals visible for the indicated (*) resonances.

¹³C NMR (151 MHz, CDCl₃): δ 162.26 (d, J = 246.6 Hz), 156.03, 138.43, 138.26, 129.38 (d, J = 3.2 Hz,), 128.37 (d, J = 8.0 Hz), 115.37 (d, J = 21.5 Hz), 99.32, 80.19, 45.87, 40.70, 28.48.



¹⁹F NMR (**564** MHz, CDCl₃): δ -114.96.

Synthesis of 2-(5-bromo-4-(4-fluorophenyl)-1H-imidazol-1-yl)ethan-1-amine dihydrochloride **3.7-diHCl**

A 1-L three-necked round-bottomed flask equipped with an overhead stirrer, septum, and nitrogen inlet adapter was charged with *tert*-butyl (2-(5-bromo-4-(4-fluorophenyl)-1*H*-imidazol-1-yl)ethyl)carbamate **3.7-Boc** (24.0 g, 62.5 mmol, 1.0 equiv) and anhydrous *n*-butanol (240 mL, 10V) at 25 °C. Stirring was initiated (200-300 rpm) and a homogenous, pale, yellow solution resulted. A commercial solution of 2M HCl in ethyl acetate (125 mL, 250 mmol, 4.0 equiv) was added dropwise over 10-20 minutes at 25 °C. No immediate change in appearance was observed. The solution was heated to 50 °C and maintained at this temperature for 2-3 hours; within the first 15 minutes, an off-white suspension was observed. After full conversion was observed by HPLC, the suspension was cooled to 25 °C and the white precipitate was collected by vacuum filtration. The solid was slurry washed with ethyl acetate (168 mL, 7V) and the cake was rinsed with an additional portion of ethyl acetate (72 mL, 3V). The white solid was dried in a vacuum oven (40 Torr, 50 °C, 2 hr) to afford **3.7-HCl** salt (22.2 g, 96% yield, 77.6 wt% assay (of **3.7**), 99.7 LCAP at 254 nm).

¹**H NMR (600 MHz, MeOD)**: δ 9.43 (bs, 2H), 7.85–7.79 (m, 2H), 7.38–7.32 (m, 2H), 4.75 (t, J = 6.4 Hz, 2H), 3.59 (t, J = 6.3 Hz, 2H).

¹³C NMR (151 MHz, MeOD): δ 165.20 (d, J = 250.4 Hz), 138.64, 133.41, 131.57 (d, J = 8.8 Hz), 123.47 (d, J = 3.3 Hz), 117.44 (d, J = 22.5 Hz), 106.30, 46.99, 39.52.

¹⁹F NMR (**564 MHz, MeOD**): δ -110.13.



Synthesis of 2-(5-bromo-4-(4-fluorophenyl)-1H-imidazol-1-yl)ethan-1-amine dihydrobromide **3.7-diHBr**

A 500-mL three-necked round-bottomed flask equipped with an overhead stirrer, septum, and nitrogen inlet adapter was charged with *tert*-butyl (2-(5-bromo-4-(4-fluorophenyl)-1*H*-imidazol-1-yl)ethyl)carbamate **3.7-Boc** (17.0 g, 44.2 mmol, 1.0 equiv) and anhydrous *n*-butanol (120 mL, 7V) at 25 °C. Stirring was initiated (200-300 rpm) and a homogenous, pale, yellow solution resulted. A commercial solution of 33% (w/w) HBr in acetic acid (23.8 mL, 133 mmol, 3.0 equiv) was added dropwise over 10-20 minutes at 25 °C. No immediate change in appearance was observed. The solution was heated to 50 °C and maintained at this temperature for 2-3 hours; within the first 15 minutes, an off-white suspension was observed. After full conversion was observed by HPLC, the suspension was cooled to 25 °C and slurry washed with ethyl acetate (120 mL, 7V). The white precipitates were collected by vacuum filtration and the cake was rinsed with an additional portion of ethyl acetate (150 mL, 9V). The white solid was dried in a vacuum oven (40 Torr, 50 °C, 2 hr) to afford **3.7-HBr** salt (19.1 g, 97% yield, 64.3 wt% assay (of **3.7**), 99.9 LCAP at 254 nm).

¹**H NMR (600 MHz, MeOD)**: δ 9.50 (s, 1H), 7.85–7.79 (m, 2H), 7.38–7.32 (m, 2H), 4.78 (t, J = 6.4 Hz, 2H), 3.64 (t, J = 6.4 Hz, 2H).

¹³C NMR (151 MHz, MeOD): δ 165.14 (d, J = 250.4 Hz), 138.51, 133.22, 131.66 (d, J = 8.8 Hz), 123.34 (d, J = 3.4 Hz), 117.40 (d, J = 22.5 Hz), 106.65, 47.03, 39.56.

¹⁹**F NMR (564 MHz, MeOD)**: δ -110.09



Synthesis of 2-(4-fluorophenyl)-8,8-dimethyl-5,6,7,8-tetrahydroimidazo[1,2-a]pyrazine 3.4

A 300-mL stainless steel Parr reactor was charged with 2-(5-bromo-4-(4-fluorophenyl)-1H-imidazol-1-yl)ethan-1-amine dihydrochloride 3.7-HCl (15.0 g, 32.0 mmol, 1.0 equiv), zeolite aluminosilicate (15.0 g), anhydrous n-butanol (150 mL, 10 V), acetone (9.4 mL, 127.8 mmol, 4.0 equiv), and triethylamine (4.9 mL, 35.1 mmol, 1.1 equiv) resulting in a beige suspension. The Parr reactor was sealed and pressurized with nitrogen gas to 10 psi. Stirring was initiated (800 rpm) and the reactor was heated to 150 °C and maintained at this temperature for 24 hours. Conversion was monitored by HPLC (aliquots were withdrawn through the sampling valve while maintaining temperature and pressure). Upon completion, the reactor was cooled to 25 °C and the brown-black reaction mass was vacuum filtered to remove insoluble components. The filter cake was washed with n-butanol (30 mL, 2V). The filtrate was transferred to a 2-L jacketed glass reactor equipped with an overhead stirrer and vacuum distillation apparatus. The filtrate was neutralized by the addition of sat. aq. NaHCO₃ (150 mL, 10V) and the mixture was stirred for 10 minutes at 25 °C. The mixture was diluted with EtOAc (300 mL, 20V) and stirred for an additional 10 minutes at 25 °C. Stirring was stopped and the aqueous phase was drained. The aqueous phase was extracted with EtOAc (2 x 150 mL) and the extracts were added back into the reactor. The combined organic phases were washed with water (3 x 150 mL), and then washed with brine (300 mL, 20V). Distillative removal of EtOAc afforded a solution of crude 3.4 in residual n-butanol, which was further concentrated by rotary evaporation (20 Torr, 50 °C) to afford crude 3.4 as a black tar (6.7 g, 60.3 LCAP at 254 nm, 25.3 wt% purity, 22% adjusted yield). Process notes: This batch of crude 3.4 was split into several smaller portions to screen purification strategies. For this reason, the following purification protocol is demonstrated on a 1.0 g scale of crude 3.4. A 100-mL roundbottomed flask equipped with a magnetic stir bar was charged with crude 3.4 (1.0 g, 25.3 wt%



purity) and MTBE (25 mL, 25V). The heterogeneous mixture was stirred for 15 minutes at 25 °C. Insoluble components were removed by vacuum filtration and the filter cake was washed with MTBE (10 mL, 10V). The filtrate (35 mL) was transferred to a 100-mL flask with water (25 mL, 25V) and the stirred, biphasic mixture was acidified to pH 1.0-1.5 by the addition of concentrated HCl. Stirring was continued for 5 minutes at 25 °C and then the layers were separated. The aqueous phase (containing 3.4-diHCl) was washed with MTBE (20 mL, 20V) and transferred to a 100-mL flask with MTBE (20 mL, 20V). The stirred, biphasic mixture was adjusted to pH 3.0-3.5 by the addition of 7% aq. NaHCO₃ at 25 °C. Stirring was continued for 5 minutes at 25 °C and then the layers were separated. The aqueous phase (containing 3.4-diHCl) was washed with MTBE (20 mL, 20V) and transferred to a 100-mL flask with MTBE (25 mL, 25V). The stirred, biphasic mixture was adjusted to pH 4.5-5.0 by the addition of 7% ag. NaHCO₃ at 25 °C. Stirring was continued for 5 minutes at 25 °C and then the layers were separated. The aqueous phase (containing 3.4-diHCl) was transferred to a 100-mL flask with MTBE (25 mL, 25V). The stirred, biphasic mixture was adjusted to pH 8.0-9.0 by the addition of 7% aq. NaHCO₃ at 25 °C. The stirred, biphasic mixture was further adjusted to pH 11.0-12.0 by the addition of 1M aq. NaOH at 25 °C. Stirring was continued for 5 minutes at 25 °C and then the layers were separated. The aqueous phase was extracted with MTBE (40 mL, 40V). The combined organic phases (65 mL) were washed with water (25 mL), transferred to a 100-mL flask, and slurried with activated charcoal (100 mg) for 20 minutes at 25 °C. The mixture was vacuum filtered through Celite to remove charcoal, and the filter pad was rinsed with MTBE (10 mL). Concentration of the filtrate afforded **3.4** as a friable yellow solid (170 mg, 92.5 LCAP at 254 nm, 81.0 wt% purity).

¹**H NMR** (**600 MHz, CDCl**₃): δ 7.72–7.64 (m, 2H), 7.07–6.99 (m, 2H), 6.95 (s, 1H), 3.96 (t, J = 5.5 Hz, 2H), 3.30 (t, J = 5.5 Hz, 2H), 1.58 (s, 6H).

¹³C NMR (151 MHz, CDCl₃): δ 161.99 (d, J = 244.6 Hz), 150.71, 139.87, 130.95 (d, J = 3.1 Hz), 126.74 (d, J = 7.9 Hz), 115.43 (d, J = 21.5 Hz), 113.35, 52.56, 46.11, 38.69, 29.15.

¹⁹F NMR (564 MHz, CDCl₃): δ -116.73.



¹H NMR (600 MHz, DMSO-d₆): δ 7.76–7.66 (m, 2H), 7.38 (s, 1H), 7.18–7.09 (m, 2H), 3.88 (t, J = 5.4 Hz, 2H), 3.08 (t, J = 5.3 Hz, 2H), 1.39 (s, 6H). These data are in agreement with those reported in literature¹ except that the upfield methylene group is reported at 2.51 rather than 3.08 ppm.

¹³C NMR (151 MHz, DMSO- d_6): δ 160.72 (d, J = 241.8 Hz), 150.61, 137.60, 131.44 (d, J = 2.9 Hz), 125.88 (d, J = 7.9 Hz), 115.13 (J = 21.4 Hz), 114.21, 51.51, 45.41, 37.95, 28.73.



Synthesis of tert-butyl (2-(5-(4-fluorophenyl)-1H-imidazol-1-yl)ethyl)carbamate (*iso-3.3-Boc*)

KR198-X105

chromatographed

• independent synthesis of *iso*-3.3-Boc by van Leusen rxn for analytical standard (of minor alkylation regioisomer)

This procedure was adapted from a literature procedure for a similar compound.²⁸ It has not been optimized. A 100-mL round bottomed flask equipped with a magnetic stir bar was charged with 4-fluorobenzaldehyde (2.50 g, 2.14 mL, 20.14 mmol, 1.0 equiv), DMF (20 mL), water (2 mL), and *tert*-butyl (2-aminoethyl)carbamate (6.45 g, 6.38 mL, 40.29 mmol, 2.0 equiv). The resulting pale, yellow solution was stirred for 2 hours at 25 °C under nitrogen atmosphere. Then, potassium carbonate (4.17 g, 30.17 mmol, 1.50 equiv) and TosMIC (4.72 g, 24.18 mmol, 1.20 equiv) were added sequentially (lot-wise, as solids) and the resulting beige suspension was heated to 50 °C and maintained for 24 hours, at which point full consumption of TosMIC was observed by ¹H NMR. The reaction mixture was cooled to 25 °C and partitioned between ethyl acetate (75 mL) and water (75 mL) and the layers were separated. The organic phase was washed with 5% (w/v) LiCl aqueous (2 x 75 mL) and brine (1 x 75 mL), dried over MgSO₄, filtered, and concentrated to afford the crude product as a viscous orange oil. The major species are *iso-3.3-Boc* and the putative imine intermediate (uncyclized). The crude mixture was purified by flash column chromatography (silica gel, methanol-chloroform gradient elution, 2% to 20%) to afford 1.45 g (24%) of *iso-3.3-Boc* as a pale, yellow solid.

¹**H NMR** (**600 MHz, CDCl**₃): δ 7.52 (s, 1H), 7.37–7.29 (m, 2H), 7.17–7.09 (m, 2H), 7.03 (s, 1H), 4.64 (bs, 1H), 4.08 (bt, J = 5.3 Hz, 2H), 3.22 (app q, J = 6.1 Hz, 2H), 1.40 (s, 9H).

¹³C NMR (151 MHz, CDCl₃): δ 162.84 ($J_{\text{C-F}}$ = 248.4 Hz), 155.80, 138.68, 131.91, 130.91 ($J_{\text{C-F}}$ = 7.98 Hz), 128.86, 125.99 ($J_{\text{C-F}}$ = 3.32 Hz), 116.12 ($J_{\text{C-F}}$ = 21.66 Hz), 80.10, 44.89, 41.25, 28.42.

¹⁹F NMR (564 MHz, CDCl₃): δ -113.37.



Synthesis of 2-(5-(4-fluorophenyl)-1H-imidazol-1-yl)ethan-1-amine (*iso-3.3*)

A scintillation vial equipped with a magnetic stir bar was charged with *iso-3.3-Boc* (501.4 mg, 1.64 mmol, 1 equiv) and *n*-butanol (5 mL, 10V). Stirring was initiated (300 rpm) at 25 °C and a homogeneous, yellow solution resulted within 5 minutes. Then, a solution of 2M HCl in ethyl acetate (3.28 mL, 6.57 mmol, 4 equiv) was added dropwise over 1 minute. The vial was capped, heated to 50 °C, and maintained for 3 hours. Within 2 hours, a pale, yellow suspension resulted. Full conversion was confirmed by HPLC. The suspension was cooled to 25 °C and the precipitated *iso-3.3-diHCl* was collected by vacuum filtration and washed with ethyl acetate (4 x 5 mL). The pale, yellow solid was dried in a vacuum oven (40 Torr, 50 °C, 2 hours) to afford 415.8 mg (91%) of *iso-3.3-diHCl* (100 A% purity at 254 nm). ¹H NMR of the *iso-3.3-diHCl* salt was acquired in MeOD. To acquire spectra of the free base form *iso-3.3*, a small portion of the salt was partitioned between 3M aqueous NaOH and CDCl₃ (about 1 mL each) in a dram vial. The CDCl₃ phase was dried over MgSO₄, filtered, and analyzed by ¹H and ¹³C NMR.

iso-3.3-diHCl

¹**H NMR (600 MHz, MeOD)**: δ 9.26 (d, J = 1.4 Hz, 1H), 7.70 (d, J = 1.5 Hz, 1H), 7.68–7.63 (m, 2H), 7.40–7.34 (m, 2H), 4.61 (t, J = 6.8 Hz, 2H), 3.28 (t, J = 6.9 Hz).

iso-3.3

¹**H NMR** (**600 MHz, CDCl**₃): δ 7.62 (s, 1H), 7.38–7.32 (m, 2H), 7.16–7.10 (m, 2H), 7.05 (s, 1H), 4.00 (t, J = 6.2 Hz, 2H), 2.88 (t, J = 6.2 Hz, 2H).



¹³C NMR (151 MHz, CDCl₃): δ 162.81 (d, J = 248.4 Hz), 138.53, 132.05, 130.97 (d, J = 8.2 Hz), 128.75, 126.19 (d, J = 3.5 Hz), 116.04 (d, J = 21.6 Hz), 48.38, 42.50.

¹⁹F NMR (**564** MHz, CDCl₃): δ -113.54.

Synthesis of 2-(4-fluorophenyl)-2-oxoethyl formate

The following procedure is unoptimized. A scintillation vial equipped with a magnetic stir bar was charged with sodium hydroxide (183.1 mg, 4.58 mmol, 2.0 equiv), water (500 µL, 1V), and formic acid (174 µL, 4.61 mmol, 2.0 equiv) and stirred until homogeneous. The solution was diluted with denaturated ethanol (4.5 mL, 9V) which caused a white precipitate to form. Finally, 2-bromo-1-(4-fluorophenyl)ethan-1-one (500 mg, 2.30 mmol, 1.0 equiv) was added in one portion. The vial was capped and the suspension was heated to 75 °C and maintained for 2 hours. The suspension clarified to a nearly clear, colorless, homogeneous solution within 1 hour. Near complete consumption of starting material was observed by HPLC (only 2 A% remaining) and TLC. The reaction mixture was cooled to 25 °C and partitioned between water and diethyl ether. The layers were separated, and the aqueous phase was extracted with ethyl acetate. The combined organic phases were washed with sat. aq. NaHCO3 and brine, dried over MgSO4, filtered, and concentrated to afford 333.0 mg of crude product as a mixture of two major species. The crude mixture was purified by flash column chromatography (silica gel, ethyl acetate-hexanes gradient elution, 10% to 60%) to afford 72.5 mg (17%) of 2-(4-fluorophenyl)-2-oxoethyl formate as a white solid. The hydrolysis product, 1-(4-fluorophenyl)-2-hydroxyethan-1-one (104 mg, white solid) was also isolated from later-eluting fractions (several mixed fractions were discarded).



Both of these species are observed by HPLC between the first 0-45 minutes of Bredereck imidazole synthesis (Milestone 2, **3.1** to **3.2**) but disappear by 60 minutes as they are converted to further downstream intermediates.

2-(4-fluorophenyl)-2-oxoethyl formate

¹H NMR (600 MHz, CDCl₃): δ 8.25 (s, 1H), 8.00–7.93 (m, 2H), 7.22–7.14 (m, 2H), 5.40 (s, 2H). These data match those reported in the literature.²⁹

¹³C NMR (151 MHz, CDCl₃): δ 189.73, 166.40 (d, J = 256.6 Hz), 160.14, 130.69 (d, J = 9.5 Hz), 130.56 (d, J = 3.1 Hz), 116.38 (d, J = 22.1 Hz), 65.26. These data match those reported in the literature.²⁹

HPLC: elution time 6.3 min (refer to ADR for method information)

1-(4-fluorophenyl)-2-hydroxyethan-1-one

¹H NMR (600 MHz, CDCl₃): δ 8.01–7.91 (m, 2H), 7.23–7.14 (m, 2H), 4.85 (d, J = 4.7 Hz, 2H), 3.46 (t, J = 4.7 Hz, 1H). These data match those reported in the literature. ³⁰

¹³C NMR (151 MHz, CDCl₃): δ 196.97, 166.53 (d, J = 256.8 Hz), 130.57 (d, J = 9.5 Hz), 129.99 (d, J = 3.1 Hz), 116.43 (d, J = 22.1 Hz), 65.46. These data match those reported in the literature.³⁰

HPLC: elution time 2.8 min (refer to ADR for method information)



3.2 NMR & HPLC spectra

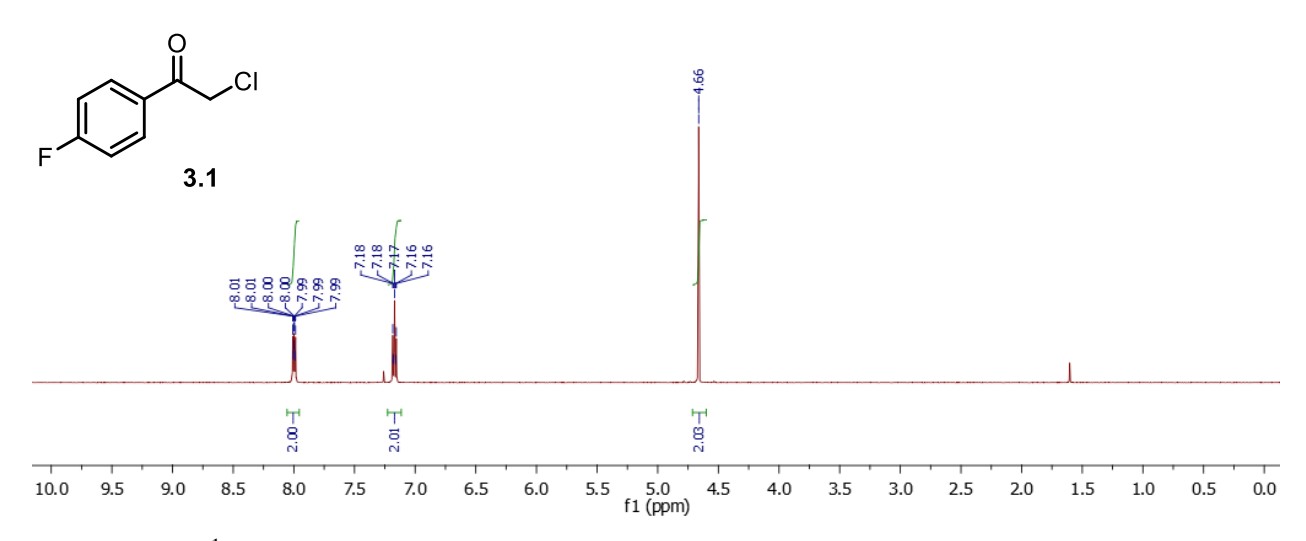


Figure 3.2.1. ¹H NMR spectrum of 3.1 in CDCl₃.

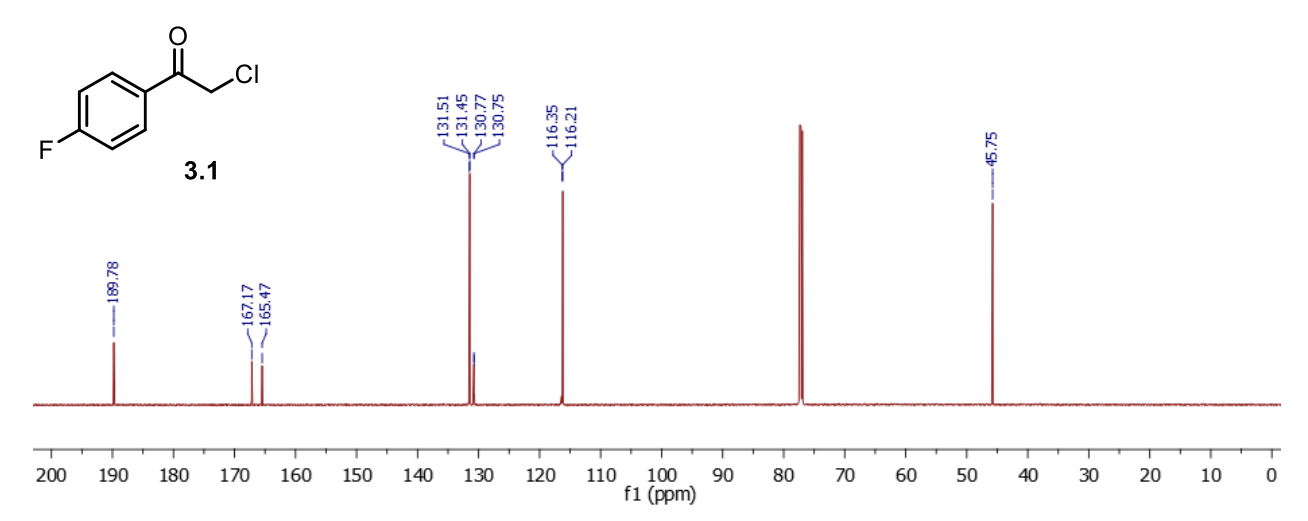


Figure 3.2.2. ¹³C NMR spectrum of 3.1 in CDCl₃.



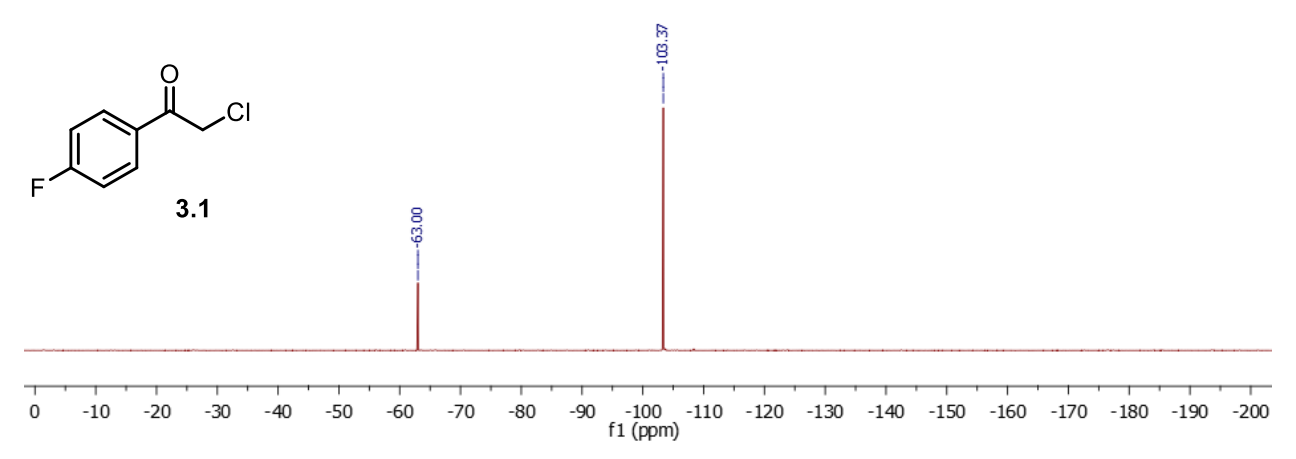


Figure 3.2.3. ¹⁹F NMR spectrum of 3.1 in CDCl₃.

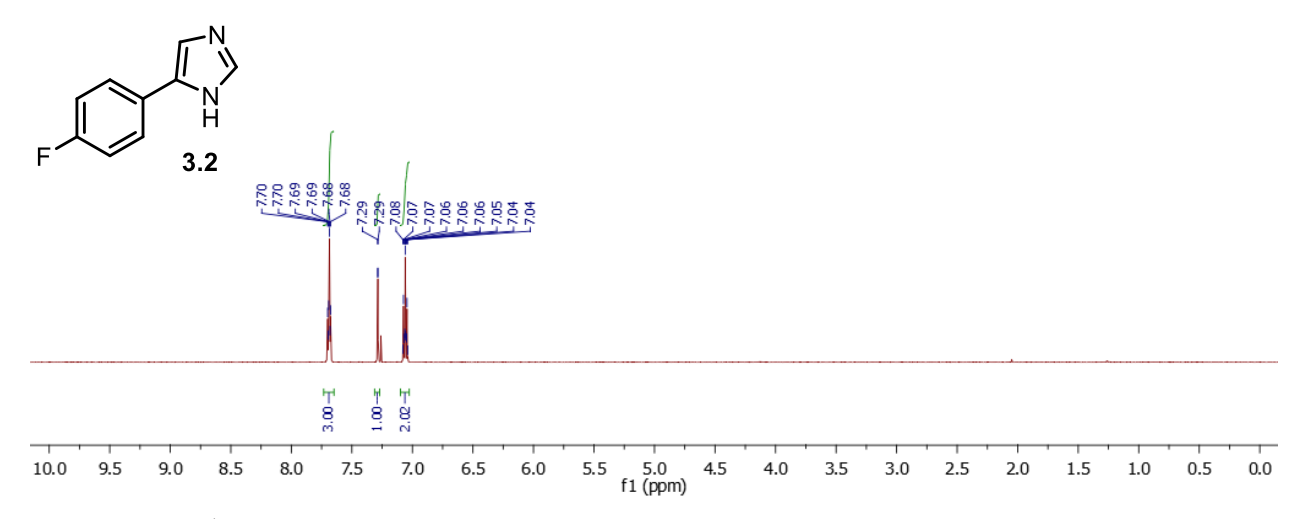


Figure 3.2.4. ¹H NMR spectrum of 3.2 in CDCl₃.



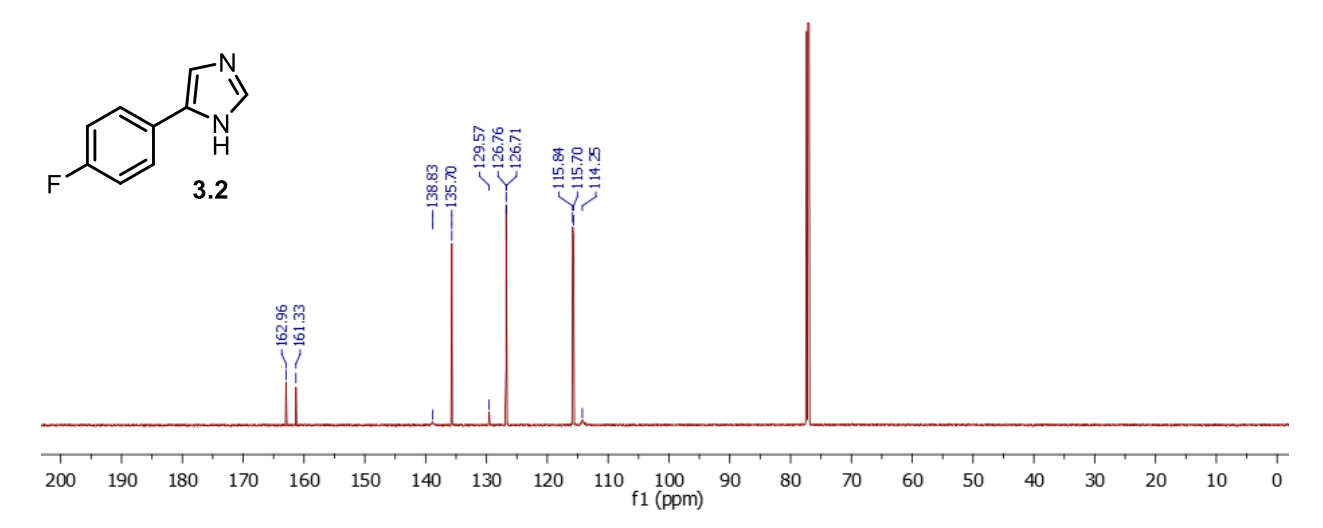


Figure 3.2.5. ¹³C NMR spectrum of 3.2 in CDCl₃.

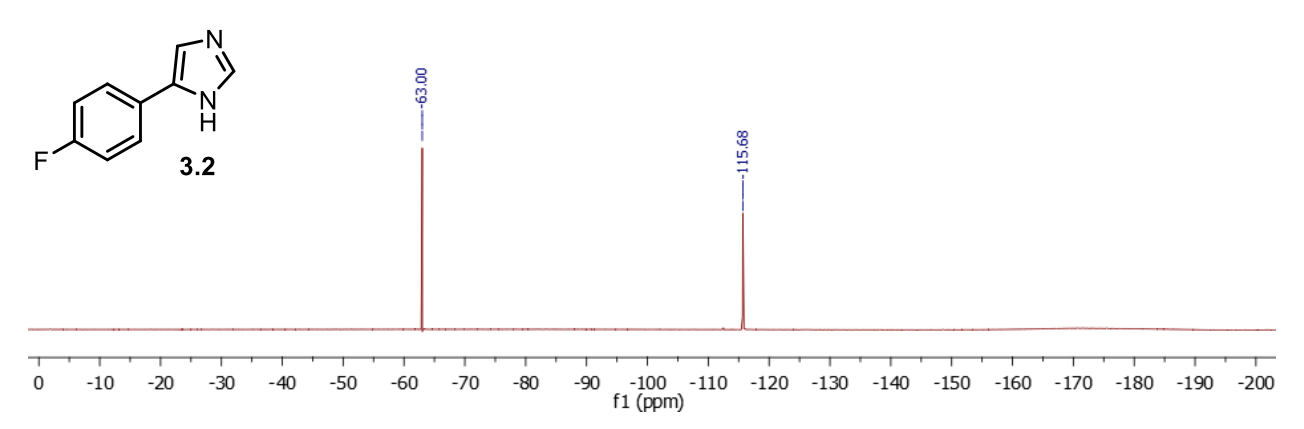


Figure 3.2.6. ¹⁹F NMR spectrum of 3.2 in CDCl₃.



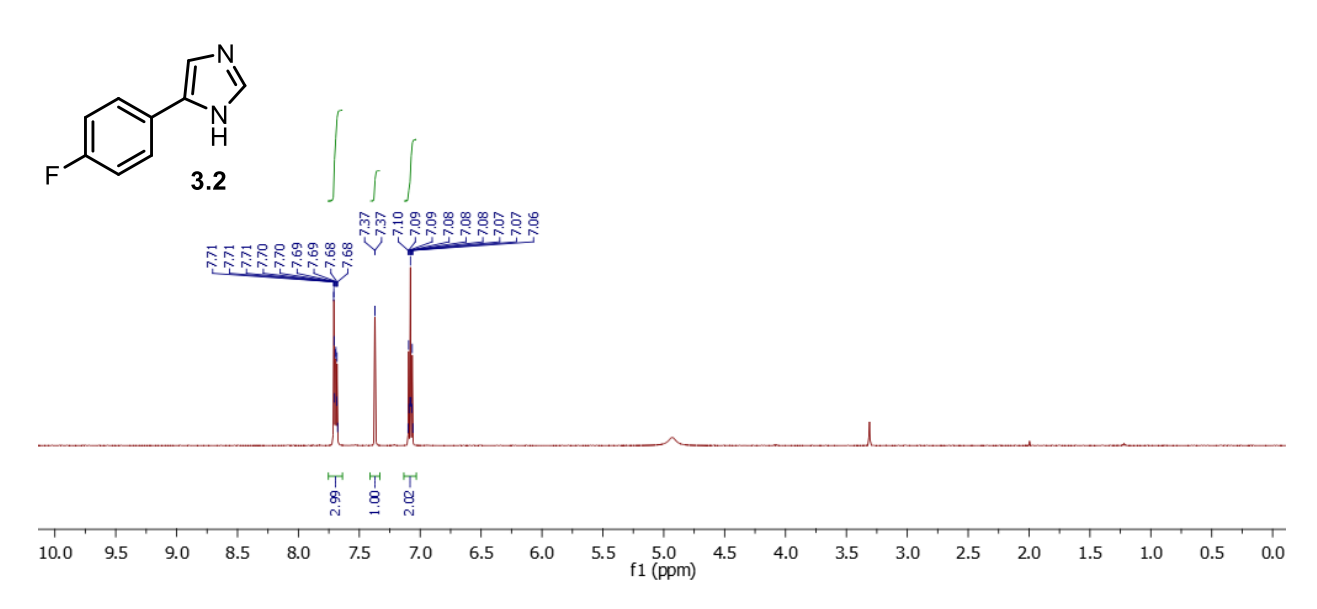


Figure 3.2.7. ¹H NMR spectrum of 3.2 in MeOD.

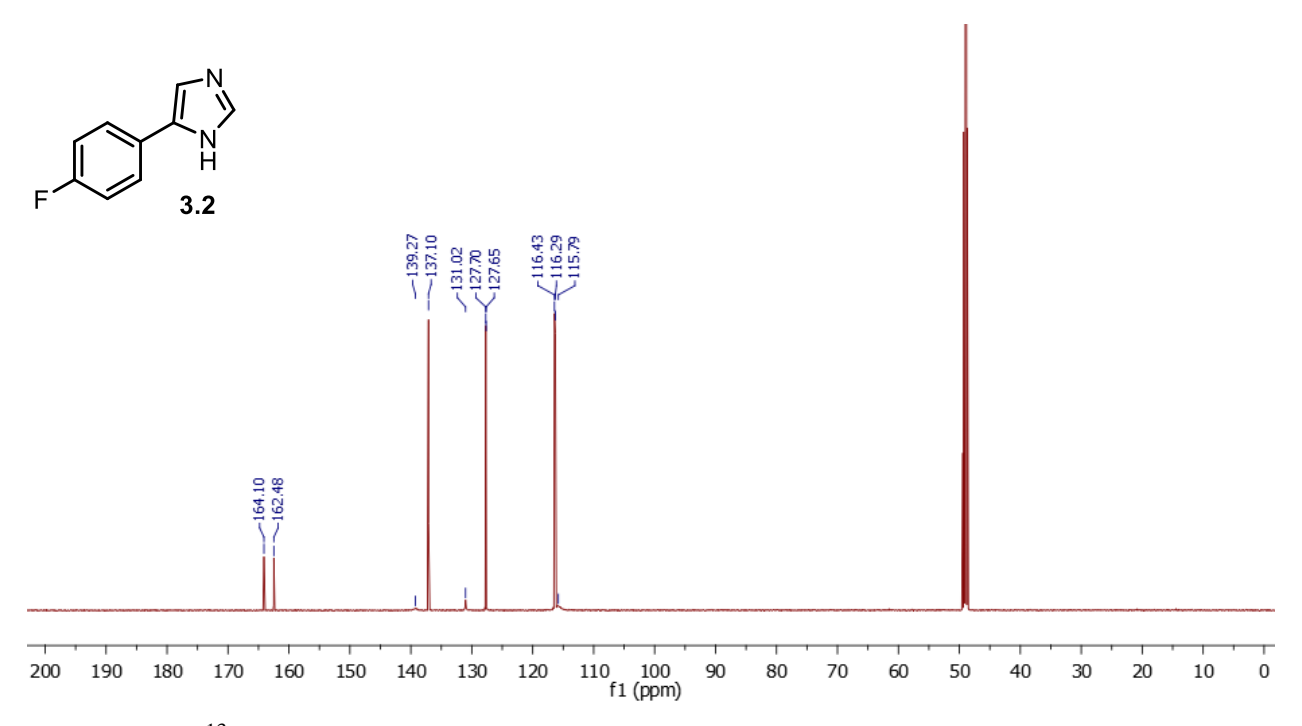


Figure 3.2.8. ¹³C NMR spectrum of 3.2 in MeOD.



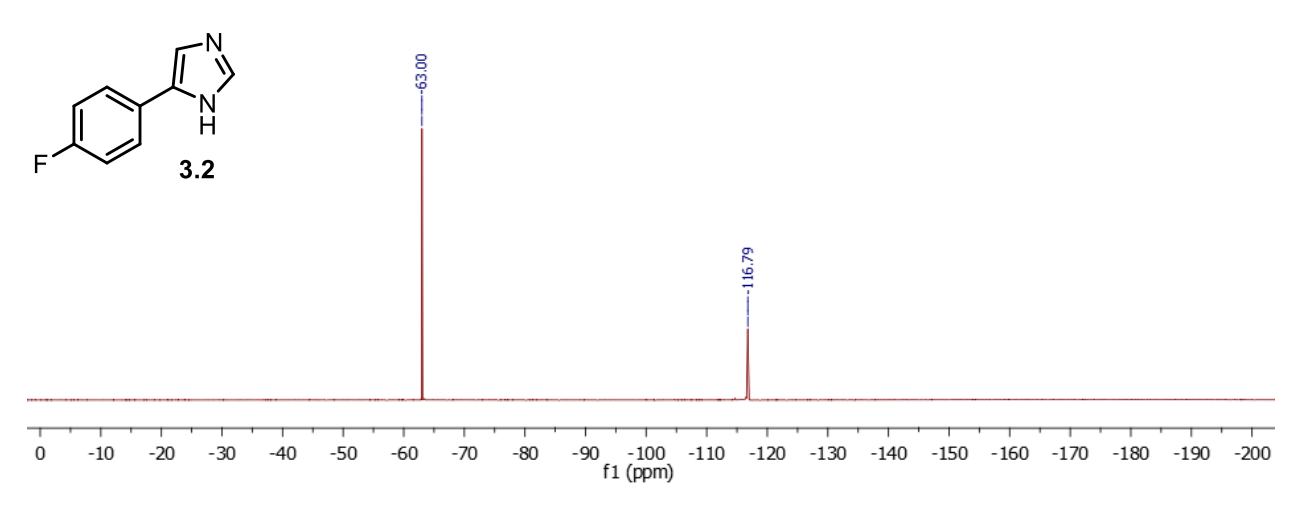


Figure 3.2.9. ¹⁹F NMR spectrum of 3.2 in MeOD.

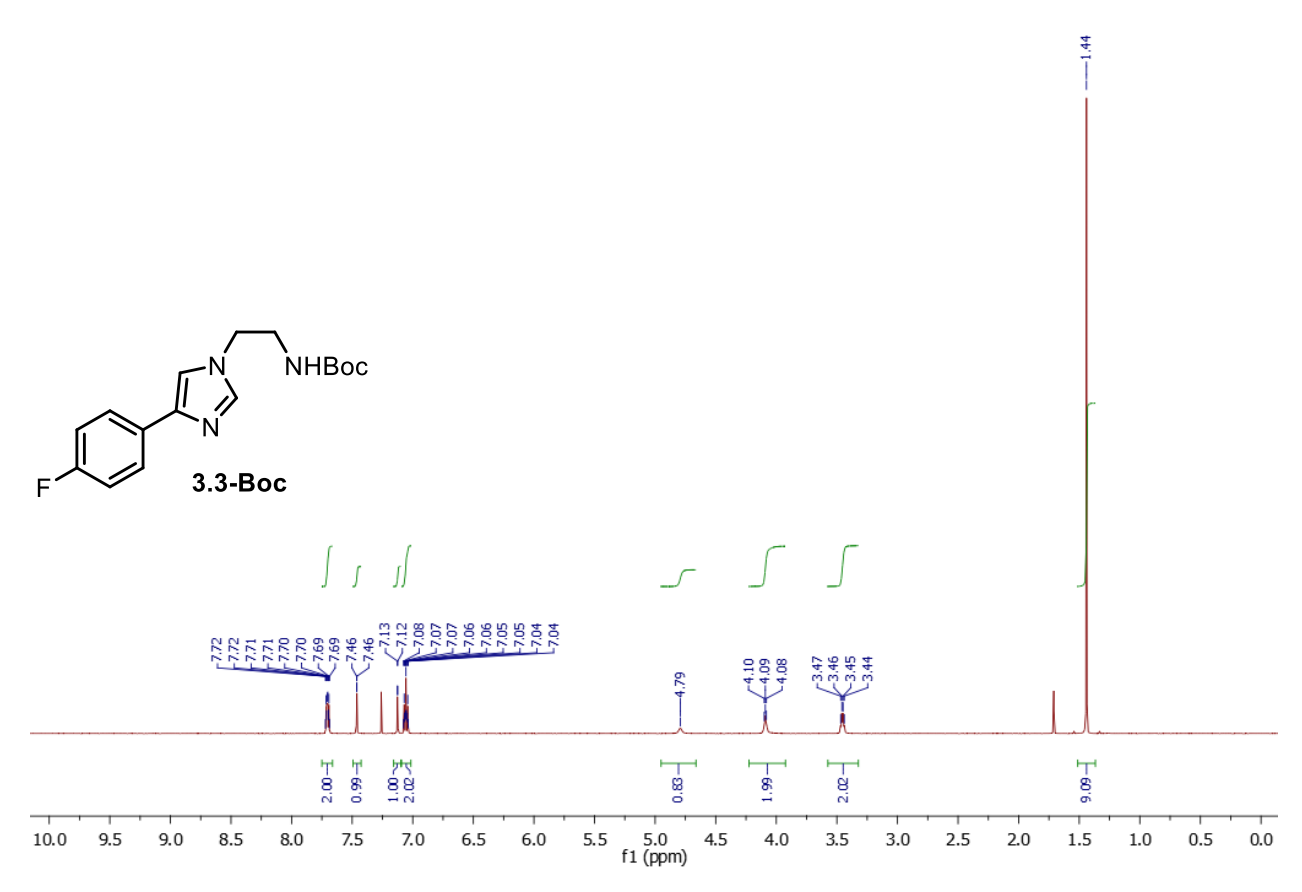


Figure 3.2.10. ¹H NMR spectrum of 3.3-Boc in CDCl₃.



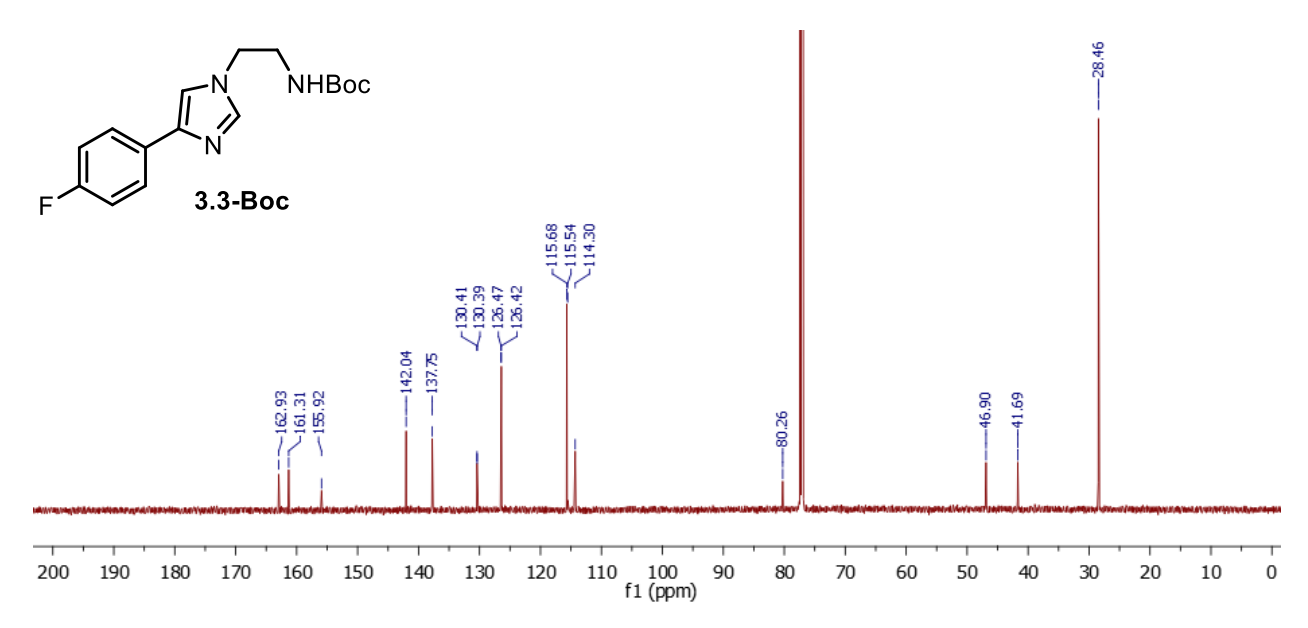


Figure 3.2.11. ¹³C NMR spectrum of 3.3-Boc in CDCl₃.

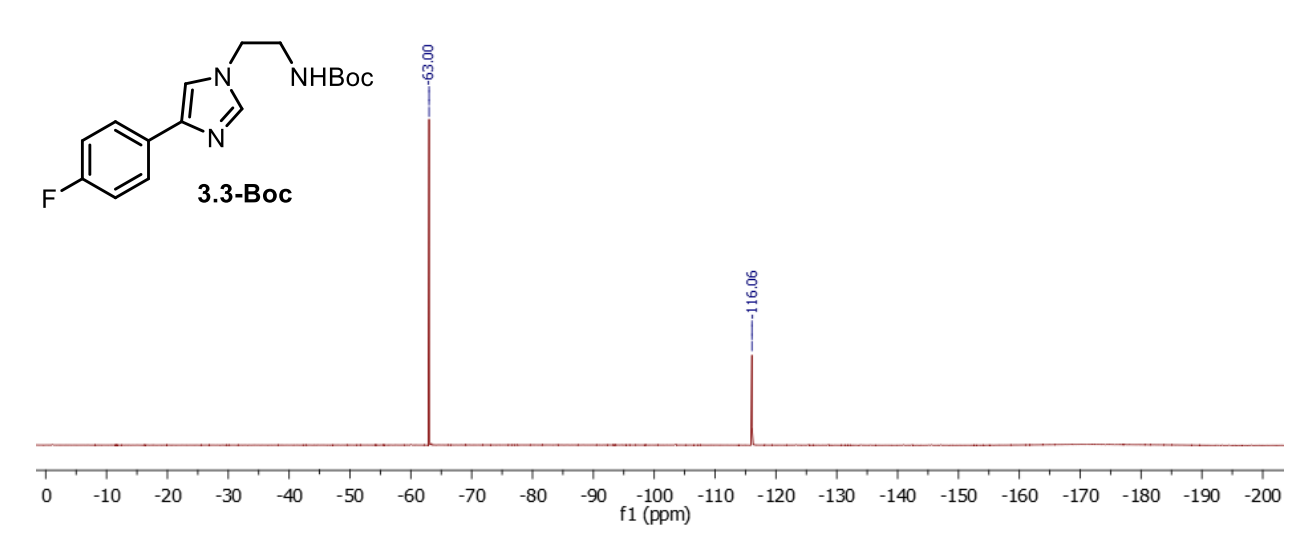


Figure 3.2.12. ¹⁹F NMR spectrum of 3.3-Boc in CDCl₃.



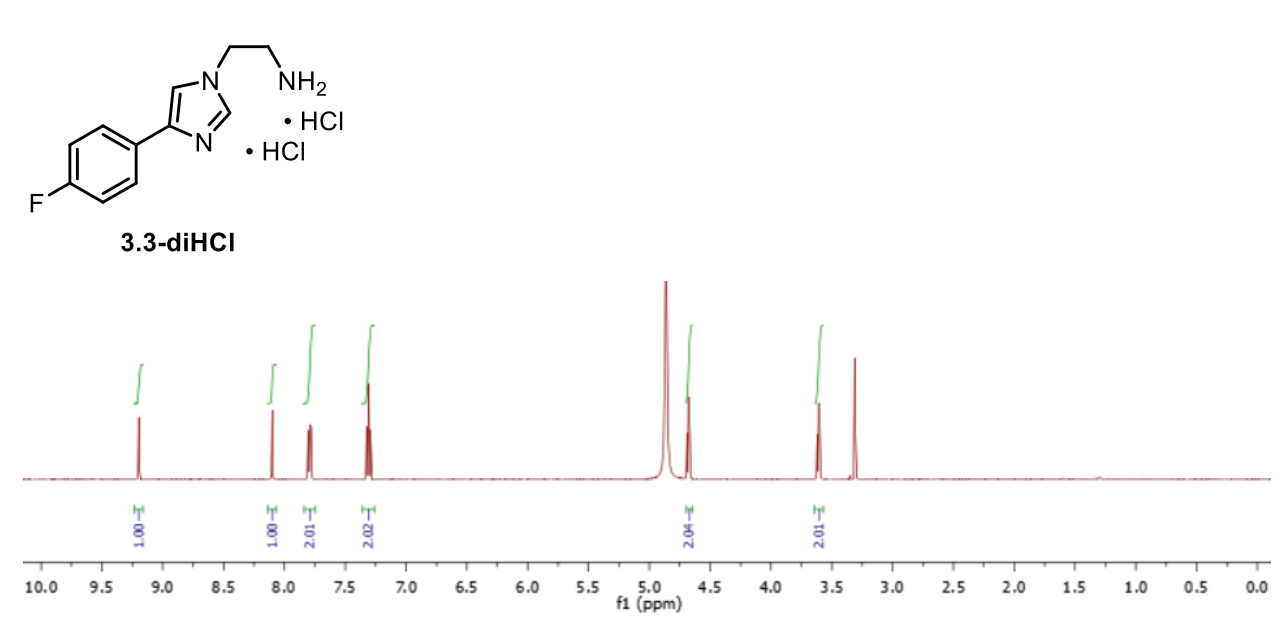


Figure 3.2.13. ¹H NMR spectrum of 3.3-diHCl in MeOD.

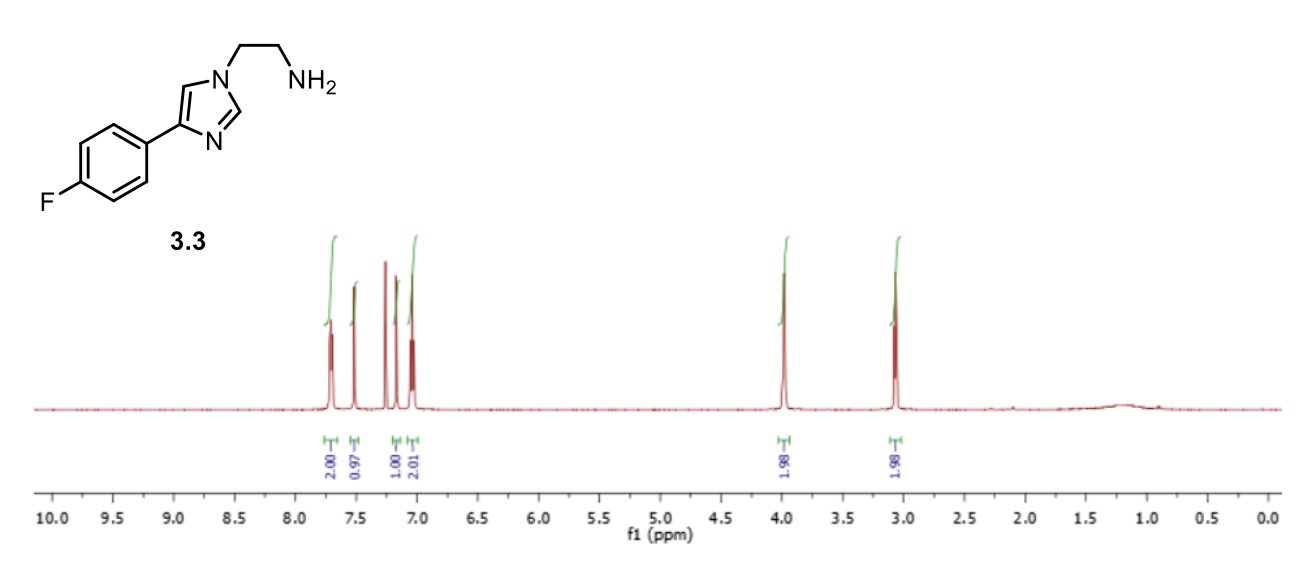


Figure 3.2.14. ¹H NMR spectrum of 3.3 in CDCl₃.



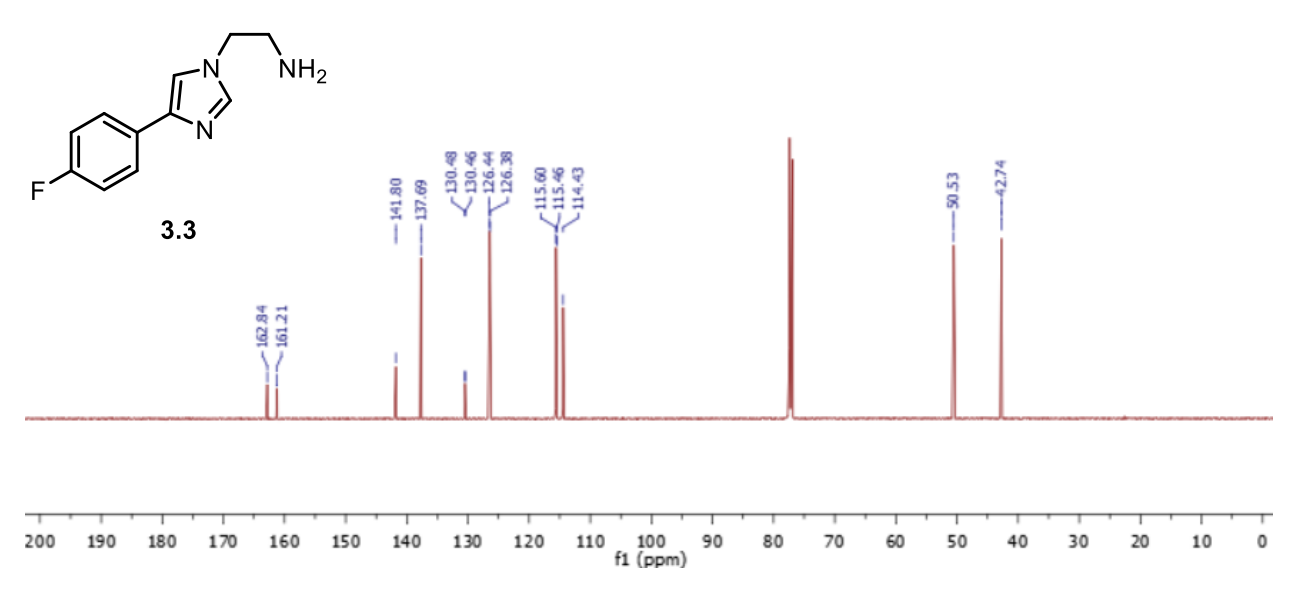


Figure 3.2.15. ¹³C NMR spectrum of 3.3 in CDCl₃.

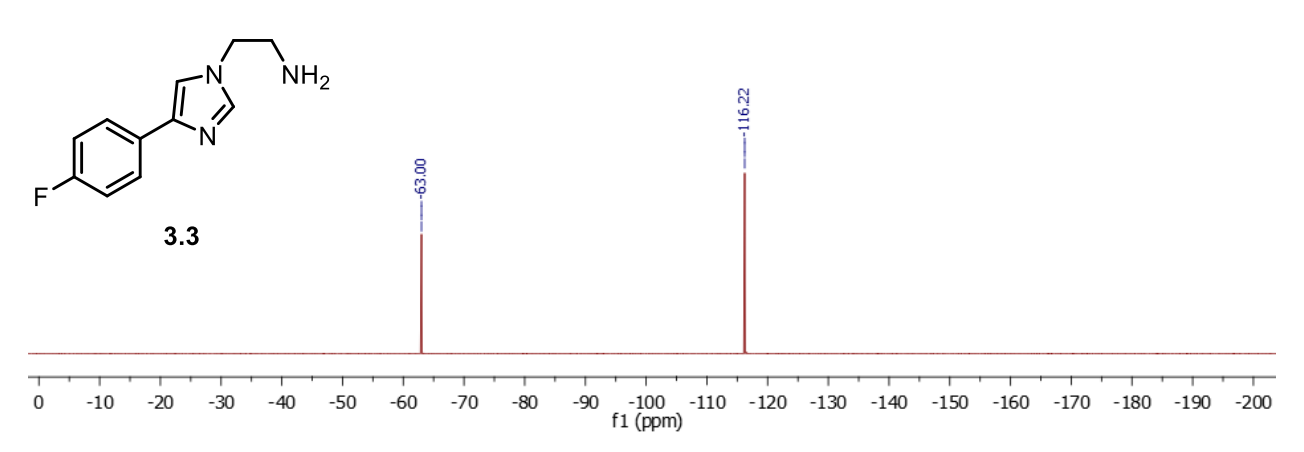


Figure 3.2.16. ¹⁹F NMR spectrum of 3.3 in CDCl₃.



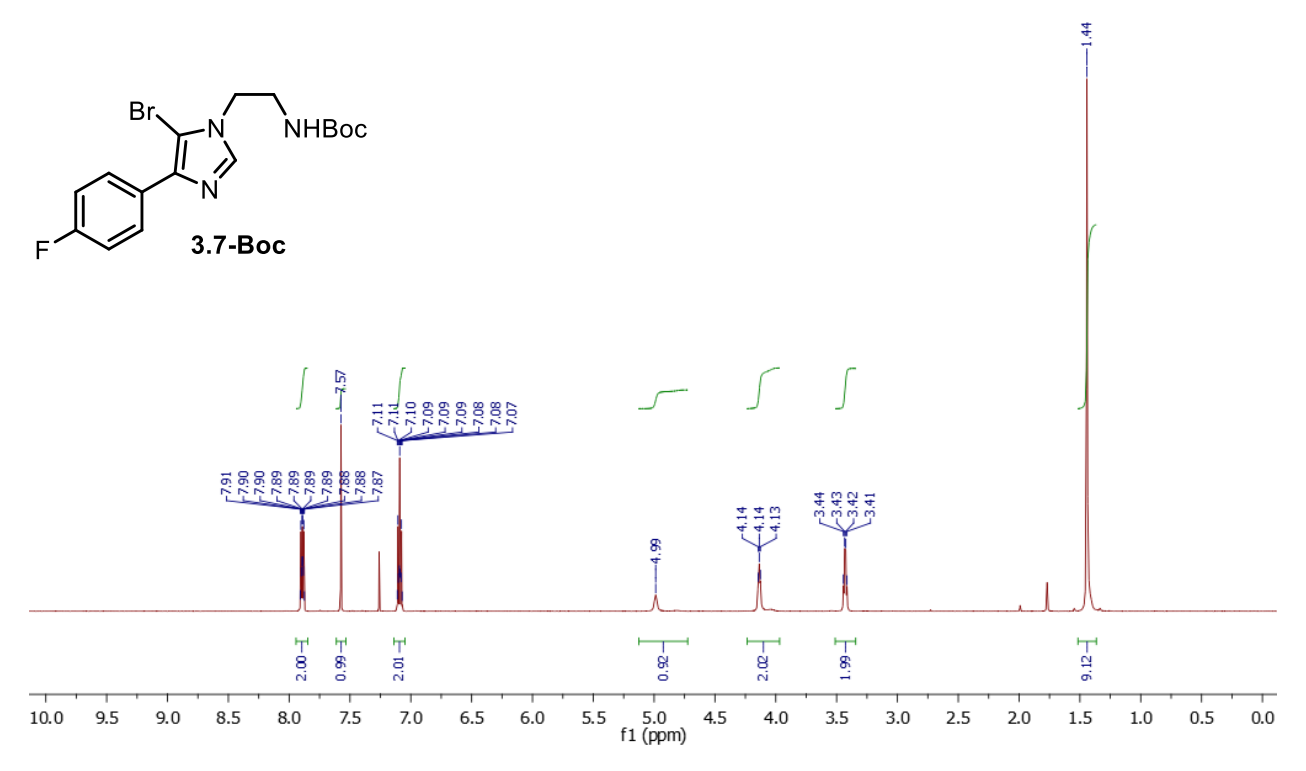


Figure 3.2.17. ¹H NMR spectrum of 3.7-Boc in CDCl₃.

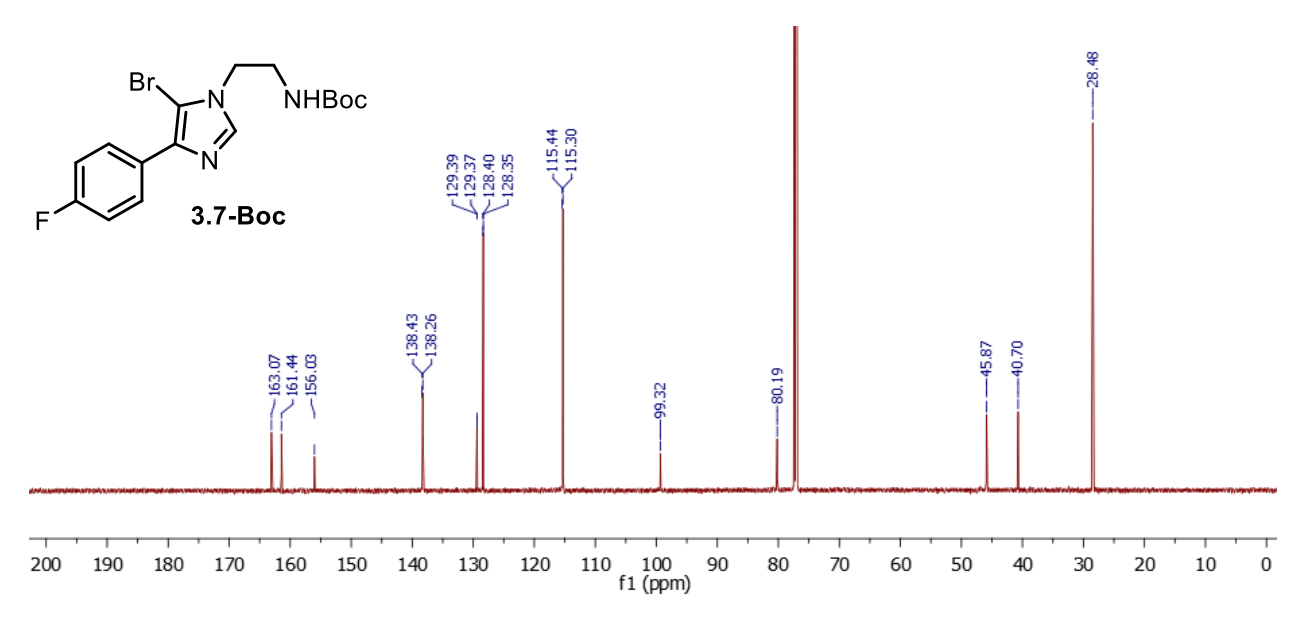


Figure 3.2.18. ¹³C NMR spectrum of 3.7-Boc in CDCl₃.



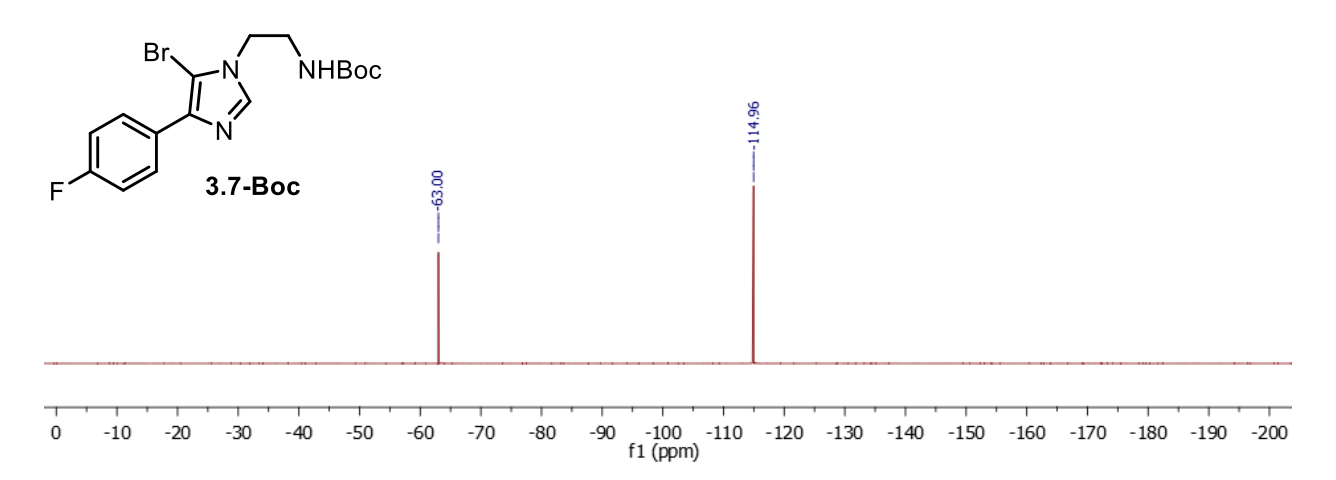


Figure 3.2.19. ¹⁹F NMR spectrum of 3.7-Boc in CDCl₃.

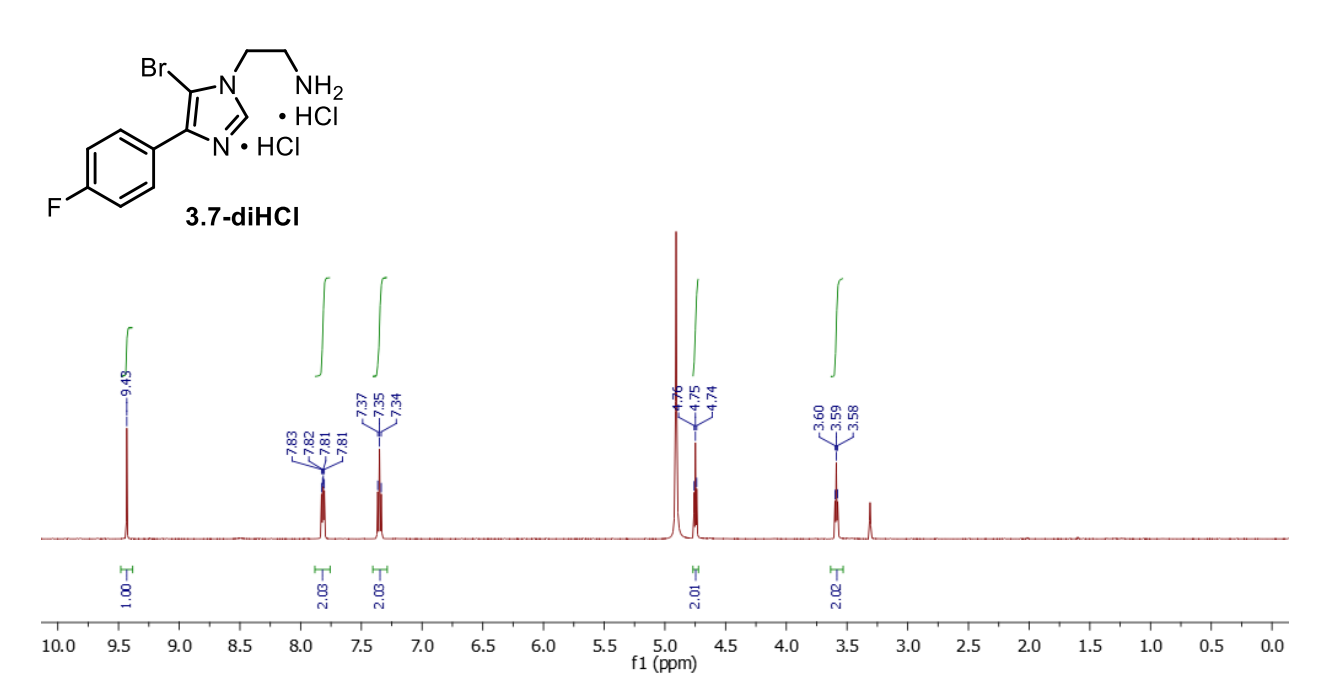


Figure 3.2.20. ¹H NMR spectrum of 3.7-diHCl in MeOD.



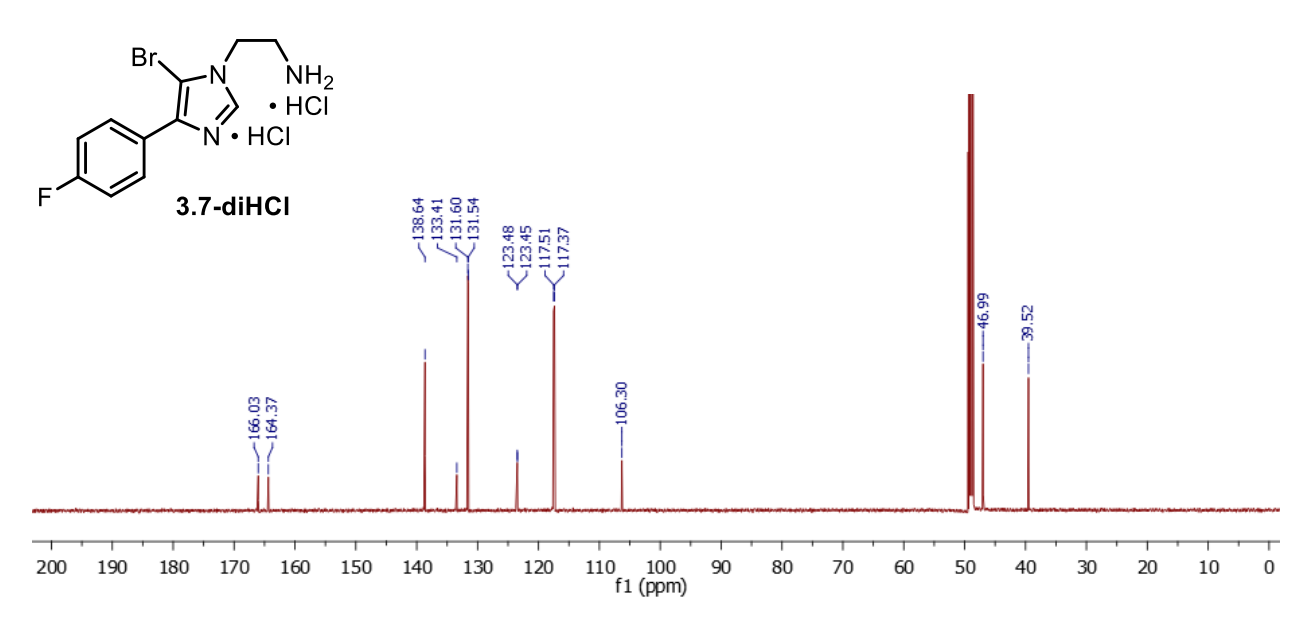


Figure 3.2.21. ¹³C NMR spectrum of 3.7-diHCl in MeOD.

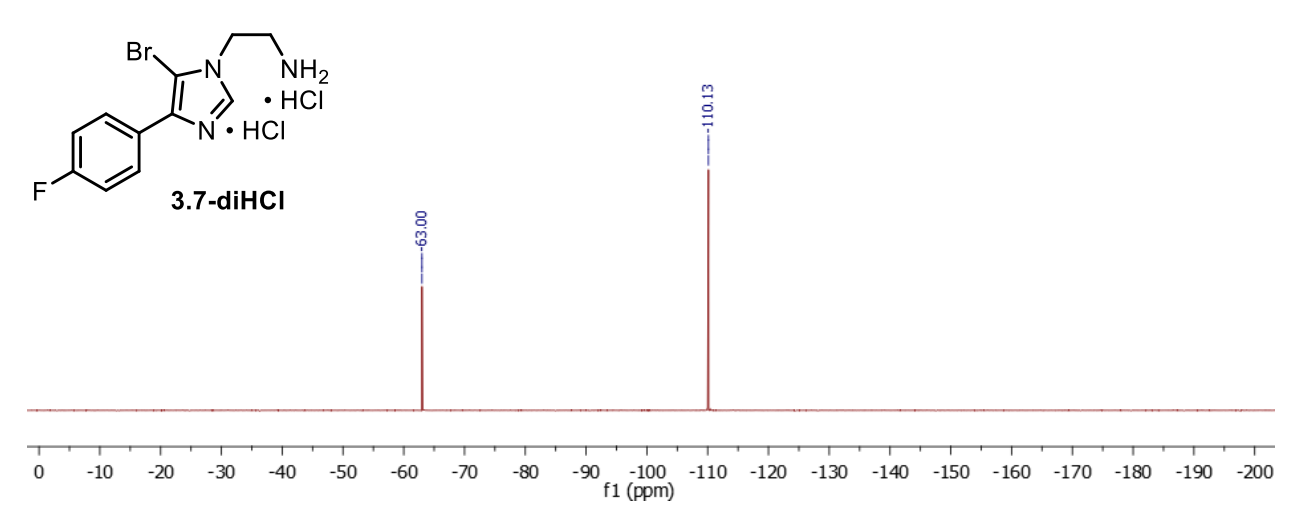


Figure 3.2.22. ¹⁹F NMR spectrum of 3.7-diHCl in MeOD.



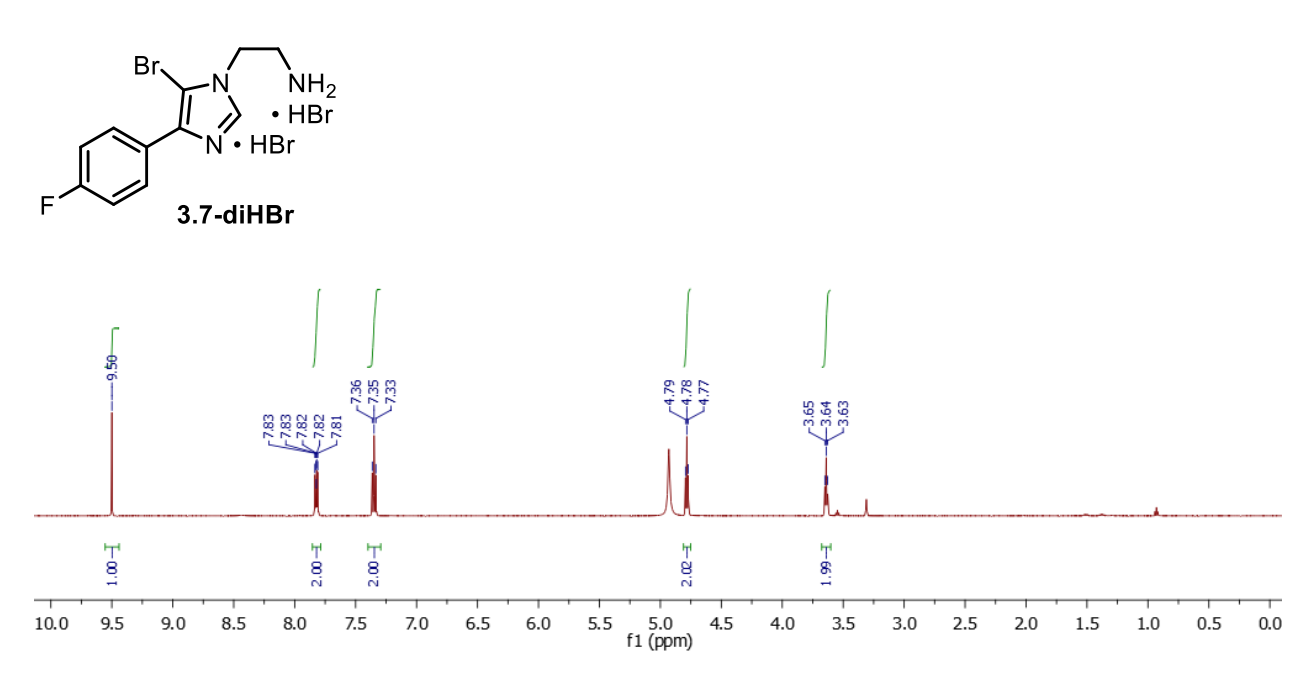


Figure 3.2.23. ¹H NMR spectrum of 3.7-diHBr in MeOD.

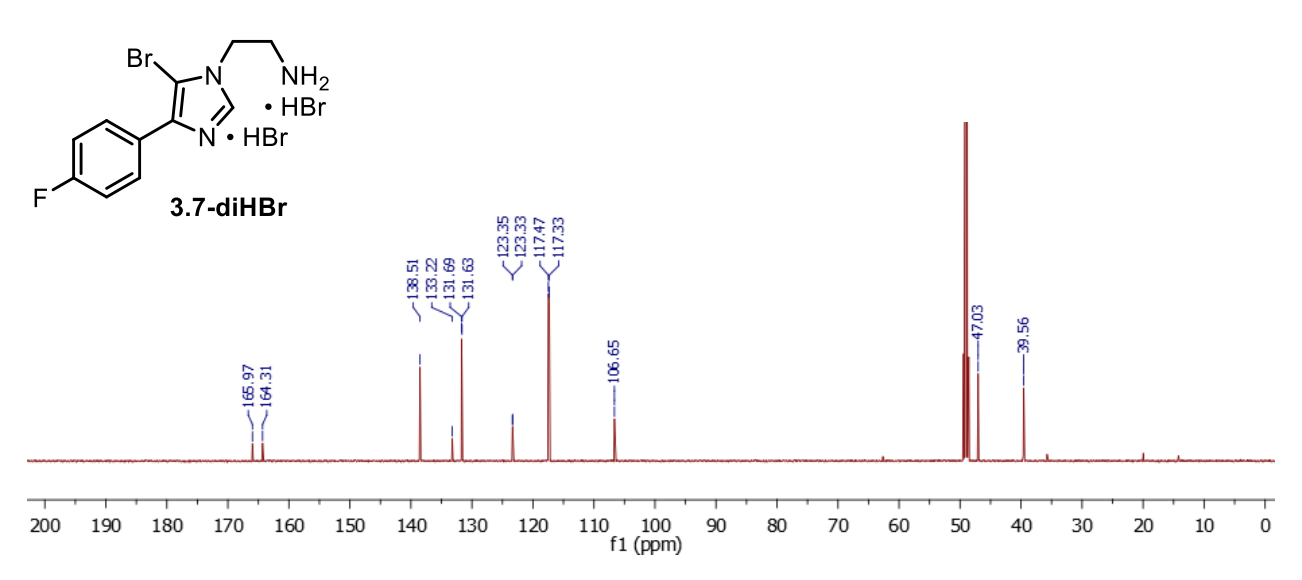


Figure 3.2.24. ¹³C NMR spectrum of 3.7-diHBr in MeOD.



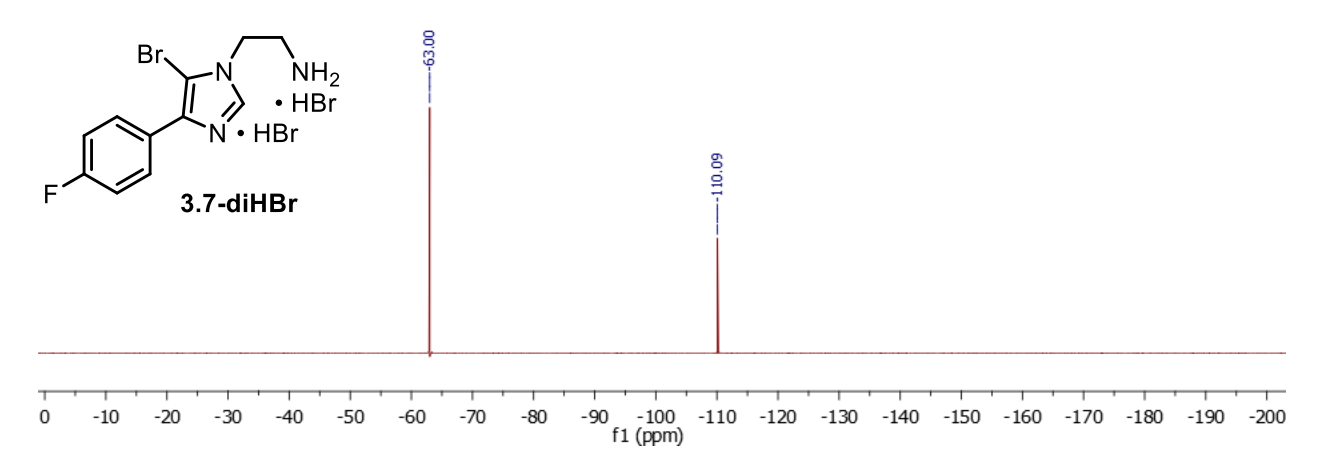


Figure 3.2.25. ¹⁹F NMR spectrum of 3.7-diHBr in MeOD.



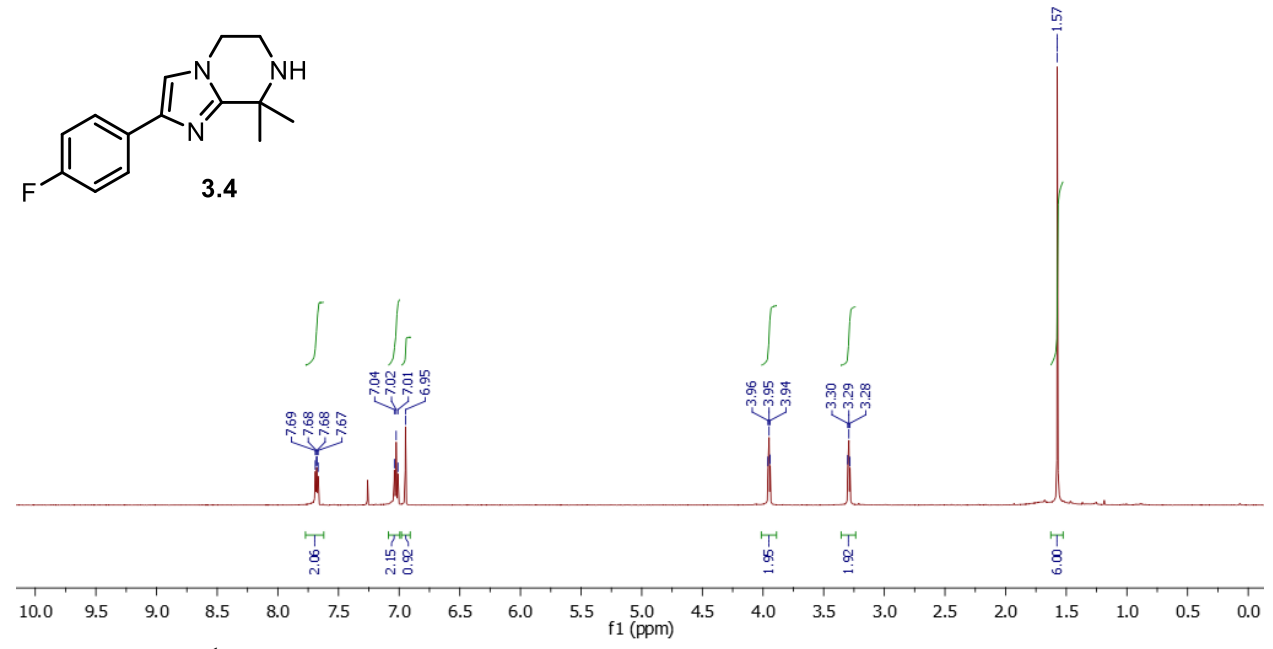


Figure 3.2.26. ¹H NMR spectrum of 3.4 (prepared by M4ALL route) in CDCl₃.

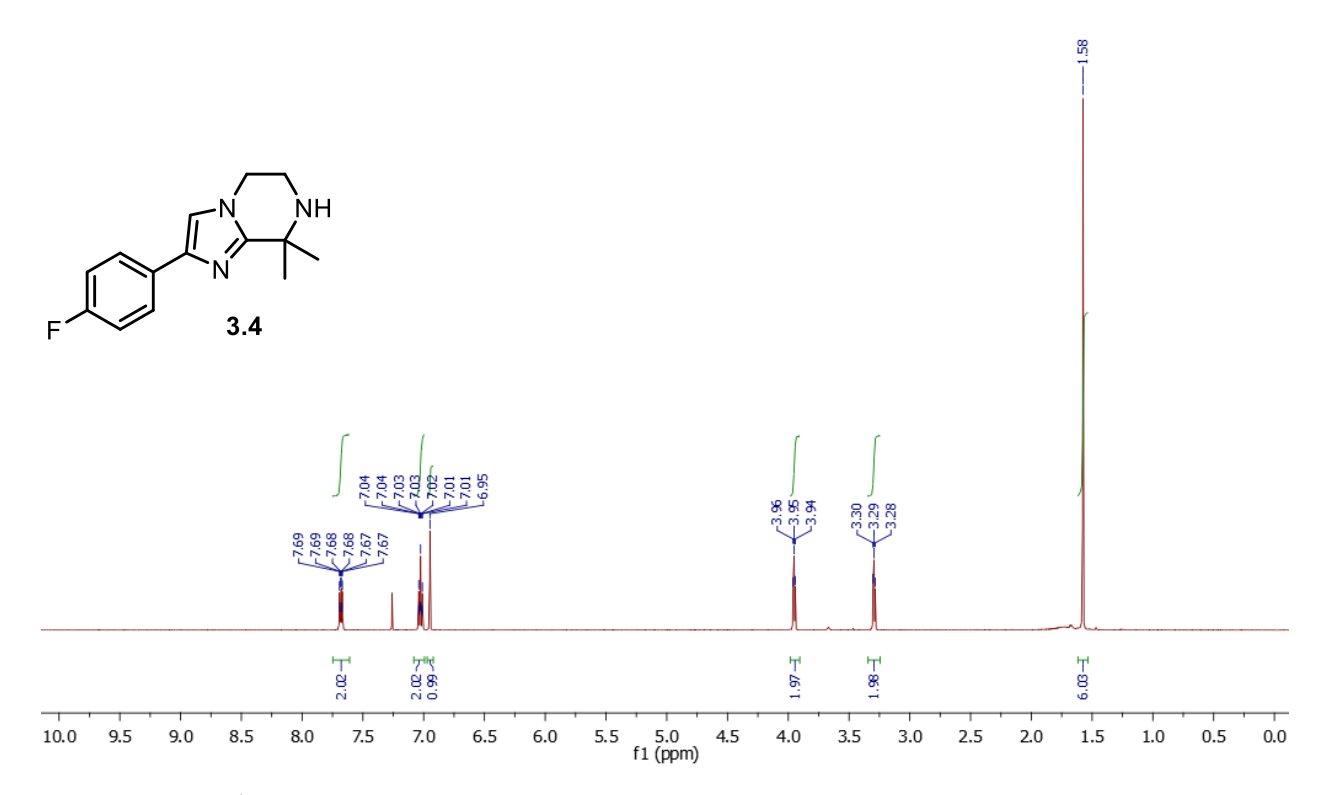


Figure 3.2.27. ¹H NMR spectrum of 3.4 (prepared by literature route) in CDCl₃.



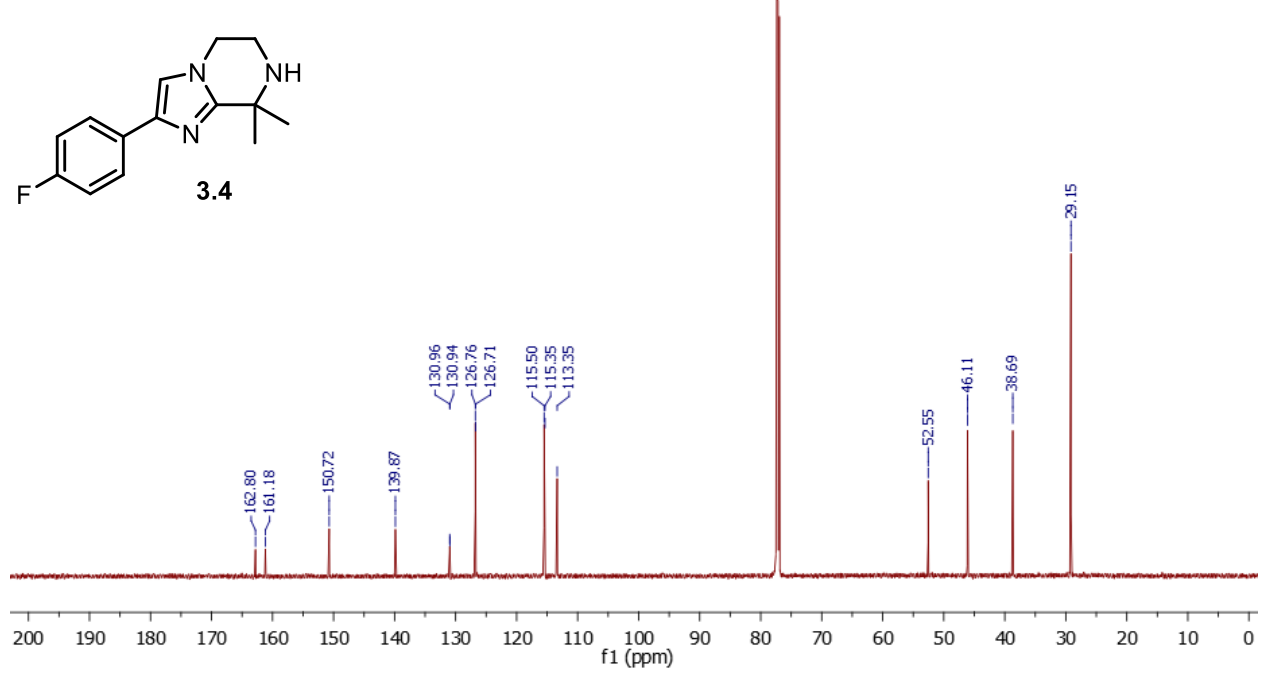


Figure 3.2.28. ¹³C NMR spectrum of 3.4 (prepared by M4ALL route) in CDCl₃.

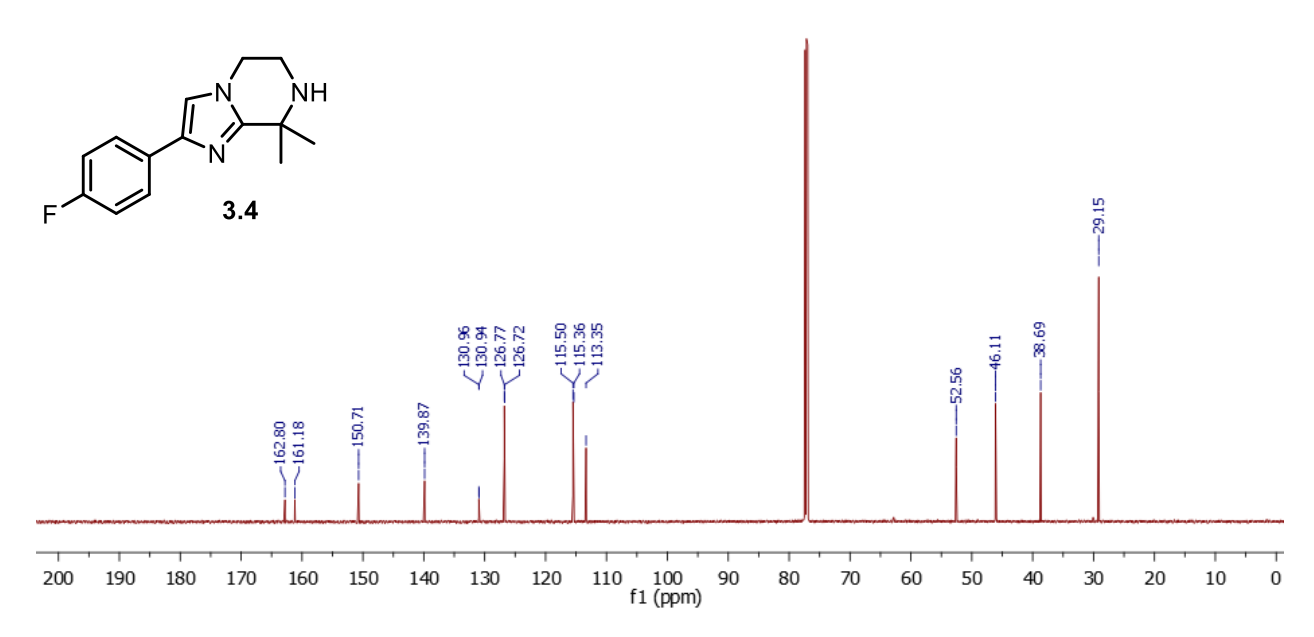


Figure 3.2.29. ¹³C NMR spectrum of 3.4 (prepared by literature route) in CDCl₃.



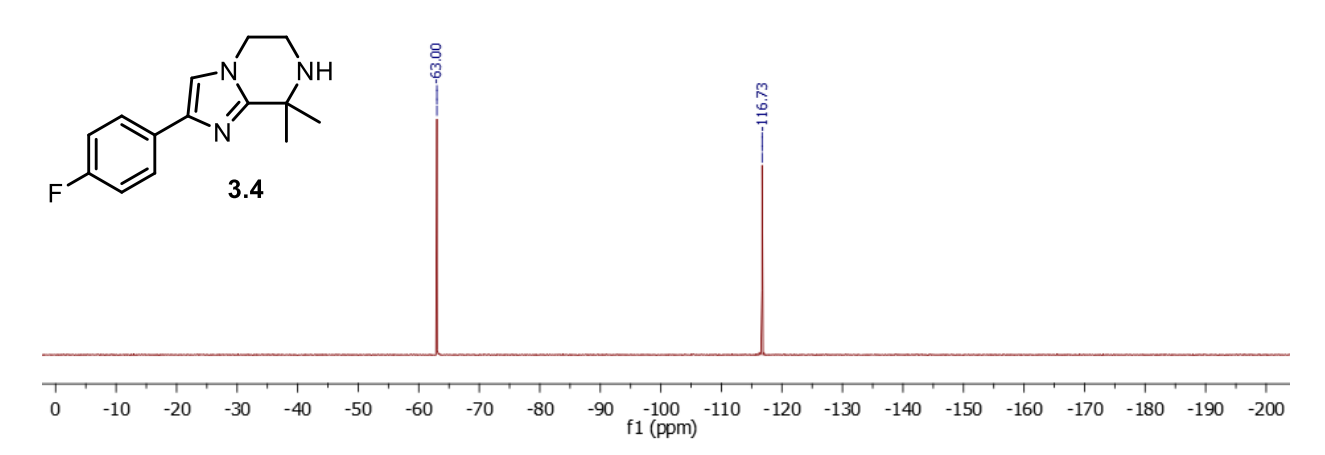


Figure 3.2.30. ¹⁹F NMR spectrum of 3.4 (prepared by M4ALL route) in CDCl₃.

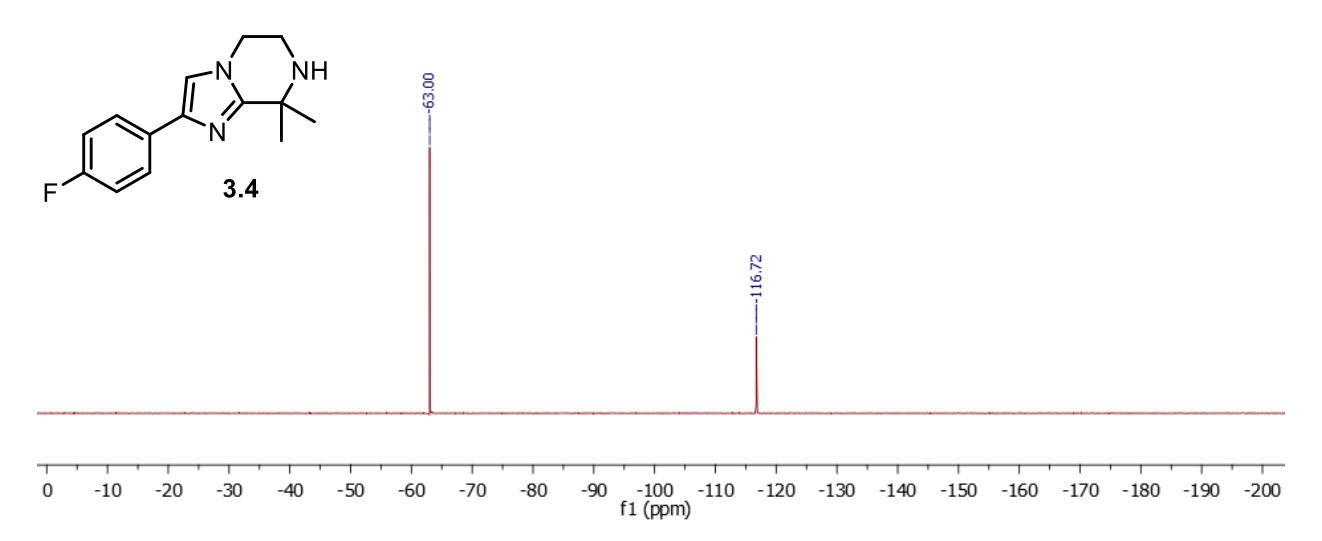


Figure 3.2.31. ¹⁹F NMR spectrum of 3.4 (prepared by literature route) in CDCl₃.



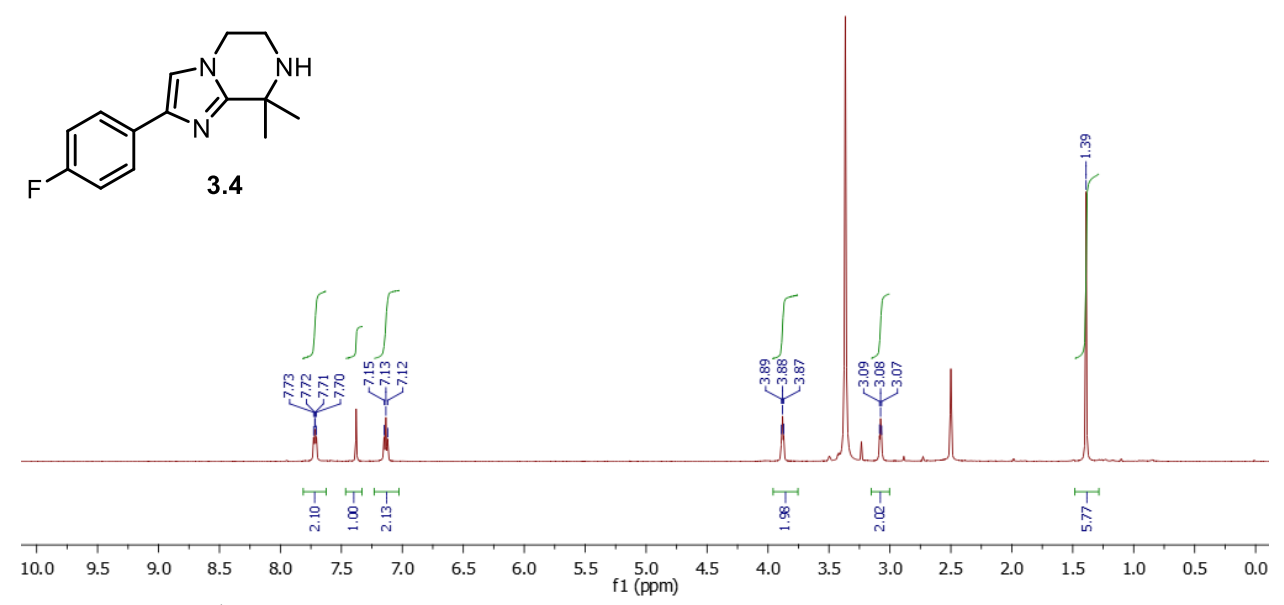


Figure 3.2.32. ¹H NMR spectrum of **3.4** (prepared by M4ALL route) in DMSO-*d*₆.

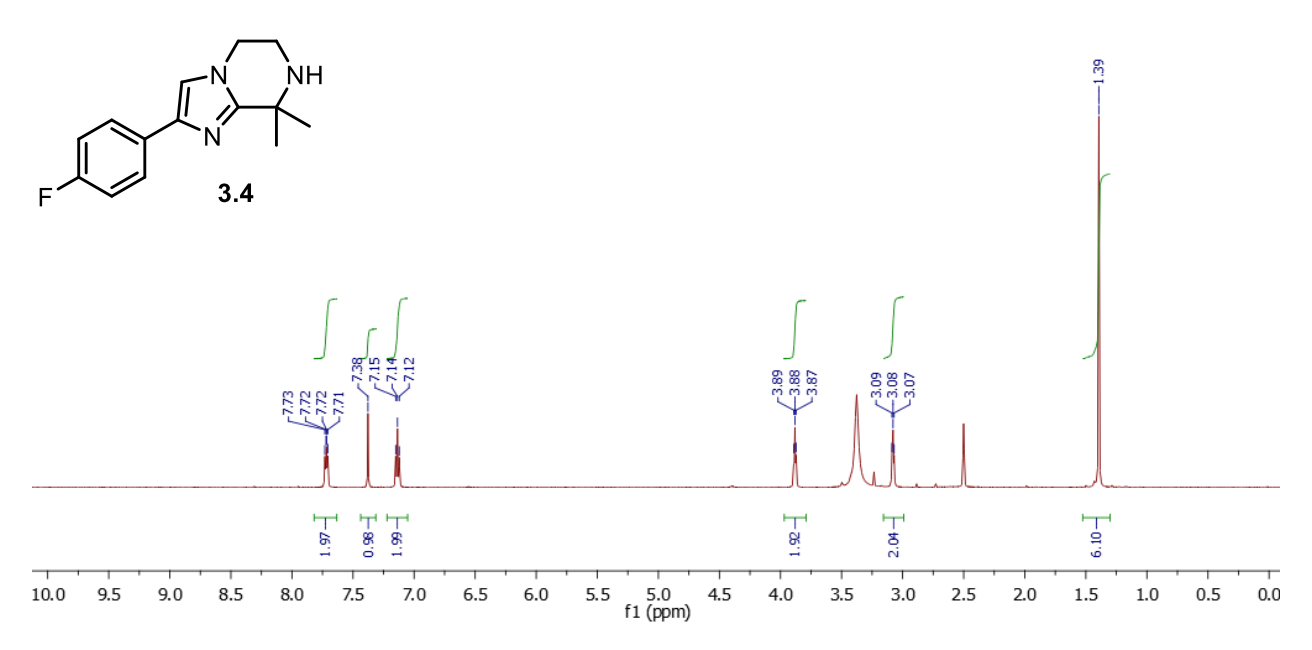


Figure 3.2.33. ¹H NMR spectrum of **3.4** (prepared by literature route) in DMSO- d_6 .



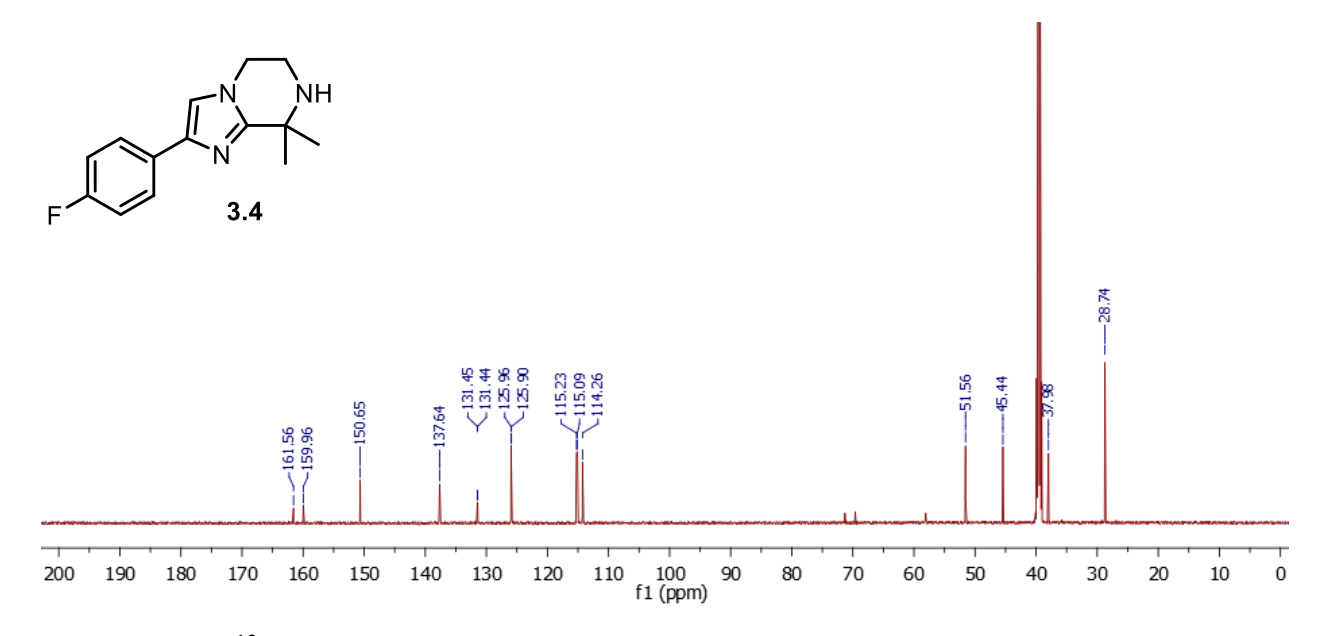


Figure 3.2.34. ¹³C NMR spectrum of 3.4 (prepared by M4ALL route) in DMSO-d₆.

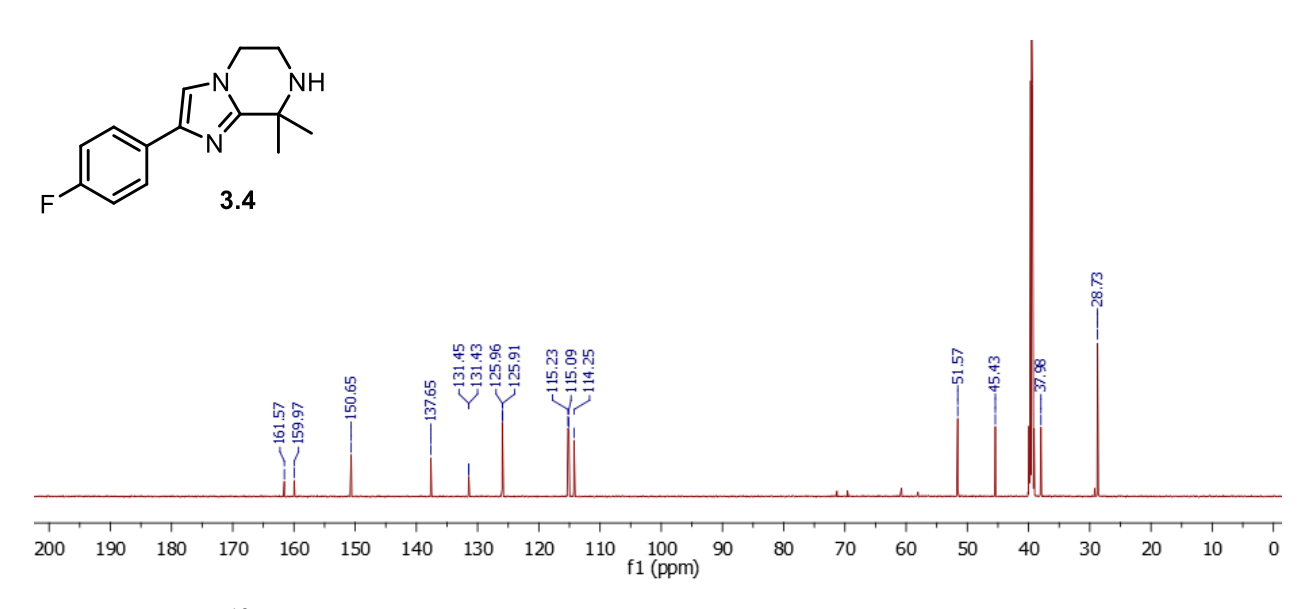


Figure 3.2.35. 13 C NMR spectrum of 3.4 (prepared by literature route) in DMSO- d_6 .



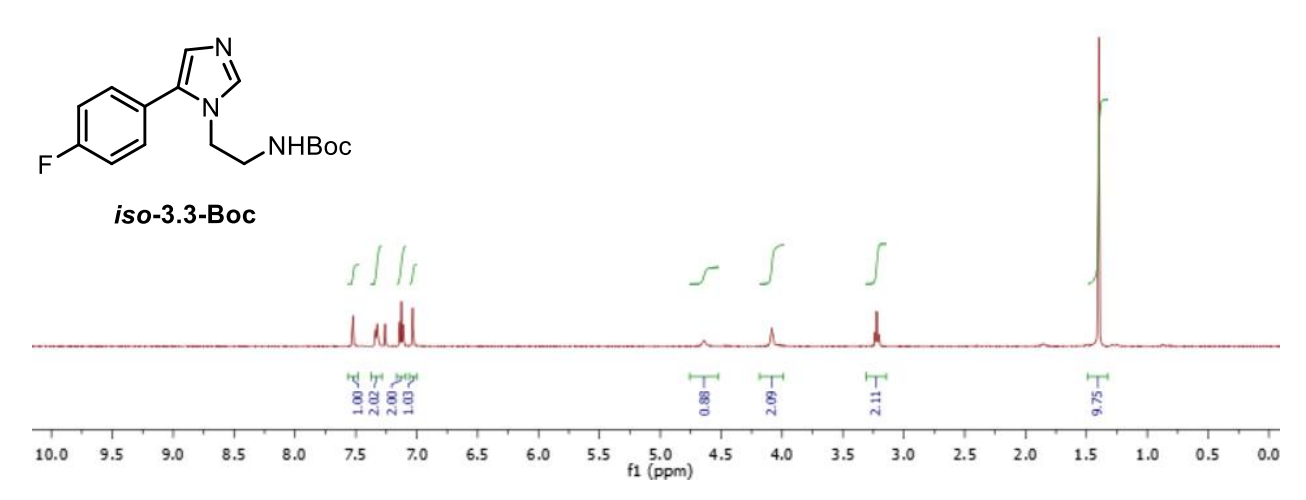


Figure 3.2.36. ¹H NMR spectrum of *iso-3.3-Boc* in CDCl₃.

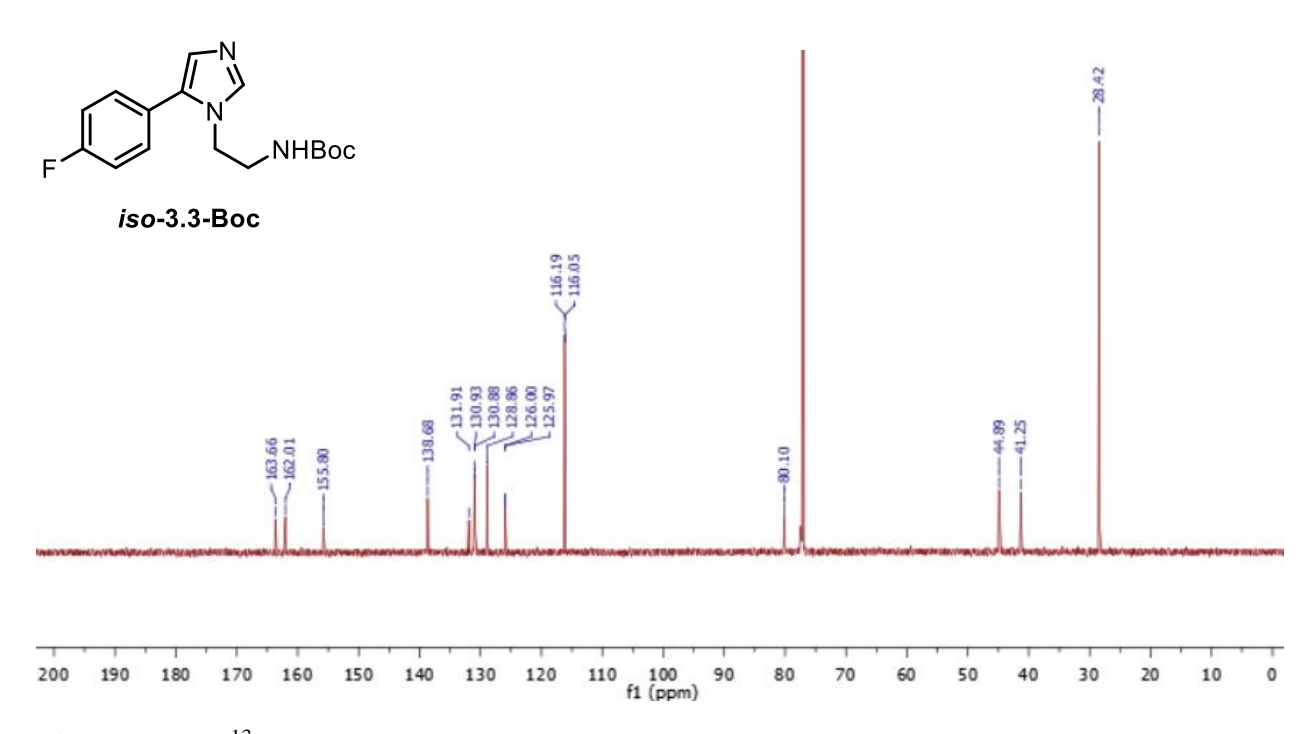


Figure 3.2.37. ¹³C NMR spectrum of *iso-*3.3-Boc in CDCl₃.



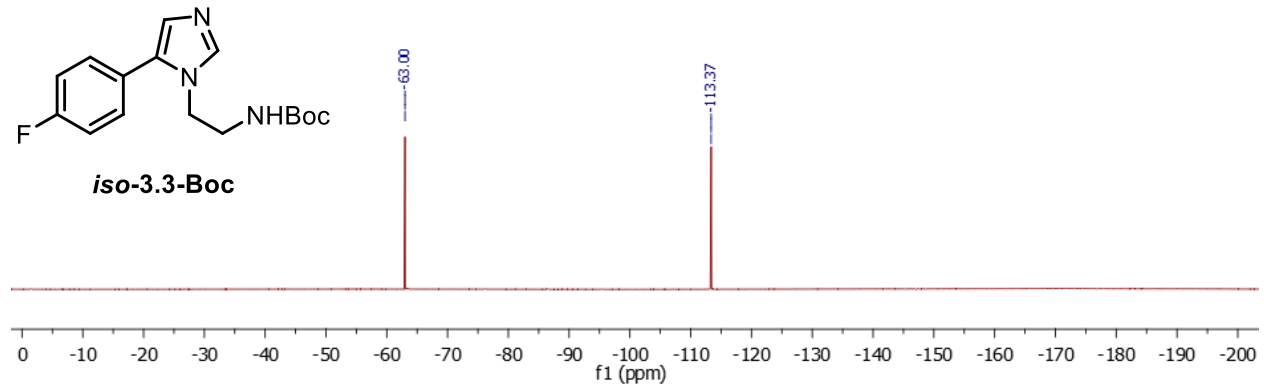


Figure 3.2.38. ¹⁹F NMR spectrum of *iso-*3.3-Boc in CDCl₃.

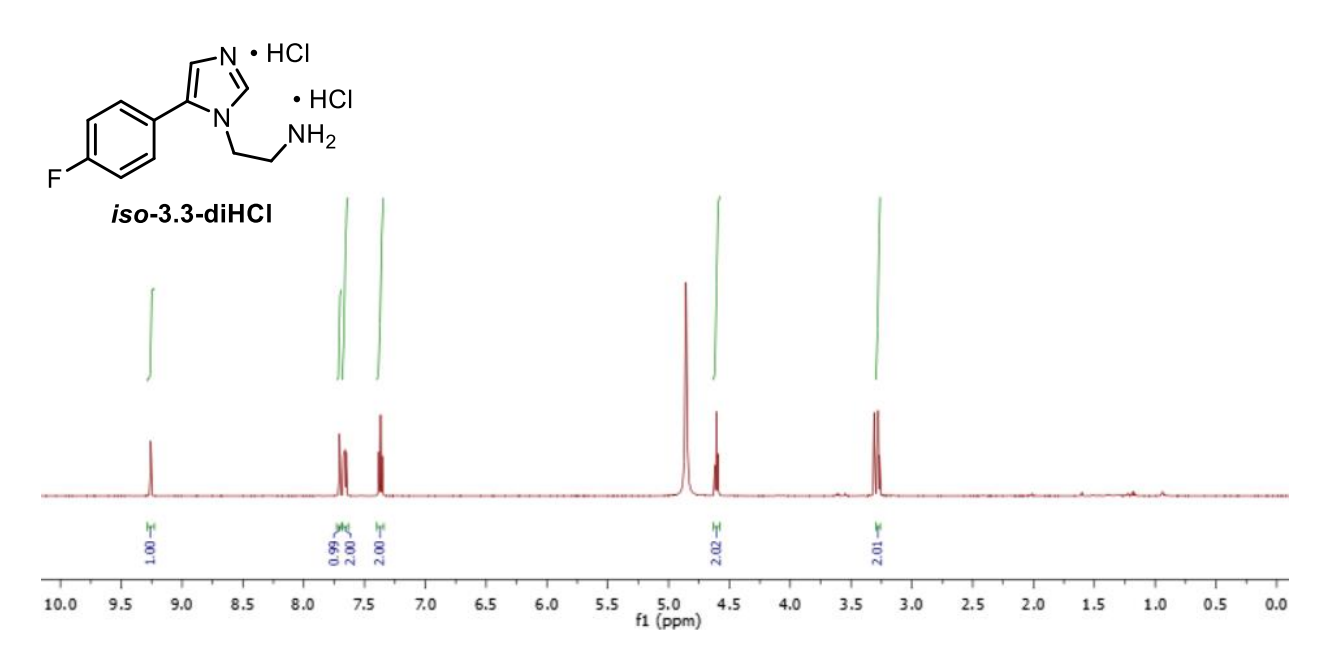


Figure 3.2.39. ¹H NMR spectrum of *iso-*3.3-diHCl in MeOD.



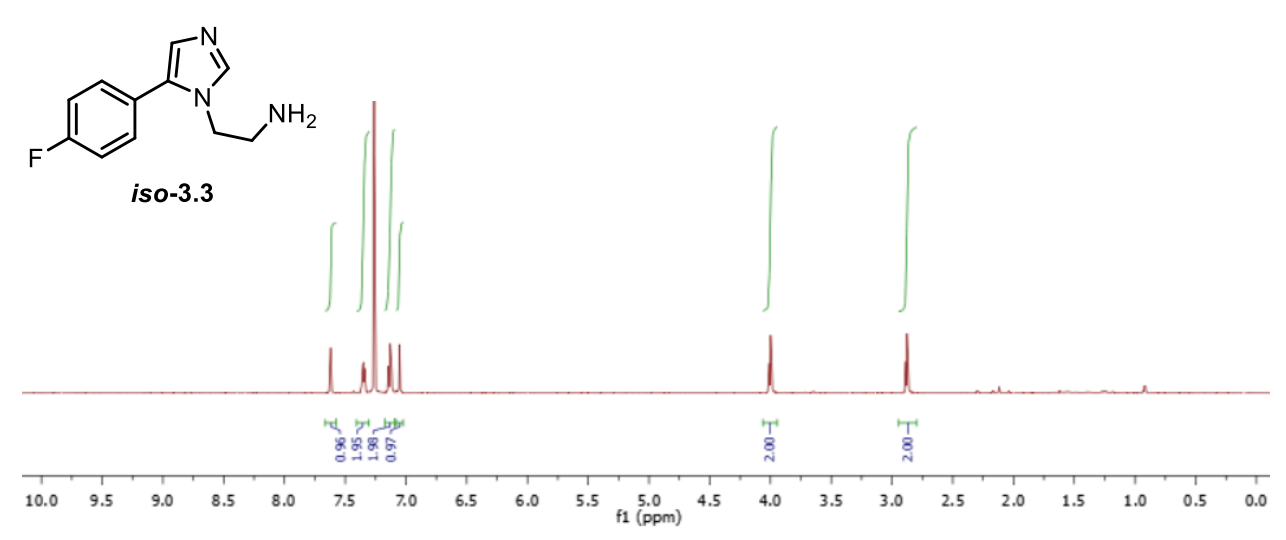


Figure 3.2.40. ¹H NMR spectrum of *iso-3.3* in CDCl₃.

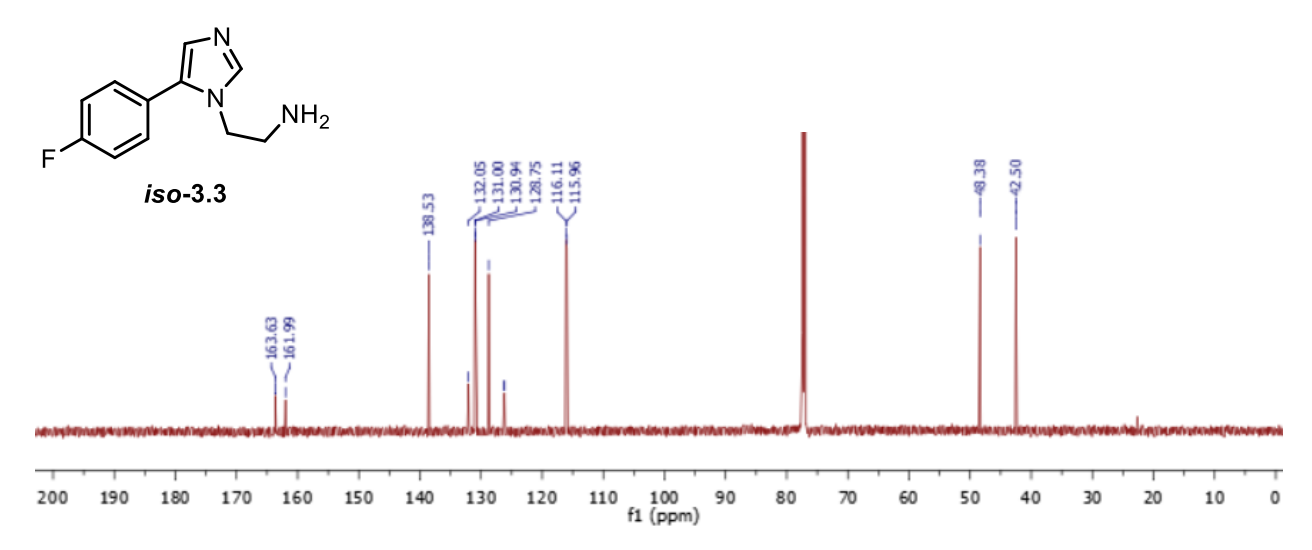


Figure 3.2.41. ¹³C NMR spectrum of *iso-3.3* in CDCl₃.



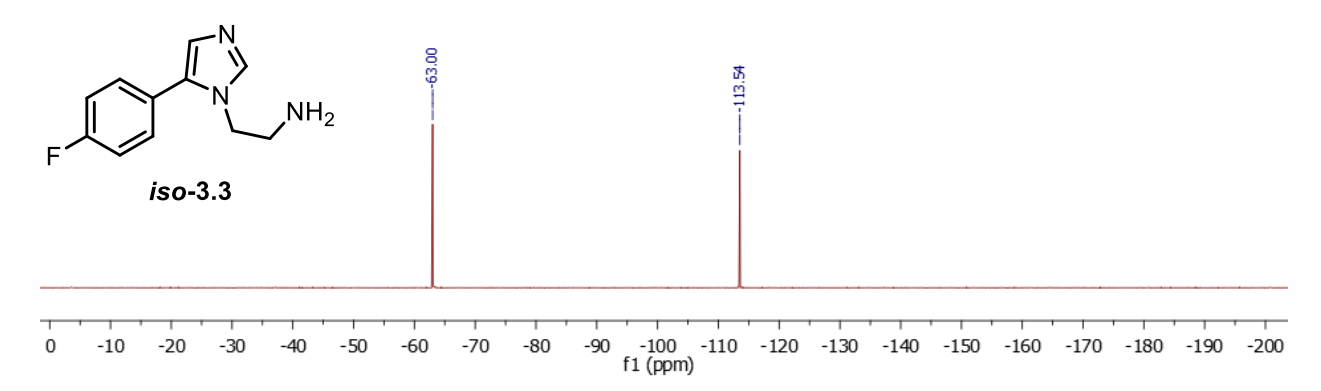


Figure 3.2.42. ¹⁹F NMR spectrum of *iso-3.3* in CDCl₃.

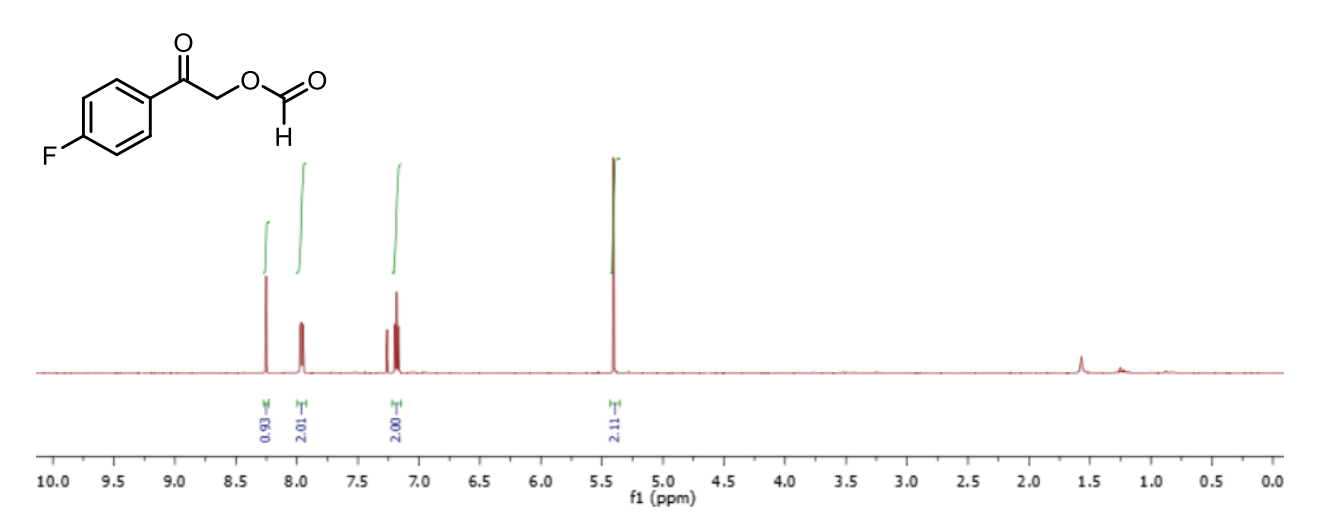


Figure 3.2.43. ¹H NMR spectrum of 2-(4-fluorophenyl)-2-oxoethyl formate in CDCl₃.



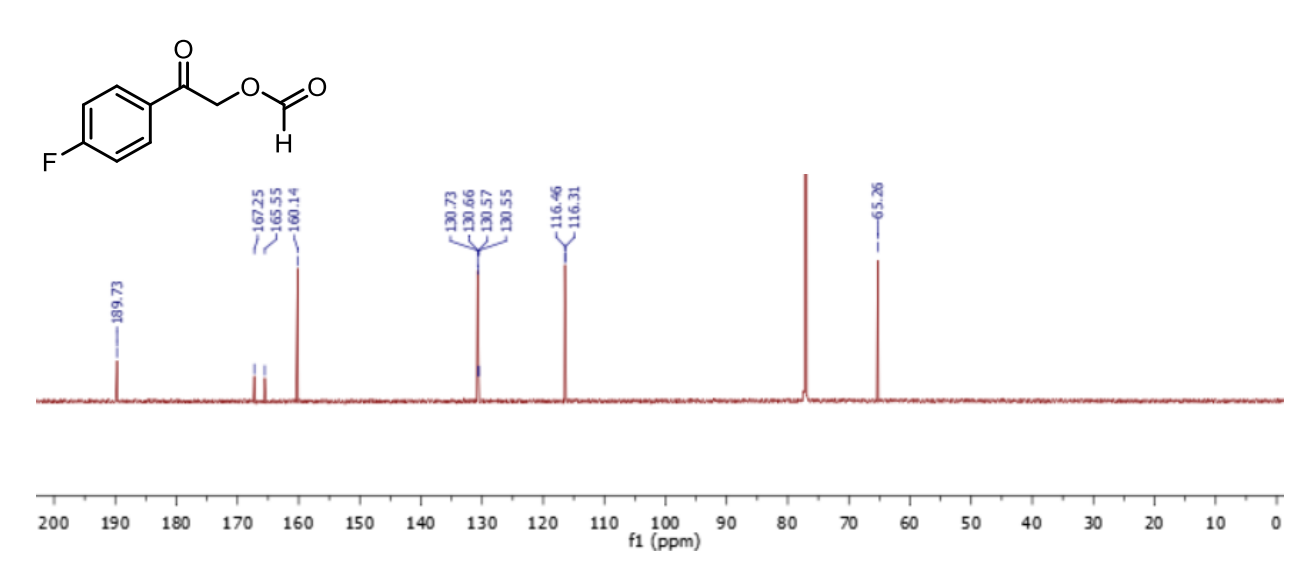


Figure 3.2.44. ¹³C NMR spectrum of 2-(4-fluorophenyl)-2-oxoethyl formate in CDCl₃.

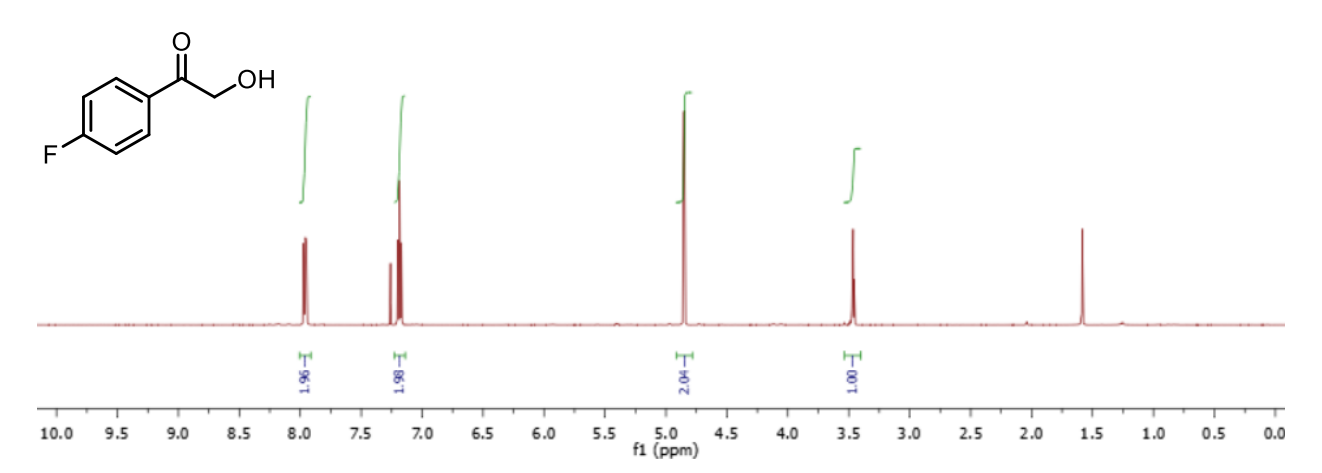


Figure 3.2.45. ¹H NMR spectrum of 1-(4-fluorophenyl)-2-hydroxyethan-1-one in CDCl₃.



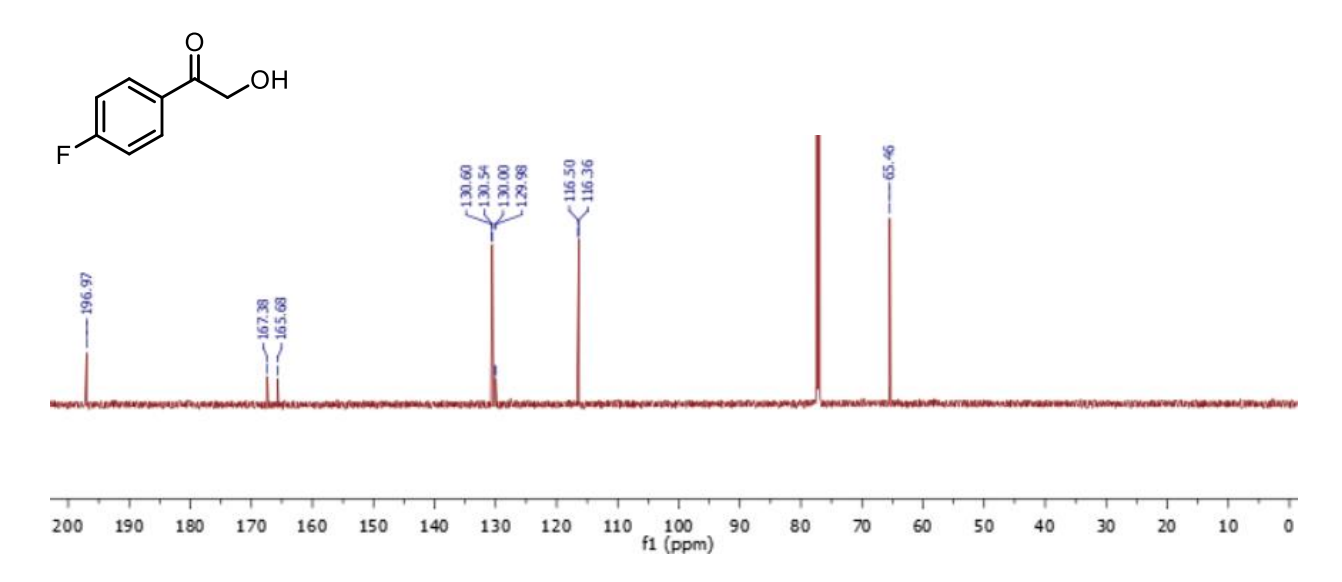


Figure 3.2.46. ¹³C NMR spectrum of 1-(4-fluorophenyl)-2-hydroxyethan-1-one in CDCl₃.



4 Acknowledgements

This work was supported with funding from the Gates Foundation. M4ALL would like to express our gratitude to Dr. Trevor Laird, Dr. John Dillon, and Dr. Mark Krook for their helpful technical guidance throughout this project, as well as Dr. John Walker and Scott Rosenblum for the ongoing collaboration and support of the M4ALL mission. The authors thank Dr. Saeed Ahmad and his team for their boundless effort in TE analysis. We also would like to thank Dr. B. Frank Gupton, Dr. Douglas Klumpp, Dr. G. Michael Laidlaw, and Michael Osberg for their input on this work.

5 References

- (1) Nagle, A.; Wu, T.; Kuhen, K.; Gagaring, K.; Borboa, R.; Francek, C.; Chen, Z.; Plouffe, D.; Lin, X.; Caldwell, C.; Ek, J.; Skolnik, S.; Liu, F.; Wang, J.; Chang, J.; Li, C.; Liu, B.; Hollenbeck, T.; Tuntland, T.; Isbell, J.; Chuan, T.; Alper, P. B.; Fischli, C.; Brun, R.; Lakshminarayana, S. B.; Rottmann, M.; Diagana, T. T.; Winzeler, E. A.; Glynne, R.; Tully, D. C.; Chatterjee, A. K. Imidazolopiperazines: Lead Optimization of the Second-Generation Antimalarial Agents. *J. Med. Chem.* **2012**, *55* (9), 4244–4273. https://doi.org/10.1021/jm300041e.
- (2) Chatterjee, A. K.; Nagle, A.; Wu, T.; Tully, D.; Kuhen, K. L. Compounds and Compositions for the Treatment of Parasitic Diseases. WO2011006143A2, January 13, 2011.
- (3) Bredereck, H.; Effenberger, F.; Maruez, F.; Ockewitz, K. Säureamid-Reaktionen, XXIII. Darstellung von Imidazolen Aus Ketonen. https://doi.org/10.1002/cber.19600930927.
- (4) Fact sheet about malaria. https://www.who.int/news-room/fact-sheets/detail/malaria (accessed 2025-08-30).
- (5) LaMonte, G. M.; Rocamora, F.; Marapana, D. S.; Gnädig, N. F.; Ottilie, S.; Luth, M. R.; Worgall, T. S.; Goldgof, G. M.; Mohunlal, R.; Santha Kumar, T. R.; Thompson, J. K.; Vigil, E.; Yang, J.; Hutson, D.; Johnson, T.; Huang, J.; Williams, R. M.; Zou, B. Y.; Cheung, A. L.; Kumar, P.; Egan, T. J.; Lee, M. C. S.; Siegel, D.; Cowman, A. F.; Fidock, D. A.; Winzeler, E. A. Pan-Active Imidazolopiperazine Antimalarials Target the Plasmodium Falciparum Intracellular Secretory Pathway. *Nat. Commun.* **2020**, *11* (1), 1780. https://doi.org/10.1038/s41467-020-15440-4.
- (6) Kreutzfeld, O.; Orena, S.; Okitwi, M.; Tumwebaze, P. K.; Byaruhanga, O.; Katairo, T.; Conrad, M. D.; Legac, J.; Garg, S.; Crudale, R.; Aydemir, O.; Giesbrecht, D.; Nsobya, S. L.; Blasco, B.; Duffey, M.; Rouillier, M.; Bailey, J. A.; Cooper, R. A.; Rosenthal, P. J. Ex Vivo Susceptibilities to Ganaplacide and Diversity in Potential Resistance Mediators in Ugandan Plasmodium Falciparum Isolates. *Antimicrob. Agents Chemother.* 2024. https://doi.org/10.1128/aac.00466-24.
- (7) Ogutu, B.; Yeka, A.; Kusemererwa, S.; Thompson, R.; Tinto, H.; Toure, A. O.; Uthaisin, C.; Verma, A.; Kibuuka, A.; Lingani, M.; Lourenço, C.; Mombo-Ngoma, G.; Nduba, V.; N'Guessan, T. L.; Nassa, G. J. W.; Nyantaro, M.; Tina, L. O.; Singh, P. K.; Gaaloul, M. E.; Marrast, A. C.; Chikoto, H.; Csermak, K.; Demin, I.; Mehta, D.; Pathan, R.; Risterucci, C.; Su, G.; Winnips, C.; Kaguthi, G.;



- Fofana, B.; Grobusch, M. P. Ganaplacide (KAF156) plus Lumefantrine Solid Dispersion Formulation Combination for Uncomplicated Plasmodium Falciparum Malaria: An Open-Label, Multicentre, Parallel-Group, Randomised, Controlled, Phase 2 Trial. *Lancet Infect. Dis.* **2023**, *23* (9), 1051–1061. https://doi.org/10.1016/S1473-3099(23)00209-8.
- (8) Novartis and Medicines for Malaria Venture announce decision to move to Phase 3 study for novel ganaplacide/lumefantrine-SDF combination in adults and children with malaria. Novartis. https://www.novartis.com/news/media-releases/novartis-and-medicines-malaria-venture-announce-decision-move-phase-3-study-novel-ganaplacidelumefantrine-sdf-combination-adults-and-children-malaria (accessed 2025-08-30).
- (9) *Ganaplacide-lumefantrine*. Medicines for Malaria Venture. https://www.mmv.org/mmv-pipeline-antimalarial-drugs/ganaplacide-lumefantrine (accessed 2025-08-30).
- (10) Wu, T.; Nagle, A.; Kuhen, K.; Gagaring, K.; Borboa, R.; Francek, C.; Chen, Z.; Plouffe, D.; Goh, A.; Lakshminarayana, S. B.; Wu, J.; Ang, H. Q.; Zeng, P.; Kang, M. L.; Tan, W.; Tan, M.; Ye, N.; Lin, X.; Caldwell, C.; Ek, J.; Skolnik, S.; Liu, F.; Wang, J.; Chang, J.; Li, C.; Hollenbeck, T.; Tuntland, T.; Isbell, J.; Fischli, C.; Brun, R.; Rottmann, M.; Dartois, V.; Keller, T.; Diagana, T.; Winzeler, E.; Glynne, R.; Tully, D. C.; Chatterjee, A. K. Imidazolopiperazines: Hit to Lead Optimization of New Antimalarial Agents. *J. Med. Chem.* **2011**, *54* (14), 5116–5130. https://doi.org/10.1021/jm2003359.
- (11) Tichniouin, M.; Sauleau, J.; Sauleau, A.; Lacroix, P. Synthesis, psychotropic activity and effect on experimental arrhythmias of unsaturated hydroxyhydrazines. *Eur. J. Med. Chem.* **1985**, *20* (2), 181–186
- (12) US EPA, O. Biden-Harris Administration Finalizes Ban on Most Uses of Methylene Chloride, Protecting Workers and Communities from Fatal Exposure. https://www.epa.gov/newsreleases/biden-harris-administration-finalizes-ban-most-uses-methylene-chloride-protecting (accessed 2025-09-11).
- (13) A GUIDE TO COMPLYING WITH THE 2024 METHYLENE CHLORIDE REGULATION UNDER THE TOXIC SUBSTANCES CONTROL ACT (TSCA) (RIN 2070-AK70). **2024**.
- (14) Guillaume, M. J. M.; Lang, Y. L.; Roessler, A.; Ulmer, L.; Leurs, S. M. H.; De, S. D. Process for the Production of `2- (4-Fluoro-Benzyl) -Phenyl! -Acetic Acid. WO2006024630A1, March 9, 2006.
- (15) Kiss, L. E.; Learmonth, D. A.; Rosa, C. P. D. C. P.; Gusmao, D. N. R.; Palma, P. N. L.; Soares, D. S. P. M. V. A.; Beliaev, A. Pharmaceutical Compounds. WO2010074588A2, July 1, 2010.
- (16) Carneiro, P. F.; Gutmann, B.; de Souza, R. O. M. A.; Kappe, C. O. Process Intensified Flow Synthesis of 1H-4-Substituted Imidazoles: Toward the Continuous Production of Daclatasvir. *ACS Sustain. Chem. Eng.* **2015**, *3* (12), 3445–3453. https://doi.org/10.1021/acssuschemeng.5b01191.
- (17) Kumar, S.; Jaller, D.; Patel, B.; LaLonde, J. M.; DuHadaway, J. B.; Malachowski, W. P.; Prendergast, G. C.; Muller, A. J. Structure Based Development of Phenylimidazole-Derived Inhibitors of Indoleamine 2,3-Dioxygenase. *J. Med. Chem.* **2008**, *51* (16), 4968–4977. https://doi.org/10.1021/jm800512z.
- (18) Xiao, H.-Y.; Wu, D.-R.; Malley, M. F.; Gougoutas, J. Z.; Habte, S. F.; Cunningham, M. D.; Somerville, J. E.; Dodd, J. H.; Barrish, J. C.; Nadler, S. G.; Dhar, T. G. M. Novel Synthesis of the Hexahydroimidazo[1,5b]Isoquinoline Scaffold: Application to the Synthesis of Glucocorticoid Receptor Modulators. *J. Med. Chem.* **2010**, *53* (3), 1270–1280. https://doi.org/10.1021/jm901551w.
- (19) Dhar, T. G. M.; Xiao, H.-Y. Nonsteroidal Compounds Useful as Modulators of Glucocorticoid Receptor Ap-1 and/or Nf-?B Activity and Use Thereof. WO2009058944A2, May 7, 2009.
- (20) Elejalde-Cadena, N. R.; García-Olave, M.; Figueroa, D.; Vidossich, P.; Miscione, G. P.; Portilla, J. Influence of Steric Effect on the Pseudo-Multicomponent Synthesis of N-Aroylmethyl-4-Arylimidazoles. *Molecules* **2022**, 27 (4), 1165. https://doi.org/10.3390/molecules27041165.



- (21) Taveras, A. G.; Doll, R. J.; Cooper, A. B.; Ferreira, J. a; Guzi, T.; Rane, D. F.; Girijavallabhan, V. M.; Aki, C. J.; Chao, J.; Alvarez, C.; Kelly, J. M.; Lalwani, T.; Desai, J. a; Wang, J. J.-S. Farnesyl Protein Transferase Inhibitors. US6372747B1, April 16, 2002.
- (22) Kudo, K.; Kageyama, H. Method for Preparing N-(2-Aminoethyl)Azole Compound. JP2010215610A, September 30, 2010.
- (23) Li, Q.; Zhu, J.; Zhang, Y.; Li, M.; Liu, Y. Isobaric Vapor–Liquid Equilibria for Ethyl Acetate + Acetonitrile + 1-Butyl-3-Methylimidazolium Bis(Trifluoromethylsulfonyl)Imide at 101.3 kPa. *J. Chem. Eng. Data* **2016**, *61* (11), 3705–3709. https://doi.org/10.1021/acs.jced.5b00995.
- (24) Kim, H. Y.; Talukdar, A.; Cushman, M. Regioselective Synthesis of N-β-Hydroxyethylaziridines by the Ring-Opening Reaction of Epoxides with Aziridine Generated in Situ. *Org. Lett.* **2006**, 8 (6), 1085–1087. https://doi.org/10.1021/ol0529703.
- (25) Kumar, M.; Joshi, G.; Arora, S.; Singh, T.; Biswas, S.; Sharma, N.; Bhat, Z. R.; Tikoo, K.; Singh, S.; Kumar, R. Design and Synthesis of Non-Covalent Imidazo[1,2-a]Quinoxaline-Based Inhibitors of EGFR and Their Anti-Cancer Assessment. *Molecules* **2021**, *26* (5), 1490. https://doi.org/10.3390/molecules26051490.
- (26) Jing, Y.; Daniliuc, C. G.; Studer, A. Direct Conversion of Alcohols to α-Chloro Aldehydes and α-Chloro Ketones. *Org. Lett.* **2014**, *16* (18), 4932–4935. https://doi.org/10.1021/ol5024568.
- (27) Wang, Z.; Richter, S. M.; Rozema, M. J.; Schellinger, A.; Smith, K.; Napolitano, J. G. Potential Safety Hazards Associated with Using Acetonitrile and a Strong Aqueous Base. *Org. Process Res. Dev.* **2017**, *21* (10), 1501–1508. https://doi.org/10.1021/acs.oprd.7b00158.
- (28) Stucchi, M.; Grazioso, G.; Lammi, C.; Manara, S.; Zanoni, C.; Arnoldi, A.; Lesma, G.; Silvani, A. Disrupting the PCSK9/LDLR Protein–Protein Interaction by an Imidazole-Based Minimalist Peptidomimetic. *Org. Biomol. Chem.* **2016**, *14* (41), 9736–9740. https://doi.org/10.1039/C6OB01642A.
- (29) Kumar, S.; Kumar, A.; Gupta, R. K.; Kumar, D. One-Pot Synthesis of α-Formyloxy Ketones from Enolizable Ketones. *Synth. Commun.* **2008**, *38* (3), 338–345. https://doi.org/10.1080/00397910701767049.
- (30) McLaughlin, M.; Belyk, K. M.; Qian, G.; Reamer, R. A.; Chen, C. Synthesis of α-Hydroxyacetophenones. *J. Org. Chem.* **2012**, 77 (11), 5144–5148. https://doi.org/10.1021/jo3005556.